Texas Medical Center Library
DigitalCommons@TMC

UT GSBS Dissertations and Theses (Open Access) | Graduate School of Biomedical Sciences

12-2016

MAGUK SCAFFOLDS ORGANIZE A KEY SYNAPTIC COMPLEX IN HORIZONTAL CELL PROCESSES CONTACTING PHOTORECEPTORS

Alejandro Vila, Ph.D.

Follow this and additional works at: http://digitalcommons.library.tmc.edu/utgsbs_dissertations

Part of the Medicine and Health Sciences Commons, Molecular and Cellular Neuroscience Commons, and the Systems Neuroscience Commons

Recommended Citation
Vila, Ph.D., Alejandro, "MAGUK SCAFFOLDS ORGANIZE A KEY SYNAPTIC COMPLEX IN HORIZONTAL CELL PROCESSES CONTACTING PHOTORECEPTORS" (2016). *UT GSBS Dissertations and Theses (Open Access)*. 727.
http://digitalcommons.library.tmc.edu/utgsbs_dissertations/727

This Dissertation (PhD) is brought to you for free and open access by the Graduate School of Biomedical Sciences at DigitalCommons@TMC. It has been accepted for inclusion in UT GSBS Dissertations and Theses (Open Access) by an authorized administrator of DigitalCommons@TMC. For more information, please contact laurel.sanders@library.tmc.edu.

MAGUK SCAFFOLDS ORGANIZE A KEY SYNAPTIC COMPLEX IN HORIZONTAL CELL PROCESSES CONTACTING PHOTORECEPTORS

by

Alejandro Vila. M.S

APPROVED:

_____
John O'Brien, Ph.D.
Advisory Professor

_____
Stephen Mills, Ph.D.

_____
Christophe P. Ribelayga, Ph.D.

_____
Kartik Venkatachalam, Ph.D.

_____
Jeffrey A. Frost, Ph.D.

APPROVED:

_____
Dean, The University of Texas
Graduate School of Biomedical Sciences at Houston

MAGUK SCAFFOLDS ORGANIZE A KEY SYNAPTIC COMPLEX IN HORIZONTAL CELL PROCESSES CONTACTING PHOTORECEPTORS

A

DISSERTATION

Presented to the Faculty of

The University of Texas

Health Science Center at Houston

and

The University of Texas

MD Anderson Cancer Center

Graduate School of Biomedical Sciences

in Partial Fulfillment

of the Requirements

for the Degree of

DOCTOR OF PHILOSOPHY

By

Alejandro Vila. M.S

Houston, Texas

December, 2016

Acknowledgements

First and foremost I want to thank my mother and father for giving me life and always being there for me. My parents are wonderful human beings, and I am very thankful for the joy and love they have brought throughout my life. I am extremely grateful to them for teaching me from a young age to believe in myself and never give up in my dreams. This dissertation is a testament to their hard work to make sure my sister and I had more opportunities than they had. I will always be thankful to them for allowing me to take ownership of my own life and become the person I am today. I want to thank my dearest sister Elsa for her support when times were difficult and specially for bringing Hudson and Bella V to our family. Most importantly, I am very grateful to have met my wife here in Houston. Kellyn is the source of my inspiration and has always given me the strength to overcome many obstacles throughout graduate school. I am very proud of my wife for her support and specially for giving me the space to prepare for my defense the months leading up to completing my dissertation. No words can describe how grateful I am for the birth of our precious son Ethan Alexander. I am also extremely fortunate to be parent of Sofia who I care and love as my own daughter.

There are numerous people who have contributed to my success and whom I would like to acknowledge. Specifically I would like to thank my best friend Michael Kopple, whom I met my first year as an international student in Davis, CA, and who encouraged me to transfer to UCLA to continue my education. I would also like to thank Dr. Sotirious Tetradis at UCLA for giving me the opportunity to experience as an undergraduate what it is like to get your work published. I will always be grateful to my

former supervisor Dr. Nicholas C. Brecha at UCLA for teaching me so much about the retina and providing me with the necessary tools to be a successful neuroscientist. I am extremely grateful to Dr. David Marshak and Ruth Heidelberger for recruiting me to the PhD graduate program and allowing me to flourish as a scientist through their mentorship and numerous collaborations. I am also extremely thankful to Dr. Iris Fahrenfort, to whom I owe a great deal for taking time out of her grant writing to help me prepare for my qualifying exam. I want to thank Christopher Whitaker for his technical expertise and unforgettable jamming sessions at home. I am very thankful to our lab manager Ya-Ping Lin whose invaluable technical support and impeccable lab management skills contributed to the publication of my work. Next, I want to thank the entire Neuroscience staff and Ophthalmology and Vision Department and some of their students including, Natalie Sirisaengtaksin, Monica Gireud, Madeline Farley, Jonathan Flynn, Sahily Reyes, Andrea Bordt and Helen Yanran Wang for their input throughout our numerous presentations and interactions inside and outside of the lab.

I also want to thank my supervisory committee Dr. Stephen Mills, Dr. Christophe Ribelayga and members of his team for their encouragement, support and excellent technical expertise and, Dr. Kartik Venkatachalam and Dr. Jeffrey Frost for their years of mentoring and guidance. Most importantly, I would like to extend my greatest gratitude to my Ph.D advisor Dr. John O'Brien. There are no words to express how grateful I am to John for accepting me to work in his laboratory with his excellent guidance, continuous encouragement, and caring. I am eternally indebted to him for his support and patience, which helped me to overcome many crisis situations and complete my Ph.D.

MAGUK SCAFFOLDS ORGANIZE A KEY SYNAPTIC COMPLEX IN HORIZONTAL CELL PROCESSES CONTACTING PHOTORECEPTORS

Alejandro Vila, Ph.D.

Supervisory Professor: John O'Brien, Ph.D

Abstract

Synaptic processes and plasticity of synapses are mediated by large suites of proteins. In most cases, many of these proteins are tethered together by synaptic scaffold proteins. Scaffold proteins have a large number and typically a variety of protein interaction domains that allow many different proteins to be assembled into functional complexes. As each scaffold protein has a different set of protein interaction domains and a unique set of interacting partners, the presence of synaptic scaffolds can provide insight into the molecular mechanisms that regulate synaptic processes. In studies of rabbit retina, we found SAP102 and Chapsyn110 selectively localized in the tips of B-type horizontal cell processes where they contact cone and rod photoreceptors. We further identified some known SAP102 binding partners, kainate receptor GluR6/7 and inward rectifier potassium channel Kir2.1, closely associated with SAP102 in the processes of invaginating HCs. In contrast, in the mouse retina we identified Chapsyn110 as the major scaffold in the tips of horizontal cells contacting photoreceptors. Kir2.1 was found to be assembled with SAP102 into a complex with

GluR6/7 in photoreceptor invaginations in Rabbit. GluR6/7 and Kir2.1 presumably are involved in synaptic processes that govern cell-to-cell communication, and could both contribute in different ways to synaptic currents that mediate feedback signaling. Notably, we failed to find evidence for the presence of Cx57 or Cx59, but Pannexin1 immunolabeling was positive in the OPL of mouse retina suggesting that it could play a role in ephaptic and pH mediated signaling. Polyamines regulate many ion channels including Kir2.1. During the day polyamine immunolabeling was unexpectedly high in photoreceptor terminals compared to other areas of the retina. If polyamines are released, they may regulate the activity of Kir2.1 channels located in the tips of HCs. Alternatively, the presence of polyamines may potentiate GluR6/7 by reducing the transition to desensitized state causing an increase in channel conductance. The presence of SAP102 and Chapsyn110 and their binding partners in both cone and rod invaginating synapses suggests that whatever mechanism is supported by this protein complex is present in both types of photoreceptors.

Table of Contents

Acknowledgements …….. III

Abstract ……...VI

Table of Contents ……VIII

List of Illustrations……...X

Chapter 1. Introduction ……... 1

1.1. Lateral inhibition in the outer plexiform layer ……1

1.1.1. GABA …… 4

1.1.2. Ephaptic signal ……6

1.1.3. Proton ……..…….. 11

1.1.4. Summary ……. 14

1.2 Synaptic Scaffolds ……15

1.2.1 Glutamate receptors ..……..……..16

1.2.2 Potassium channels …… 21

Chapter 2. Methodology

2.1 Tissue Preparation …… 23

2.2 Injection of Neurobiotin and Alexa 568 ……... 24

2.3. Immunolabeling ..……..…… 25

2.4. In situ Proximity ligation assay (PLA) ...…….. 29

2.5. Confocal Microscopy . …..……. 30

2.6. Intensity Measurements of polyamines at different times of the day….. 31

Chapter 3. Synaptic Scaffolds in rabbit retina

3.1. Introduction……32

3.2. Distribution of MAGUK-containing synaptic scaffold proteins in the retina .34

3.2.1 SAP102 is a post synaptic element of photoreceptor synapses…….36

3.2.2 SAP102 is located in B-type HC ……..40

3.3. SAP102 complex in rabbit retina

3.3.1 Proteins known to bind to SAP102 are present in HC synapses…….43

3.3.2 Proteins thought to mediate ephaptic feedback signaling were not present in the scaffold complex…….47

3.3.3 Close associations of SAP102 with ion channels in the OPL……...49

3.4 Discussion …… 52

Chapter 4. Synaptic scaffolds in mouse retina

4.1. Introduction .,…… 59

4.2. Distribution of MAGUK-containing synaptic scaffold proteins in the retina .59

4.2.1 Chapsyn110/PSD93 is a post-synaptic element ……...63

4.2.2 Chapsyn is located in HCs ……...64

4.3. Chapsyn-110 (PSD93) complex in mouse retina ……...66

4.3.1 Chapsyn110 collects inward rectifying channels in HC synapses ….66

4.4 Evidence for pannexin channels in the mouse retina ……70

4.5 Changes of polyamine content in the OPL ……...71

4.5.1 Immunohistochemical evidence for polyamine transporter …… 76

4.6. Discussion …… 79

Chapter 5. Future Directions …… 82

Literature Cited …… 88

Vita …..……105

List of Illustrations

Fig.1.1 The synaptic complex of cone pedicles ……..2

Fig.1.2 Current voltage relationship of an isolated Ca^{2+} current …….3

Fig.1.3 Proposed mechanisms of horizontal cell feedback .....……....8

A. The ephaptic mechanism

B. The PANX1/ATP-mediated mechanism

Fig.1.4 Potential mechanism for HC feedback onto cones in the retina ..……..13

Fig.1.5 Structure and domain organization of glutamate receptors…….....……17

A. Linear view

B. Crystal structure

Fig.1.6 Conformational changes in the functioning AMPA receptors ……. 18

Fig.1.7 AMPA receptors: binding sites and modulators …..……..19

Fig.1.8 NMDA receptors: binding sites and modulators ……20

Fig.1.9 Architecture of inwardly rectifying potassium channels …….. 22

Table 1 Antibodies used in this study ...…….. .28

Fig.3.1 Membrane-Associated Guanylate Kinase (MAGUK) protein in rabbit retina …35

Fig.3.2 Clustered scaffolds are associated with cone photoreceptors ……37

Fig.3.3 Association of SAP102 with synaptic elements in OPL ……...39

Fig.3.4 SAP102 is located in B-type HCs ……...42

Fig.3.5 Association of SAP102 with kainate receptor GluR6/7 ……44

Fig.3.6 Association of SAP102 with Kir2.1 ..……....46

Fig.3.7 Connexins 57 and 59 make gap junctions in OPL ……48

Fig.3.8 In situ proximity ligation assays (PLA) to show SAP102 association with ion channels ……51

Fig.4.1 SAP102 distribution in mouse retina ……60
Fig.4.2A PSD95 immunolabeling in the mouse retina ……61
Fig.4.2B High magnification of PSD95 immunolabeling in the mouse OPL ……61
Fig.4.3 Chapsyn110 distribution in mouse retina ……..62
Fig.4.4 Association of Chapsyn110 with synaptic elements in the OPL ……64
Fig.4.5 Chapsyn110 is located in mouse HCs ……65
Fig.4.6 Higher magnification of Chapsyn in the tips of HC dendrites ……..……66
Fig.4.7 Kir2.1 is located in tips of HCs contacting rod and cone photoreceptors …….. 68
Fig.4.8 High magnification of Kir2.1 in tips of horizontal cells …….. 69
Fig.4.9 Pannexin 1 immunolabeling in the mouse retina ……71
Fig.4.10 Association of Spermine with glial cells in the retina …….. 72
Fig.4.11 Spermine immunolabeling throughout the entire mouse retina …… 73
Fig.4.12 Polyamine immunolabeling varies across photoreceptors and with time of the day ……..……..74
Fig.4.13 Polyamine intensity measurements in the OPL day vs night animals …….. 76
Fig.4.14A Distribution of vesicular polyamine transporter SLC18B1 (solute carrier family 18 member B1) in the mouse retina ……..78
Fig.4.14B High magnification of double labeling with PSD95 and vesicular polyamine transporter SLC18B1in the OPL ……..79

Chapter 1: Introduction

1.1 Lateral inhibition in the outer plexiform layer

More than half a century ago, a significant advancement in understanding signal processing was accomplished with the study of retinal circuits in lower vertebrates. The discovery of photoreceptor pathways in the retina of these species demonstrated that lateral interactions with one another accentuated the edges of objects and enhanced contrast (Hartline and Ratliff, 1957). To extract the useful portions of information and discard the rest, the retina has to use a lot of synaptic mechanism and horizontal cells are the first retinal neuron that provides part of that service. The HC, through its extreme receptive field and extensive coupling to other HC (Kaneko, A, 1971; McMahon et al., 1989), samples a very large area of photoreceptor output and takes average information from that photoreceptor output and subtracts it from each individual photoreceptor. This is what initiates the center surround antagonist field, which allows the contrast information from each local photoreceptor to be sent through bipolar cells and on to subsequent circuitry. At the heart of this process, invaginating bipolar cell dendrites and horizontal cell processes come together in close apposition at photoreceptor terminals (Figure 1.1).

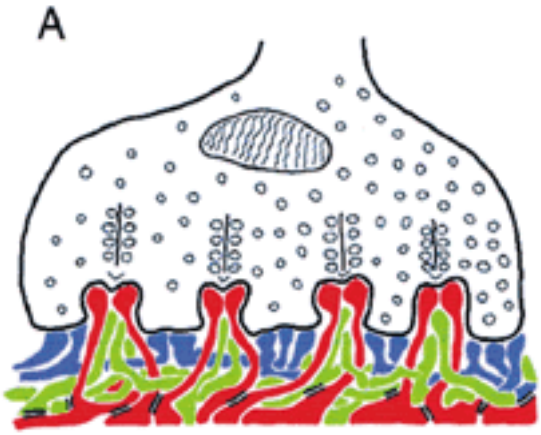

Fig. 1.1. **The synaptic complex of cone pedicles**. **A.** Schematic drawing of the cone pedicle with the dendrites of horizontal (red), ON cone bipolar (green), and OFF cone bipolar (blue) cells. The desmosome-like junctions are indicated by the black double lines. Figure 1.1 was reproduced with permission from Haverkamp S, Grunert U, Wassle H. 2000. The cone pedicle, a complex synapse in the retina. Neuron 27(1):85-95.The Journal of General Physiology 40 (3): 357-376

Beyond cell circuitry trying to understand the subcellular mechanism underlying synaptic signaling at the triad synapse between photoreceptor, HC and bipolar cells (BC) has been a challenge. Synaptic release from photoreceptor terminals is a Ca^{2+} dependent process, which is regulated by the opening and closing of Voltage gated Ca^{2+} channels (VGCC) in the membrane of the cell (Bader et al., 1982; Catterall and Few, 2008). HC serve a very important purpose and they do this by means of feedback (Verweij et al., 1996). The mechanism of HC feedback is unclear but the feedback mechanism of HC applies a certain amount of gain control to

photoreceptor synapses keeping the photoreceptor synapses within the operating range of its own Ca^{2+} channels. The mechanism of HC feedback is almost noiseless and is very fast (Baylor et al., 1971). Feedback can be manifested and observed in a few different ways. The mechanism of feedback causes a leftward shift in the activation curve of the Ca^{2+} current of the photoreceptor (Kamermans and Fahrenfort, 2004; Figure 1.2)

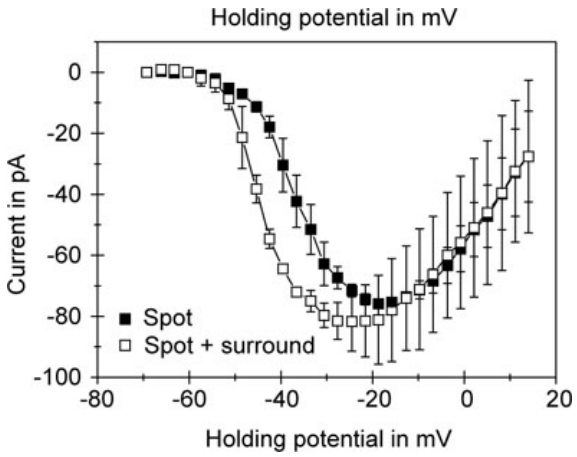

Figure 1.2: Current voltage relationship of an isolated Ca^{2+} current in the cone photoreceptor. The black dot curve is that IV curve in relation to spot illumination just in the center of the cone and the open boxes are that relationship when a surround is also present. The shift in the activation curve of Ca^{2+} current is caused by the HC feedback. Figure 1.2 was reproduced with permission from Kamermans M, Fahrenfort I. 2004. Ephaptic interactions within a chemical synapse: hemichannel-mediated ephaptic inhibition in the retina. Curr Opin Neurobiol 14(5):531-541.

As shown in Fig 1.2, in the presence of surround illumination activation of the Ca^{2+} current is shifted to more negative potentials causing a relative activation of the Ca^{2+} current. Thus, feedback is equivalent of depolarizing the photoreceptor, thereby increasing the amount of neurotransmitter released into the synaptic cleft. All together, these findings suggest that a signal is modulating the voltage dependence and amplitude of the voltage-dependent Ca^{2+} current in the cone photoreceptor and that is contributing to the properties of feedback inhibition. Hypotheses about the mechanism of lateral inhibition between HC and photoreceptors can be summarized in three main models: 1) The release of GABA from HCs onto photoreceptor terminals 2) pH buffering in the synaptic cleft 3) Ephaptic mechanism. I will present evidence for the three mechanisms in the following sections.

1.1.1 GABA

For years, it was thought that changes of voltage in HC were responsible for GABA release, which caused voltage changes in the photoreceptor terminal (Wu SM, 1992; Endeman et al., 2012). The underlying mechanism of HC feedback due to GABA signaling is a topic of long debate. In non-mammalian vertebrates, GABA was found to generate cone responses with whole cell patch clamp techniques, suggesting GABA receptors were present in photoreceptors (Verweij et al., 1996). GABA transporters are present in the plasma membrane, suggesting HCs have a mechanism for taking up GABA from the extracellular space and pump it into the HCs (Kamermans et al., 2002; Paik et al., 2003). GAD, the enzyme that synthesizes GABA, is present in rodents, suggesting a potential for GABA to be there (Guo et al., 2010). HCs can release GABA when depolarized in darkness in non-mammalian

species, which is thought to occur by both a Ca^{2+} dependent mechanism (exocytosis) as well as through a non-vesicular mechanism involving the actions of GABA transporter (Schwartz, 2002). However, knockout of vesicular transporters eliminated feedback, suggesting GABA generates a feedback signal to inhibit photoreceptors (Hirano et al., 2016).

In mammalian retina, up to more recently there has not been really good evidence for a release mechanism because it seems they lack the transporter (Johnson 1996). More recently, a number of the SNARE proteins that would be required for exocytosis have been identified (Sherry et al., 2006; Brecha and Lee, 2010). They are up in the tips of HC dendrites where they invaginate into the photoreceptors, suggesting the machinery for GABA release is present. It is unclear, however, whether GABA is acting directly on the cone or rod photoreceptor as a feedback mechanism. In non-mammalian vertebrates the evidence suggests that could happen, particularly in turtles (Tatsukawa, 2005), but the mammalian evidence is very inconsistent from the physiological and immunocytochemistry point of view. It's been suggested that may depend on the state of the retina at the time of the experiments (Yang and Wu, 1989).

Other results argue GABA may not be the sole protagonist in the generation of feedback. The amount of GABA receptors found in the cleft near the HC to cone contact sites was minimal (Yazulla, 1997). If GABA mediates feedback then GABA antagonist should eliminate the effect but GABA blockers failed to block feedback (Thoreson W and Burkhardt D, 1990; Verweij et al., 1996). Furthermore, GABA blockers failed to eliminate the center surround field measured in ganglion cells

(GCs; McMahon et al., 2004), suggesting changes of the voltage in the photoreceptors could not account for the shift of VGCC. GABA-gated Cl^- channels reduced the size of feedback responses in both HC and cones (Kammermans et al., 2012). More recently, it has been demonstrated that GABA autoreceptors are activated on the plasma membrane of HC resulting in high conductance for bicarbonate suggesting GABA regulates pH buffering in the synaptic cleft (Liu et al., 2013).

1.1.2. Proton-mediated lateral inhibition

A competing hypothesis is a completely different mechanism in which the synaptic cleft is acidified by protons from unknown source and causing inhibition of Voltage-gated Ca^{2+} channels (VGCC) and that the concentration of protons is reduced when HCs hyperpolarize through some mechanism (Barnes et al., 1993; Fahrenfort et al., 2005). As you decrease the pH in the synaptic cleft the activation of Ca^{2+} current is shifted to the right and the amplitude is reduced (Barnes and Bui, 1991). These protons inhibit the calcium current by either plugging the channel pore or affecting the electrical field seen by the channel voltage sensor by (Iijima et al., 1986; Krafte and Kass, 1988).

Recently, one study indicates that Na^+-H^+ exchanger in the membrane of HCs is the principal source of protons that mediate lateral inhibition with photoreceptors (Warren et al., 2016). Probably other types of channels are going to be affected by changes in pH to some extent, suggesting variations in proton flux may cause changes in pH locally at that synapse. Thus, changes in proton concentration can

modulate the gating of VGCC and how much Ca^{2+} comes in and is released (Hirasawa and Kaneko, 2003). Together these findings suggest protons are directly inhibiting the Ca^{2+} channel causing a shift of the activation curve. To determine whether pH was responsible for changes in HC voltage HEPES was used as buffer (Hirasawa and Kaneko, 2003; Fahrenfort, 2009). High levels of HEPES in solution did not cause modulation of VGCC (Thoreson et al., 2008). However, application of non-aminosulfonate buffers also eliminates feedback, suggesting that the block of feedback is due to the buffering not to HEPES block of hemichannels (Trenholm and Baldridge, 2010; Vessey et al., 2005).

With the discovery of pH indicators it is now possible to measure the effects of protons at specific synaptic sites within the cleft. A missing link in neuroscience is to image whether changes in proton concentrations mediate lateral inhibition. Addressing this question is very difficult in an intact retina because the synaptic cleft is minuscule compared to everything else and the concentration of protons is miniscule (10^{-7}M). To get around this problem a genetically coded pH sensitive GFP variant (pHluorin) attached to α2 δ4 subunit of the L-type channel was engineered to be expressed exclusively in cone photoreceptor terminals (Wang et al., 2014). In the presence of light, HCs are hyperpolarized causing alkalinization in the cleft, consistent with a proton-mediated feedback signal.

One possible underlying mechanism that controls feedback between HC and photoreceptors is ATP release via Pannexin 1 channels in HC tips contacting photoreceptors (Vroman et al., 2014). This report suggests that there is an entire ATP degradation apparatus in the extracellular space, which would take ATP that is

released by Pannexin channels and degrade it to produce phosphate and protons, which may inhibit Ca^{2+} channels. The idea is that hydrolysis is going to release a couple of protons and phosphate into the synaptic cleft to create a phosphate buffer of PKa=7.2. When cells hyperpolarize hyperpolarization, ATP release is diminished, the protons diffuse away and the cleft alkalinizes resulting in increase of Ca^{2+} current. This mechanism underlies the slow component of feedback. (Figure 1.3B)

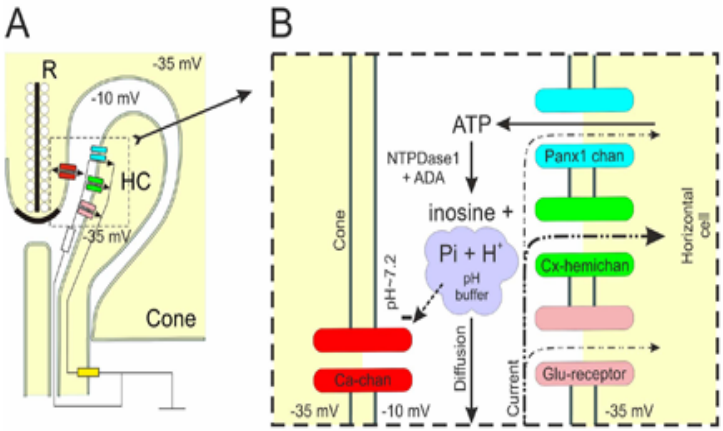

Figure 1.3: Proposed mechanisms of horizontal cell feedback. A. The ephaptic mechanism. Cone photoreceptors release glutamate in the dark via Ca^{2+} dependent mechanism through Ca^{2+} channels (red) at the presynaptic ribbon (R) synapse. Lateral elements formed by HC dendrites end at the cone synaptic ribbon. Cx hemichannels (green) and Panx1 channels (blue) are expressed on the dendrites of HCs. When HC hyperpolarize, a current will flow through the extracellular resistance (white resistor) into the HC dendrites, which invaginate the cone synaptic terminal. The current that flows into HCs via the Cx hemichannels and Panx1 channels has to pass this resistor, which will induce a slight negativity deep in the synaptic cleft. The result will be that the voltage-gated Ca^{2+} channels sense a slightly depolarized

membrane potential. When HCs hyperpolarize, the current through the Cx hemichannels will increase and so will the negativity in the synaptic cleft leading to a further decrease of the potential sensed by the cone Ca^{2+} channels. This is the fast component of feedback. **B. The Panx1/ATP-mediated mechanism**. Expanded view of the pre- and postsynaptic membranes of cones and HCs. ATP is released by HCs via Panx1 channels. Through a number of steps ATP is converted into inosine, protons, and a phosphate buffer with a pKa of 7.2. This makes the synaptic cleft acidic relative to the extrasynaptic medium (pH 7.4), which inhibits Ca^{2+} channels and shifts their activation potential to positive potentials. Hyperpolarization of HCs will eventually reduce conductance of Pannexin 1 channels which prevents HCs from releasing ATP, thereby stopping the production of phosphate buffer leading to alkalization of the synaptic cleft. This alkalization disinhibits the Ca^{2+} channels and shifts their activation potential to negative potentials. Figure 1.3 was reproduced with permission from Vroman R. Klaassen LJ, Howlett MH, Cenedese V, Klooster J, Sjoerdsma T, Kamermans M Extracellular ATP Hydrolysis Inhibits Synaptic Transmission by Increasing pH Buffering in the Synaptic Cleft. PLoS Biol. 2014 May; 12(5):e1001864.

There is no evidence of ATP being released via vesicular mechanisms in HC but it is possible. In fact, ATP could be vesicular because almost every vesicle contains ATP (Forgac et al., 1983). This would suggest ATP is released day and night. Recently, ATP release was measured from isolated HC when stimulated with AMPA resulting in an increase in the amount of luminescence signal (Vroman et al., 2014). When medium was treated with probenecid, an inhibitor of Pannexin

channels, the amount of ATP was decreased relative to the baseline, suggesting some ATP is released at rest coming out of these HCs that is dependent on Pannexin channels. Consequently, stimulating HC by depolarization would trigger release of more ATP and probenecid block the effect. Since Pannexin are only found in the tips of HC (Kranz et al., 2012) it is possible that during dissociation of HC cells many pannexins were lost in the process. The possibility that ATP may act on purine or adenosine receptors was investigated with selective blockers but they had no effect on feedback, suggesting that feedback is not mediated by adenosine or purine receptors (Vroman et al., 2014)

In the dark, the effects of adenosine receptors are associated with inhibition of voltage gated channels and reduction of calcium conductance in cone photoreceptor terminals in tiger salamander (Stella et al., 2007). More recently, evidence of adenosine receptors was found in zebra fish and mouse retina (Li et al., 2013 and 2014). The presence of adenosine receptors suggests modulation of currents via PKA mechanism. These receptors are not going to operate on a short time scale but rather in a quasi-steady state condition. There is going to be a change in the average activation of currents that can be regulated by adenosine receptors. We cannot rule out the effects of additional buffering systems in the regulation of pH in the synaptic cleft. An attractive alternative to the GABA model for feedback has emerged implicating the passage of bicarbonate ions through $GABA_A$ receptors in horizontal cells (Liu et al., 2013). In this model, activation of voltage-gated Ca^{2+} channels in HCs increases GABA release, which increases chloride and bicarbonate permeability through GABA receptor channels. Thus, the acidification of the synaptic

cleft would cause inhibition of L-type Ca^{2+} channels in the photoreceptor (Liu et al., 2013).

1.1.3. Ephaptic signal

The original premise for the ephaptic hypothesis was based on a theoretical model to describe the HC effects on photoreceptor terminals. These were purely non experimental and proposed feedback was a positive effect. In this scenario there is no messenger that is mediating communication between HC and cone terminals; rather, it is an electrical effect. HCs send an inhibitory signal to cone photoreceptors that alters their calcium channel conductance without affecting their voltage (Byzov and Shura-Bura, 1986). It was postulated an ephaptic signal was responsible, meaning communication signals at the triad are mediated by local changes of electrical fields. Figure 1.4 shows this potential mechanism for HC feedback onto cones in the retina. In this circuit, the membrane potential of the cone controls the release of glutamate. When the cone is depolarized glutamate is released and activates glutamate receptors on the tips of HC dendrites. Because the synaptic cleft has finite resistance the current flowing through this space causes a voltage drop between the interior of the invaginating synapse and the surrounding extracellular space. Thus, the change in voltage generates a relative depolarization in the cone membrane resulting in Ca channels opening up and release of NT. The size of the synaptic cleft is consistent with how much resistance is needed to produce a voltage drop (Dowling, 2012). In the presence of illumination glutamate receptors are closed which leads to less current flowing through the synaptic cleft and hyperpolarization of Ca^{2+} channels. It is unclear, however, how ephaptic signals are generated. Little

information is available on how much resistance is produced by extracellular matrix and other factors (Anastassiou & Koch, 2015). According to Byzov's model, when glutamate is released, current flows into channels in HC tips and through the cleft, causing a voltage drop. If current flowing into HC tips slows down so does the cleft current. Thus, there would be either less voltage drop or none at all.

There have been several hypothesis for ephaptic feedback. Among these competing mechanisms, the hemichannel-mediated ephaptic mechanism has drawn a lot of attention because of the requirement for connexin channel expression by HCs at photoreceptor terminals. The work of Iris Fahrenfort during her PhD thesis proposed ephaptic feedback signal could be generated by the presence of a channel that stays open all the time. Thus, in the presence of illumination, HC hyperpolarization would result in an increase in the current through the synaptic cleft. Presumably this channel would allow more flow and then suddenly whether you are in the center or the surround, an ephaptic signal be generated that could antagonize the hyperpolarization of the cone (Kamermans et al., 2001). This observation was further supported with the use of carbenoxolone, a hemichannel blocker, which was found to reduce feedback (Kamermans et al., 2001). However, the use of carbenoxolone, a non-specific gap junctional blocker, resulted in the inhibition of L-type Ca^{2+} channels in cones (Vessey et al., 2004). For the ephaptic hypothesis, it is not straightforward case due to lack of specific hemichannel blockers. In sum, when Ca^{2+} channels are opened, transmitter is being released; glutamate receptor channels are activated and current flows in (Fig 1.4A). That current flow will cause a relative depolarization of the pre-synaptic membrane and

increase the transmitter release. That is positive feedback in its steady state. If light shines in the surround but not on the cone, the horizontal cell is hyperpolarized and glutamate is released causing an increase in current flow into the HC due to larger driving force, which drives cations into those glutamate receptor channels (Fig 1.4B).

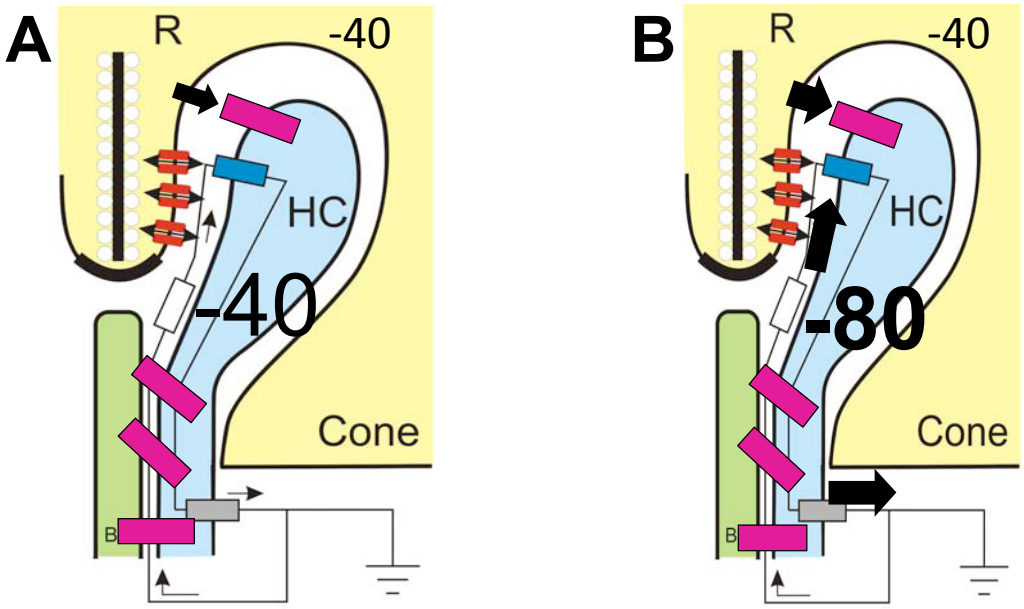

Figure 1.4: Potential mechanism for HC feedback onto cones in the retina. When light is in the center of the cone glutamate receptors close and the feedback goes away (Fig 1.4A). Under surround illumination conditions negative feedback is increased fighting against the cone's hyperpolarizing response (Fig 1.4B). When the HC hyperpolarizes, the opened channels cause an increase in current flow through the extracellular space and that increases the voltage differences within the synapse and causes a relative depolarization of the pre-synaptic membrane causing Ca^{2+} channels to open up a little bit again. So the communication causes a change in how active these channels are and how much NT is released. That would be a form of feedback. Figure 1.4 was reproduced with permission from Fahrenfort I, Steijaert M,

Sjoerdsma T, Vickers E, Ripps H, van Asselt J, Endeman D, Klooster J, Numan R, ten Eikelder H, von Gersdorff H, Kamermans M. 2009. Hemichannel-mediated and pH-based feedback from horizontal cells to cones in the vertebrate retina. PLoS One 4(6):e6090.

1.1.4. Summary

For the last fifty years a plethora of evidence has emerged to decipher whether the signal that drives HC feedback to cone photoreceptors is either chemical or electrical. When it comes to GABA the jury is out. There is very little support for the release of GABA from HCs into the cleft and the amount of receptors present in cone terminals is found to be sparse. But perhaps the most conclusive evidence is the failure of GABA receptor antagonists to block feedback suggesting GABA does not play a role. The premise of the ephaptic hypothesis is that voltage changes in the HCs lead to an apparent change in voltage in cones but is hard to imagine such mechanism without taking into account changes of pH or the release of chemical signals. There is no direct evidence for the existence of hemichannels in the tips of HCs and to make matters worse specific hemichannel blockers are unavailable. However, the specific expression of encoded fluorescent voltage indicators in cone terminals could shed some light in the measurement of local voltage changes. The proton-mediated hypothesis is a competing hypothesis with a completely different mechanism in which the synaptic cleft is acidified by protons and causing inhibition of the Ca^{2+} channel when HC is depolarized and the concentration of protons is reduced when HCs hyperpolarize. Although there is a lot of support for this mechanism, it is unknown whether the source of protons is due to

a release mechanism or changes in the concentration of bicarbonate and phosphate in the synaptic cleft. It is possible, however, that a combination of effects including GABA, protons and ephaptic feedback contribute together to mediate HC feedback

1.2 Synaptic Scaffolds

For these mechanisms to work is critically important that all of the elements that are doing the feedback are localized right inside that synapse. Photoreceptors have a unique deeply invaginated synapse which appears to be structurally design to allow this kind of signal to take place. All photoreceptor synapses throughout the vertebrate world have this deeply invaginated synapse that appears to be necessary for this type of synaptic signaling. These elements have to be in that place for feedback to work, so we propose examining synaptic scaffolds because they are responsible for assembling those components and anchor them in place.

Precise physical localization of synaptic proteins is essential for effective synaptic transmission and for control of the signaling pathways that impose plasticity. At most synapses, large suites of proteins form complex networks, which play an important role in synaptic plasticity. The following work will focus on synaptic scaffolds that may influence synaptic events in horizontal cells. Membrane-associated guanylate kinase (MAGUK) proteins are responsible for anchoring many of the necessary components that regulate synaptic transmission in opposing membranes (Oliva et al., 2012; Chen et al., 2015). It is well known that excitatory synapses are rich in MAGUKs, including postsynaptic density protein 95 (PSD95), PSD93 (Chapsyn-110), synapse-associated protein 102 (SAP102) and SAP97

(Koulen et al., 1998). These synaptic scaffolding proteins share homologous PDZ, SH3, and guanylate kinase domains, which mediate protein-protein interactions to form multi-protein complexes. The complexes of synaptic scaffolds often include a variety of transmitter receptors, ion channels, protein kinases, phosphatases, and AKAPs (Zheng et al., 2011). Synaptic scaffolds play an important role in assembling signaling pathways to specific parts of the cell. We have identified a few ion channels likely to be involved in horizontal cell synaptic signaling, which will be described in more detail below.

1.2.1 Glutamate receptors

The most prominent proteins anchored by synaptic scaffolds in excitatory synapses are the glutamate receptors. AMPA and Kainate receptors are ligand-gated channels, which share similar structures and have fast activating largely Na^{2+} or cation conductances. Their different subunit types have some different properties and there are spliced variants of some of these genes so there is quite a bit of diversity in each of them. The GluRs form multimers and they can form heteromeric multimers so there is a lot of diversity among these different types of glutamate receptors. The ionotropic receptors are generally grouped into what is called non-NMDA type, which include the GluA AMPA receptors and GluK Kainate receptors and the NMDA type, the GluN type receptors. The GluA type receptors typically have fast activation kinetics and inactivate or desensitize fairly quickly; GluKs have slower inactivation kinetics but they have a more profound desensitization. The GluNs, on the other hand, have somewhat slower activation and much slower deactivation kinetics and so, even though they have typically the similar peak

amplitude of current, the NMDA type receptors will often stay open for much longer period of time (Lüscher and Malenka, 2012). These are largely conserved in vertebrates (Glanzman, 2010).

The ionotropic GluRs have a structure similar to Figure 1.5A**:** they have a ligand binding domain (LBD) extracellular and N-terminal domain (ATD). They form a tetramer in their final form. They typically form dimers of monomers and then dimers of dimers. The key point is that these channels can form heterotetramers with different isoforms as seen in Figure 1.5B. However, there is no evidence of GluK receptors making heterotetramers with GluA receptors.

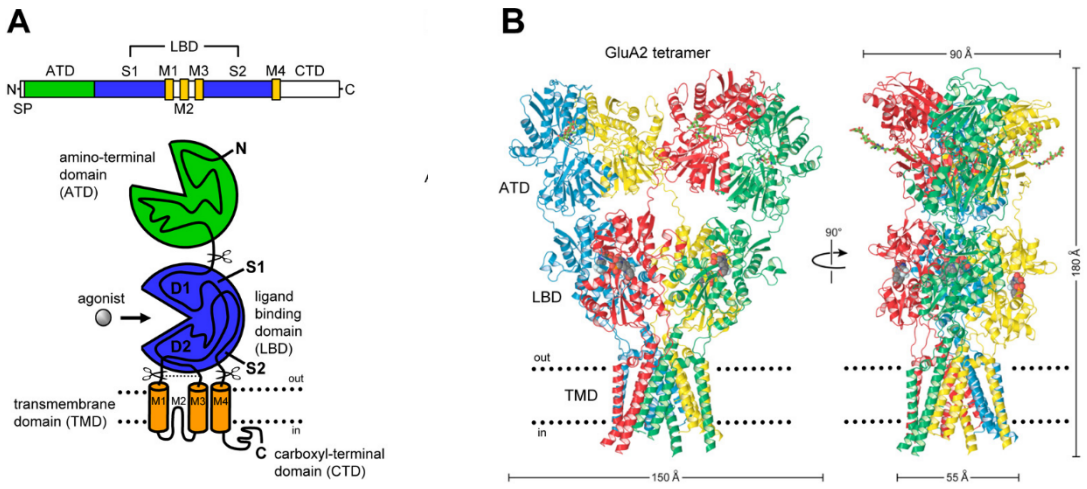

Figure 1.5: Structure and domain organization of glutamate receptors: **A.** Linear representation of the subunit polypeptide chain and schematic illustration of the subunit topology. LBD: ligand binding domain in blue; ATD: amino terminal domain in green. **B.** Crystal structure at 3.6 Å of the GluA2 AMPA receptor. (Figure 1.5 Structure and domain organization of glutamate receptors was reproduced with permission from Traynelis SF, Wollmuth LP, McBain CJ, Menniti FS, Vance KM,

Ogden KK, Hansen KB, Yuan H, Myers SJ, Dingledine R. 2010. Glutamate receptor ion channels:structure, regulation, and function.62(3): 405-96

There is a ligand binding cleft on each of the subunits, and when at least 2 of those are bound to glutamate AMPA and Kainate type receptors will open and the current increase up to 4 of them bound. This current will open transiently and will start to desensitize. The opening involves a conformational change that opens that channel pore and desensitization involves a second relaxation conformation that brings some of the transmembrane domains (TM) domains back together to close the channel pore (Figure 1.6).

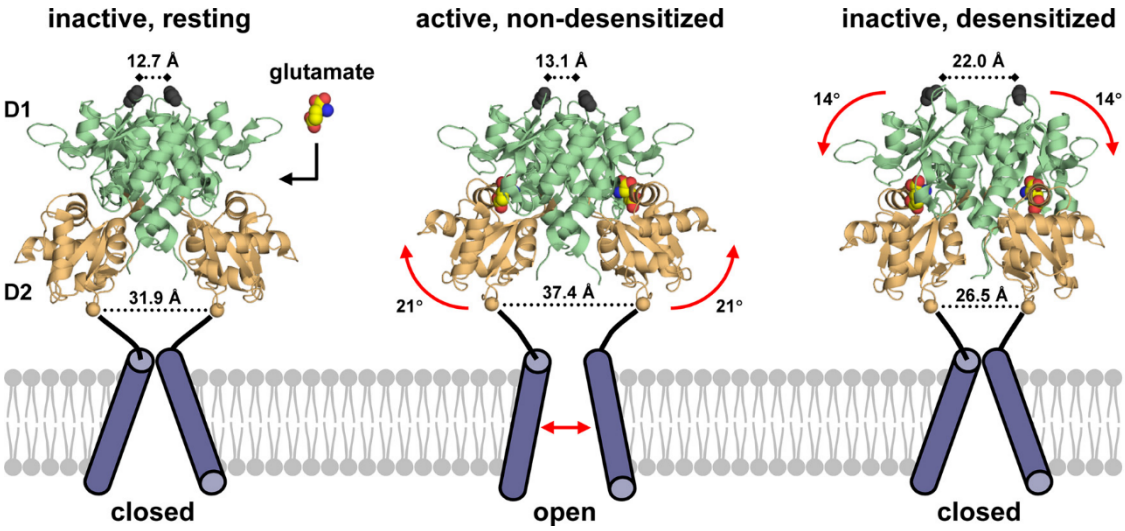

Figure 1.6: Conformational changes in the functioning AMPA receptor: ribbon diagrams of the crystal structures of the GluA2 ligand binding dimer in conformations that correspond to the resting state, active state (glutamate-bound), and desensitized state (glutamate-bound). D1 and D2 correspond to the two lobes of extracellular ligand binding domains seen in Fig 1.5A in blue. Figure 1.6 Conformational changes in the functioning AMPA receptor was reproduced with

permission from Traynelis SF, Wollmuth LP, McBain CJ, Menniti FS, Vance KM, Ogden KK, Hansen KB, Yuan H, Myers SJ, Dingledine R. 2010. Glutamate receptor ion channels: structure, regulation, and function.62(3): 405-96

In the AMPA and kainate type receptors, all 4 of those ligand binding sites bind glutamate. The AMPA and Kainate type receptors can be modulated by a variety of things but they are relatively simple in this activation and desensitization type of behavior (Figure 1.7).

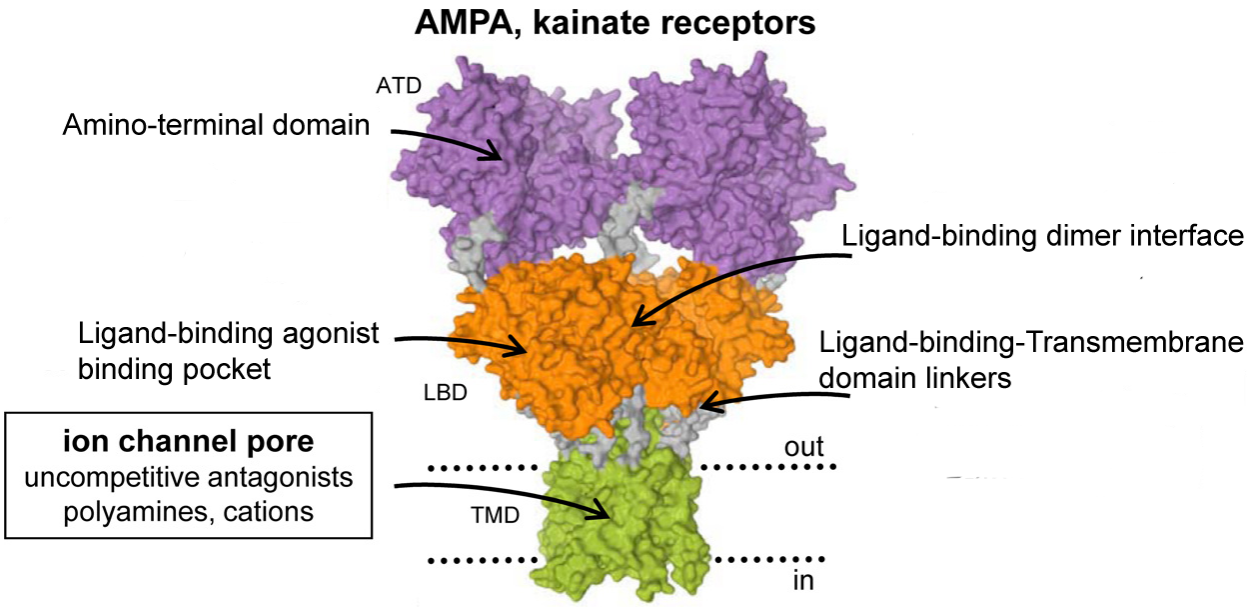

Figure 1.7: Binding sites for the agonists, and modulators are shown for the glutamate receptor AMPA. AMPA and kainate indicates that the ligand selectively targets GluA or GluK receptor subunits, respectively. Note polyamine target in the ion channel pore. Figure 1.7 Binding sites for the agonists, and modulators are shown for the glutamate receptor was reproduced with permission from Traynelis SF, Wollmuth LP, McBain CJ, Menniti FS, Vance KM, Ogden KK, Hansen KB, Yuan

H, Myers SJ, Dingledine R. 2010. Glutamate receptor ion channels:structure, regulation, and function.62(3): 405-96.

NMDA receptors are different. They are formed by a set of 5 genes, 1 GluN1 and 4 GluN2 subtypes (A-D). NMDA receptors obligatorily require the assembly of 2 GluN1 subunits and 2 GluN2 subunits. The GluN2 subunits bind glutamate the same way the other glutamate receptors do but the GluN1 subunits do not. Instead, GluN1 binds co-agonist glycine, but more recently has also been shown that amino acid D-serine also binds to GluN1 with higher affinity than glycine (Miller, 2004). The mechanism of NMDA receptor opening requires binding both agonist and co-agonist and further NMDA receptor have a Mg^{2+} binding site in the middle of the pore. When Mg^{2+} is bound that blocks channel function. In order to remove Mg^{2+} the cell has to be depolarized. So NMDA receptors are considered to be coincidence detectors because they require the presence of glutamate, co-agonist and depolarization of cell to unbind Mg^{2+} (Figure 1.8).

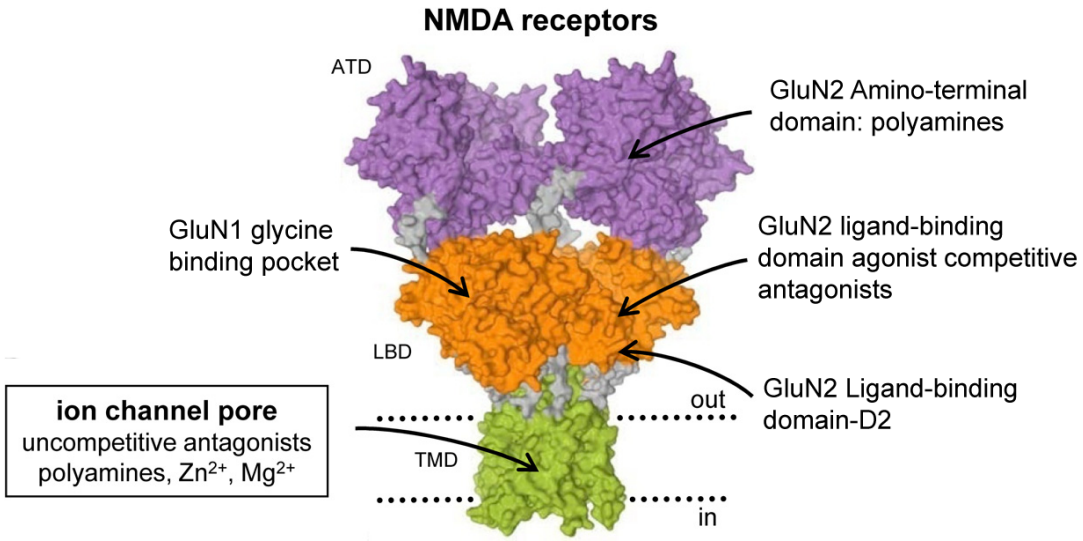

Figure 1.8: Binding sites for the agonists, and modulators are shown for the glutamate receptor NMDA. Note polyamine targets in the amino terminal domain and ion channel pore. Figure 1.8 Binding sites for the agonists, and modulators are shown for the glutamate receptor was reproduced with permission from Traynelis SF, Wollmuth LP, McBain CJ, Menniti FS, Vance KM, Ogden KK, Hansen KB, Yuan H, Myers SJ, Dingledine R. 2010. Glutamate receptor ion channels:structure, regulation, and function.62(3): 405-96

Ionotropic glutamate receptors play an important role in vision. It is well known that both kainate and AMPA receptors subunits are expressed by horizontal cells in the retina (Shen et al., 2004). Furthermore, AMPA subunits are localized in the base of HC tips contacting photoreceptors (Pan et al., 2007).

1.2.2 Potassium channels

In Chapter 3, I will show that I discovered inward rectifying potassium (KiR) channel 2.1 in horizontal cell complexes. Therefore I will provide more background on the KiR channels. KiR channels are tetramers that form multiple combinations resulting in functional channels. The ion channel pore can be regulated by H^+, Na^+, Mg^{2+} and lacks the S4 voltage sensor region, suggesting that KiR channels are insensitive to membrane voltage (Figure 1.9). The inward rectification is caused by the blockage of outward current due to polyamines and internal Mg^{2+} (Xie et al., 2003; Vilin et al., 2013).. In the retina, KiR channel conductance is shown to accelerate the onset rate of the hyperpolarizing light response of HCs (Dong and Werblin, 1995). Therefore, KiR channels generate a large K^+ conductance at hyperpolarized conditions but allow less current flow at depolarized potentials. This

conductance may serve to enhance the temporal resolution of the HC and there may exist a voltage-dependent mechanism in HCs that can accelerate the onset of the hyperpolarizing light response.

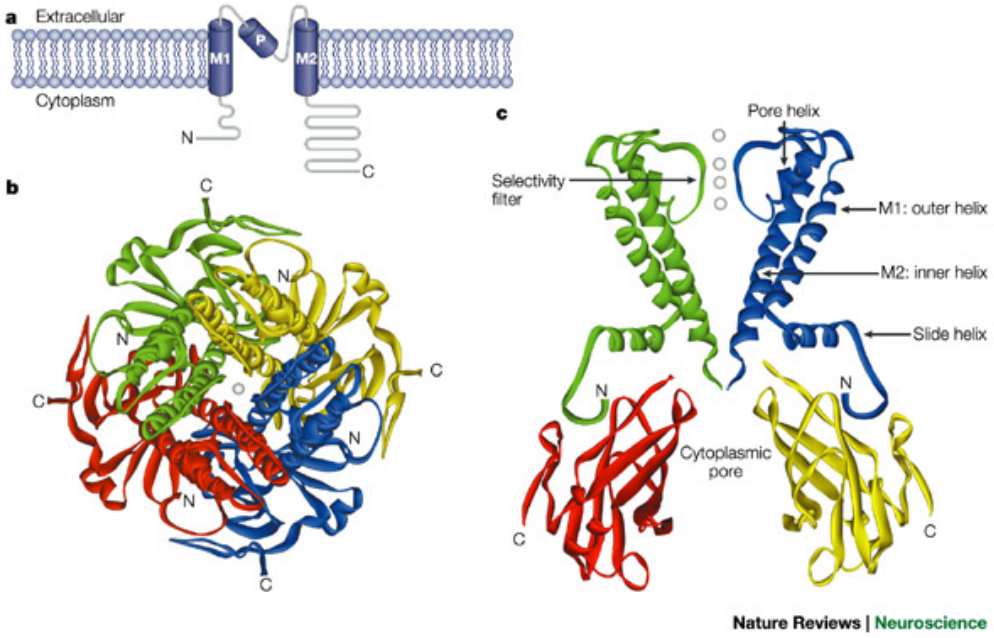

Figure 1.9: Architecture of inwardly rectifying Potassium (KiR) channels: A. Schematic Each subunit comprises two transmembrane helices (M1 and M2), a pore-forming region containing the pore-helix (P), and a cytoplasmic domain formed by the amino (N) and carboxy (C) termini. **B.** View of the tetrameric structure of the KirBac1.1 channel[4] (PDB ID: 1P7B) from the extracellular side. Monomers are individually coloured red, green, yellow and blue. A K^+ ion (white) indicates the conduction pathway. **C.** Side view of the KirBac1.1 structure showing the transmembrane domain of two subunits (green and blue) and the C-terminal domains of their neighbouring subunits (red and yellow). White spheres represent K^+ ions in the selectivity filter. Figure 1.9 Overall architecture of inwardly rectifying

Potassium (KiR) channels was reproduced with permission from Bichet D, Haass F, Jan L. 2003. Merging functional studies with structures of inward-rectifer K channels. Nature Reviews Neuroscience 4:957-967.

Chapter 2. Methodology

2.1 Tissue preparation

Retinas from New Zealand White rabbits ranging between 3-5 kg of weight and young adult mice C57BL/6 (no. 000664; The Jackson Laboratories) were used in this study. Rabbits were anesthetized with a mixture of ketamine/xylazine (40/5 mg/kg) by IM injection and euthanized with an overdose of sodium pentobarbital (100 mg/kg) whereas cervical dislocation was used for mice following protocols approved by the Institutional Animal Care and Use Committee and conforming to National Institutes of Health (NIH) guidelines. The eyes were enucleated and the anterior segment removed along the ora serrata, followed by removal of vitreous humor. The resulting retina-sclera preparation was cut into 4 to 5 sections and the tissue pieces maintained in carboxygenated Ames' medium (Sigma-Aldrich, St. Louis, MO) at ambient temperature. For light microscopy, tissue pieces were immersion fixed in either 4% (w/v) paraformaldehyde (PFA) or 4% N-(3-dimethylaminopropyl)-N′-ethylcarbodiimide hydrochloride (EDAC; Sigma-Aldrich) in 0.1M phosphate buffer (PB; pH 7.4). We found 20 minutes in 4% EDAC fixation was the best condition to visualize synaptic proteins in rabbit.

To visualize spermine immunolabeling in mouse photoreceptor terminals the best condition was 4% PFA fixation for 45 minutes. Retinal pieces were cryoprotected in 30% sucrose in PB overnight at 4°C, sectioned vertically at 12μm on a cryostat and collected on slides. For whole mount preparations, retinas were isolated from eyecup, flattened on a black nitrocellulose filter paper (Millipore, Billerica, MA) and fixed in either 4% EDAC or 4%PFA for 1 hour to preserve tissue integrity. Two to 4 month-old adult mice of either sex were used. Animals kept in a reverse light cycle were used to simplify collection of night time tissue. Mice were housed in a 12 h light/dark cycle (lights on at 7:00 A.M.) for at least 2 weeks before an experiment. Based on previous work (Jin et al., 2016), mice were sacrificed under infrared illumination with the assistance of infrared night vision goggles or under room lights during the day.

2.2 Injection of Neurobiotin and Alexa 568

Retinas from rabbits were isolated from the eyecup while immersed in carboxygenated (95% O_2 + 5% CO_2) Ames medium (US Biological, Swampscott, MA) and mounted on 0.8μm black filter paper (Millipore, Bedford, MA). Retinal cells were prelabeled with 5μM 4,6-diamino-2-phenylindole (DAPI) (Invitrogen, Carlsbad, CA) in Ames medium for 15 minutes. Retinal pieces prelabeled with DAPI were visualized on an Olympus BX-50WI microscope (Tokyo, Japan) equipped with epifluorescence. Targeted horizontal cells were impaled under visual control with 150-200 MΩ glass electrodes (Warner Instruments, Hamden, CT) pulled on a

horizontal electrode puller (Sutter Instruments, Novato, CA). Electrodes tips were filled with 4% Neurobiotin (Vector Laboratories, Burlingame, CA) and 0.5% Lucifer Yellow-NH_4 (Molecular Probes, Eugene, OR) in 0.05M PB, then backfilled with 3M LiCl. Electrodes tip-filled with Alexa 568 (Molecular Probes; A10437) were back-filled with 3M KCl. Impaled cells were injected with a biphasic current (±2.0 nA, 3Hz) for 4-5 mins. Following the last injection, retinal pieces were fixed in 4% PFA for 30 minutes prior to further immunohistochemical processing. For single cell injections, 50μM meclofenamic acid was perfused over the retina for 15 min prior to Neurobiotin injection.

2.3 Immunolabeling

Retinal sections were labeled with antiserum in tissue treated with 0.3% Triton X-100 (Sigma-Aldrich) and incubated overnight with 3% Donkey Serum in Dulbecco's Phosphate Buffered Saline (PBSA) at room temperature (RT) to block non-specific immunolabeling. For flat mount preparations, retinal pieces were incubated for a minimum of 5 days in a rotator at 4°C. Antibodies used included mouse IgG_1 anti-SAP-102 clone N19/2 (1:500; UC Davis/NIH NeuroMab Facility, Davis, CA), mouse IgG_1 anti-SAP-97 clone K64/15 (1:500, UC Davis/NIH NeuroMab Facility, Davis, CA), mouse IgG_1 anti-Chapsyn-110 clone N18/30 (1:500; UC Davis/NIH NeuroMab Facility, Davis, CA) and mouse IgG_{2a} anti-PSD-95 clone K28/43 (1:500; UC Davis/NIH NeuroMab Facility, Davis, CA). The tissue was rinsed in PBSA extensively and double- or triple-labeled with either goat IgG anti-GluR5 C-

18 (1:500, Santa Cruz Biotechnology, Santa Cruz, CA) or rabbit antibodies including anti-mGluR6, against the C-terminal peptide (KATSTVAAPPKGEDAEAHK) of human metabotropic glutamate receptor 6 (1:500; gift of Dr. Noga Vardi; {Vardi, 2000 #2823}), anti-GluR6/7 clone NL9 (1:500, Millipore), and anti-KiR2.1 (1:200, Millipore). To visualize polyamines antibodies used included rabbit anti-Spermine polyclonal (1:500; Novus, Littleton CO) and rabbit anti-Spermine (1:500, Abcam.Cambridge, MA). Both antibodies recognize polyamine species including spermine, spermidine and putrescine and their immunoreactivity was identical. Additional information about the antibodies is given on table 1 below. Most secondary antibodies were raised in donkeys and affinity purified. These included Alexa Fluor 488 and/or Cy3 anti-goat IgG (1:1,000; Jackson Immunoresearch, West Grove, PA), Alexa 488 and/or Cy3 anti-rabbit IgG (1:500; Molecular Probes, Eugene, OR) and Dyelight 647 anti-mouse IgG (1:500; Jackson Immunoresearch). Additionally, anti-mouse IgG subtype specific secondary antibodies raised in goats were used at times to double label with two mouse monoclonals. These included Alexa 488 anti-mouse IgG_1 and Cy3 anti-mouse IgG_{2a} (1:500; Jackson Immunoresearch). Sections were incubated in secondary antibodies for 1 hour at room temperature, and pieces of retina were left in secondary antibody for 1 day at $4^{o}C$. Tissue was coverslipped in Vectashield mounting medium (Vector Laboratories, Burlingame, CA) with DAPI.

Several additional antibodies were used as markers for specific cell types or for synaptic structures. Affinity-purified anti-syntaxin 3 specific antibody generated in rabbits against a peptide from the N-terminus of mouse syntaxin 3

KDRLEQLKAKQLTQDDC (1:100; gift of Dr. Roger Janz); anti-ribeye, U2656, raised in rabbits against a purified glutathione S-transferase (GST) fusion protein containing the entire B domain of rat ribeye (1:500; gift of Dr. Thomas Südhof; Schmitz et al., 2000); anti-Cx57 raised in rabbits against a mouse Cx57 C-terminal peptide, aa434-446 (1:100; Invitrogen); anti-Cx59, raised in rabbits against a C-terminal peptide of the human Cx59, aa486-501 (1:100; gift of Dr. Steve Massey); anti-Pannexin 2 raised in rabbits against a peptide corresponding to the C-terminus of mouse Panx2 (1:200; TermoFisher, Waltham, MA).

TABLE 1
Antibodies Used in This Study

Antibody	Host	Antigen	Source	Catalog No.	Dilution	References
SAP102	Ms	Fusion protein of rat SAP102 (aa1-120)	UC Davis/NIH Neuromab Facility, UC Davis, California	75-058	1:500	Haverkamp et al., 2000
PSD95	Rb	Synthetic peptide of mouse PSD95 (aa50-150)	Abcam Cambridge, MA	ab18258	1:1000	Preissmann D et al., 2012
PSD95	Ms	Fusion protein of human PSD95 (aa77-299)	UC Davis/NIH Neuromab Facility, UC Davis, California	75-028	1:500	Puthussery et al., 2014
SAP97	Ms	Fusion protein of rat SAP197 (aa1-104)	UC Davis/NIH Neuromab Facility, UC Davis, California	75-030	1:500	Koulen et al., 1999
Chapsyn110	Ms	Fusion protein of rat Chapsyn 110 (aa1-852)	UC Davis/NIH Neuromab Facility, UC Davis, California	75-057	1:500	Ogawa et al., 2008
Ribeye	Rb	U2656 against B domain of rat	Dr. Thomas Südhof; Stanford University School of Medicine, CA	N/A	1:1000	Schmitz et al., 2000
Syntaxin 3	Rb	Residues 2-264 of the mouse syntaxin 3B fused to glutathione S-transferase	Dr. Roger Janz; University of Texas Medical School, Houston	N/A	1:500	Sherry et , al., 2006
mGluR6	Rb	C-terminus of human mGluR6 (aa 8-413) coupled to KLH	Dr. Noga Vardi; University of Pennsylvania, Philadelphia, Pennsylvania	N/A	1:500	Vardi et al.,2000
GluR6/7	Rb	Rat GluR6 (aa894-908) coupled to keyhole limpet hemocyanin (KLH)	Millipore Corporation, Temecula, California	04-921	1:200	Darstein et al., 2003
GluR5	Gt	Purified peptide C-terminus of human GluR-5 (aa 900-918) and N-terminus (aa 1-20).	Santa Cruz Biotechnology Dallas, Texas	7616	1:500	Pan et al., 2007
Kir2.1	Rb	Purified peptide from human Kir2.1 (aa392-410)	Millipore Corporation Temecula, California	AB5374	1:400	Giovannardi et al., 2002
Cx57	Rb	Mouse Cx57 (aa 434-446)	Invitrogen (Zymed) Camarillo, CA	40-4800	1:100	Ciolofan et al., 2007
Cx59	Rb	Synthetic peptide derived from C-terminal of human Cx59 (aa486-501)	Dr. Stephen Massey University of Texas Medical School, Houston	N/A	1:100	N/A
Pannexin1	Rb	GST-tagged recombinant human Pannexin-1/PANX1 C-terminal fragment.	Millipore Corporation Temecula, California	ABN242	1:250	N/A
Pannexin 2	Rb	Synthetic peptide derived from C-terminal of mouse Pannexin 2	ThermoFisher Scientific Waltham, MA	42-2800	1:200	Bruzzone et al., 2008
GS	Ms	Glutamine Synthetase purified from sheep brain	Millipore Corporation Temecula, California	MAB302	1:500	Wilhelmsson et al., 2004
SLC18B1	Rb	Recombinant protein EST:FYLLEYSRRKR SKSQNILSTEEERTTLLP	Sigma Life Science St. Louis, MO	HPA029747	1:50	N/A
Spermine	Rb	Spermine conjugated to KLH	Abcam Cambridge, MA	ab26975	1:100	N/A
Spermine	Rb	Spermine conjugated to KLH	Novus Biologicals Littleton, CO	NB100-1846	1:100	N/A

2.4 In situ Proximity Ligation Assay (PLA)

Potential protein-protein interactions were assessed by in situ Proximity Ligation Assays (PLA). PLA was performed using a generalized Duolink mouse/rabbit labeling kit (Olink Bioscience, Uppsala, Sweden). To optimize results we fixed retinas with 4% EDAC in 0.1M PB for 30 minutes at room temperature followed by 4% PFA for 5 minutes. This fixation protocol worked well and was used for studying SAP102 interactions with either GluR6/7 or Kir2.1. We used conventional immunohistochemistry techniques for labeling retinal cryostat sections with mouse and rabbit primary antibodies. Briefly, retinal sections were blocked with 15% normal donkey serum in 0.1M PB with 0.3% TritonX-100 detergent and then incubated with primary antibodies in the same solution overnight at 4°C. On the following day, sections were washed three times with 0.1M PB for 10 min each with gentle shaking. After primary incubation, all further steps were done according to the Duolink manual. Incubations with the kit-derived oligonucleotide-linked secondary antibodies, PLA probe dilution/incubation time, ligation, rolling circle amplification times and polymerase concentrations were optimized for retinal sections (Leuchowius et al., 2011). PLA probes were incubated in pre-heated humidity chamber for 60 min at 37°C, briefly washed three times and left with gentle shaking for 30 min in Duolink buffer A. The slides were further processed for ligation for 60 min at 37°C, and amplification step was significantly improved when incubation time was 60min at 37°C.

To verify the selectivity of the PLA experiments, we used the antibodies

mouse anti-SAP102 (cat# 75-058, UC Davis/NIH Neuromab Facility), rabbit anti-GluR6/7 (cat#04-921, Millipore Corporation), rabbit anti-Syntaxin 3 (gift or Dr. Roger Janz) and rabbit anti-PSD95 (cat#18258, Abcam, Cambridge, MA). We performed negative controls by excluding one of the probes during antibody incubation or by probing for proteins known to be on opposite sides of the synapse (e.g. SAP102 and syntaxin 3). We performed positive controls by probing with two different antibodies to the same protein (not shown).

2.5. Confocal microscopy

Image acquisition was performed with a Zeiss LSM 510 META or LSM 780 laser scanning confocal microscope (Carl Zeiss, Thornwood, NY). All sections were imaged with dye-appropriate filters (405 nm excitation, 440–460 nm emission for DAPI; 542 nm excitation, 590–620 nm emission for Cyanine 3; 488 nm excitation, 530–550 nm emission for Alexa 488; 633 nm excitation, long-pass 650 nm emission for Dyelight 647). The detector gain and offset parameters were adjusted so that the intensity of most pixels fell within the dynamic range of the detector and the intensity of the most brightly labeled immunoreactive puncta showed very limited saturation. Images were acquired with a 40× or 63× oil-immersion objectives as a series of optical sections ranging between 0.25 to 0.5 μm in step size. Each marker was assigned a pseudocolor and the images were analyzed as single optical sections and as stacks of optical sections projected along the y or z axis. All images were processed in Adobe Photoshop (Adobe Systems CS5, San Jose, CA) to enhance

brightness and contrast. To measure polyamine levels five areas of the retina were scanned per animal and 4 animals were used for each experimental condition.

2.6 Intensity measurements of polyamines at different times of the day

Mice were sacrificed either 1 hour before noon or 1 hour past midnight corresponding to daytime and nighttime respectively. Day and night animals were used at different days. The day of the experiments mice in the inverted cycle condition were kept inside black boxes until collection of retinal tissue was performed. Retinas from both groups of animals were collected and fixed in 4% paraformaldehyde in complete darkness using infrared goggles. Immunolabeling with antibodies against spermine was performed and detected using fluorescent secondary antibodies. 12-bit images were analyzed with SimplePCI software (Hamamatsu Photonics, Bridgewater, NJ). The fluorescence intensity of Cy3 spermine labeled was measured with circles centered on photoreceptor terminals stained with PSD95. The intensity of spermine was measured in both cones and rods by using two populations, and changes in OPL intensity was evaluated between day and night. In order to compare conditions, the average of polyamine labeling intensity from the photoreceptors of 5 images was used to determine the changes in polyamine labeling of OPL in each animal. Same settings were used to measure spermine levels from animals in both conditions.

Chapter 3. Synaptic scaffolds in Rabbit retina

This chapter is based upon “MAGUK scaffolds organize a horizontal cell synaptic complex restricted to invaginating contacts with photoreceptors" by Vila, Alejandro; Whitaker, Christopher; O'Brien, John” Journal of Comparative Neurology CN-16-0115.R1 ePub August 25, 2016

3.1. Introduction

To eliminate redundancies in our visual world the retina has to compress spatial and temporal information to accommodate for these changes. In the outer plexiform layer (OPL), these redundancy reduction mechanisms are generated at the triad synapse between photoreceptors, bipolar and horizontal cells (HC), where HCs feedback to photoreceptors reviewed by (Burkhardt, 1993; Kamermans and Spekreijse, 1999; Thoreson and Mangel, 2012). The feedback mechanism of HCs applies a certain amount of gain control to photoreceptor synapses, keeping the photoreceptor synapses within the operating range of Ca^{2+} channels and thus allowing glutamate release. The mechanism of HC feedback remains controversial, with hypotheses ranging from conventional transmitters (GABA) to non-conventional transmitters (protons) and an ephaptic mechanism (Murakami et al., 1982; Hirasawa and Kaneko, 2003; Vessey et al., 2005; Kamermans et al., 2001; Klaassen et al., 2012). Evidence for the latter two mechanisms has been growing in the past decade. Both ephaptic and proton-mediated feedback mechanisms require precise localization of synaptic events in horizontal cell processes very closely apposed to photoreceptor transmitter release sites.

It is a general rule that precise physical localization of synaptic proteins is essential for effective synaptic transmission and for control of the signaling pathways that impose plasticity. At most synapses, suites of scaffold proteins form complex networks that anchor receptors and play an important role in synaptic plasticity. Membrane-associated guanylate kinase (MAGUK) proteins are responsible for anchoring many of the necessary components that regulate synaptic transmission (Oliva et al., 2012; Chen et al., 2015). It is well known that excitatory synapses are rich in MAGUKs, including postsynaptic density protein 95 (PSD95), PSD93 (Chapsyn-110), synapse-associated protein 102 (SAP102) and SAP97 (Koulen, 1999). These synaptic scaffolding proteins share homologous PDZ domains, which mediate protein-protein interactions to form multi-protein complexes. The complexes of synaptic scaffolds often include a variety of transmitter receptors, ion channels, and regulatory proteins.

To provide insight into HC synaptic mechanisms, we sought to identify neuronal scaffold proteins that reside in the synapse between photoreceptors and HCs. We systematically evaluated the distributions of several synaptic scaffold proteins in rabbit retina, finding scaffolds restricted to the tips of horizontal cells contacting photoreceptors, and further examined the localization of proteins known to interact with them. We find evidence that scaffolds assemble a complex of proteins that are likely involved in synaptic signaling between photoreceptors and horizontal cells.

3.2. Distribution of MAGUK-containing synaptic scaffold proteins in the retina

Synaptic scaffold proteins bind to and assemble unique suites of proteins that establish the functional properties of synapses. Because each scaffold may assemble different groups of proteins, certain aspects of the functional properties of a synapse can be inferred from the scaffolds that are present. To gain insight into the synaptic interactions of retinal photoreceptors, we examined the distribution of the MAGUK-containing synaptic scaffold proteins in the rabbit outer plexiform layer (OPL) by multiple-label immunofluorescence and confocal microscopy. Labeling for PSD95 followed its well-known but paradoxical labeling pattern as a pre-synaptic marker encircling the plasma membranes of both rod and cone terminals (Fig. 3.1A). SAP97 gave a similar labeling pattern (Fig.3.1B). Both SAP97 and PSD95 were also present in the inner plexiform layer (IPL), although PSD95 labeling was very weak. In contrast to the distribution of these proteins, immunoreactivity for SAP102 (Fig.3.1C) had a strong punctate distribution in both the OPL and the IPL. The distribution of Chapsyn110 was similarly punctate in the OPL (Fig. 3.1D) and quite abundant and punctate in the IPL.

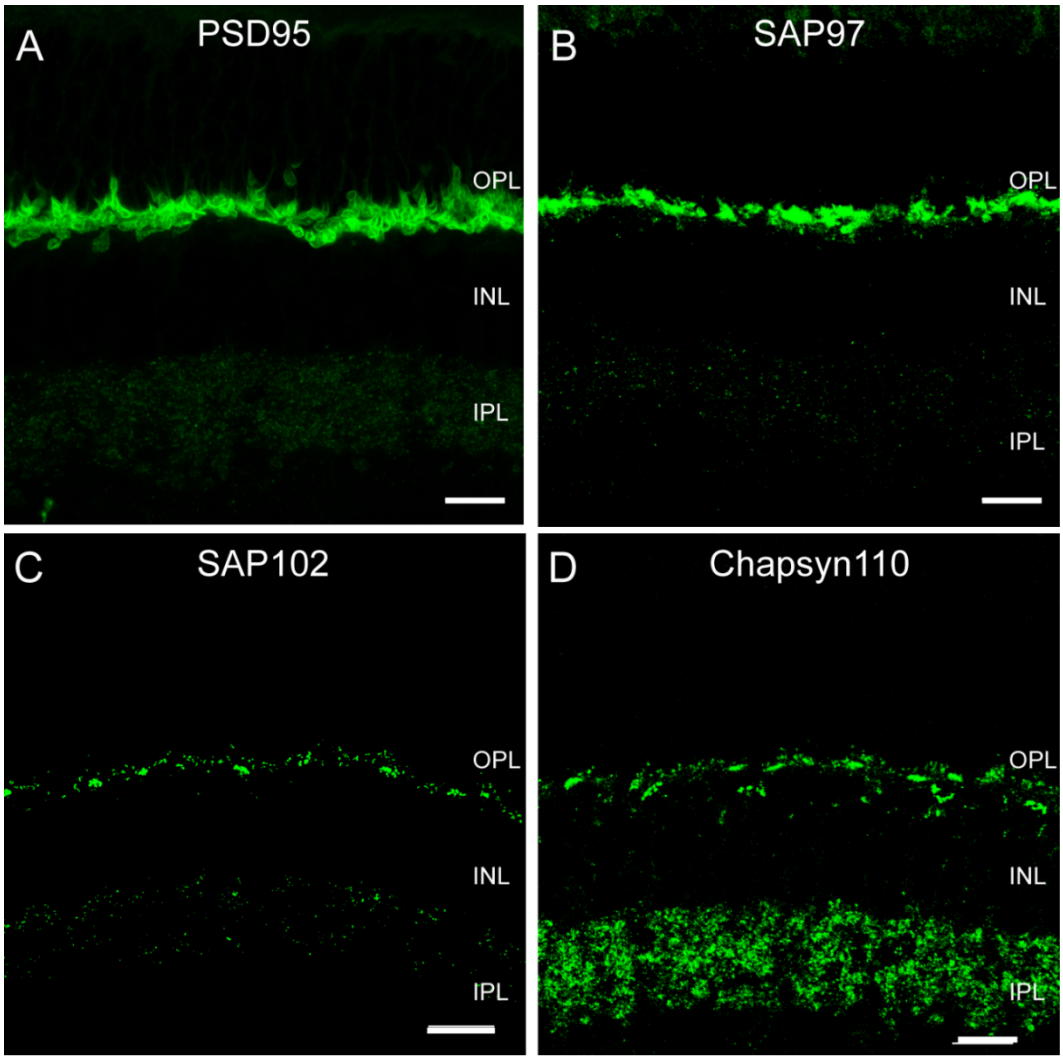

Figure 3.1. Membrane-Associated Guanylate Kinase (MAGUK) proteins in the rabbit retina. A, Vertical section of rabbit retina labeled for PSD-95. Prominent immunoreactivity in the OPL encircled photoreceptor terminals. In the IPL immunofluorescence was found in the form of sparse, very small puncta. **B**, SAP97-IR was found in the OPL, where rod and cone photoreceptor terminals were labeled intensively. Strong labeling was concentrated in the cytoplasm of rod spherules and cone pedicles. In the IPL immunofluorescence was found in the form of sparse puncta. **C,** SAP102-IR appeared as clusters of puncta in the OPL surrounded by sparser puncta. Immunolabeling in the IPL was weak and punctate. **D**, Chapsyn-

110 IR had a similar labeling pattern as observed with SAP102 in the OPL. Chapsyn-110 immunolabeling was punctate and much stronger than the other MAGUKs in the IPL. Scale bars: 10 µm.

3.2.1. SAP102 is a postsynaptic element of photoreceptor synapses

The punctate distribution of SAP102 and Chapsyn110 that did not show the outline of photoreceptor terminals suggested that these scaffolds might be post-synaptic in the OPL. To assess their distribution, we first examined the localization of SAP102 in more detail. In whole mount views of the OPL, SAP102 immunoreactivity appeared as tight clusters of round puncta surrounded by smaller, sparser puncta (Fig. 3.2A). Labeling with an antibody to GluR5, a marker that labels OFF bipolar cell dendrites at the base of cone pedicles (Haverkamp et al., 2003), revealed that the tight clusters of SAP102 labeling were located at cone pedicles (Fig. 3.2A). In vertical sections SAP102-immunoreactive (IR) puncta were located slightly above GluR5 labeling (Fig. 3.2B), a finding suggesting that SAP102 was located inside cone pedicles. Chapsyn-110 had similar distribution with clusters of puncta associated with cones and distributed individual puncta in the OPL (Fig. 3.2C).

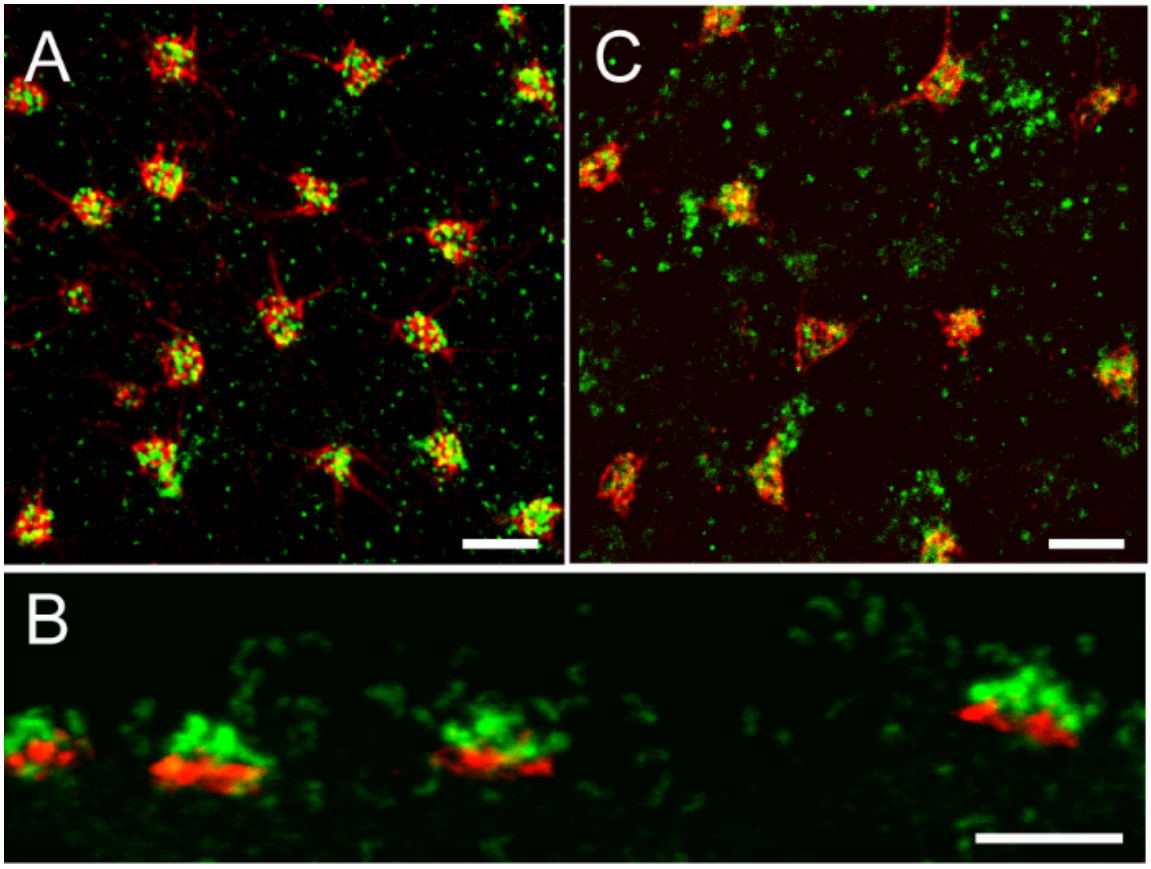

Figure 3.2. Clustered scaffolds are associated with cone photoreceptors. A. Wholemount immunofluorescence labeling in the OPL of SAP102 (green) and GluR5 (red), a marker that labels OFF bipolar cell dendrites at the base of cone pedicles. Tight clusters of SAP102 labeling were located at cone pedicles. **B.** Vertical section through the OPL with the same labeling scheme as A. SAP102 puncta were located slightly above GluR5. **C.** Chapsyn-110 (green) had similar distribution in the OPL with clusters of puncta associated with GluR5 (red) and distributed individual puncta. Scale bars: 5 μm.

To determine whether SAP102 was localized to photoreceptor terminals, retinas were double-labeled with antibodies to syntaxin 3, a membrane protein

expressed by rods and cones that is a component of the soluble N-ethylmaleimide-sensitive factor attachment protein receptor (SNARE) complex at ribbon synapses (Morgans et al., 1996). Immunolabeling of syntaxin 3 is found in the membranes of cone and rod photoreceptor synaptic terminals (Li et al., 2009; Vila et al., 2012). Strong syntaxin 3 immunolabeling was found at the plasma membrane of synaptic terminals in rods (Fig. 3.3A). In cone terminals, however, a small amount of diffuse cellular staining was present. Single optical sections through the OPL double labeled with SAP102 and syntaxin 3 antibodies showed punctate staining closely associated with each other but the two were not colocalized (Fig. 3.3B). SAP102 puncta in the form of clusters were localized slightly above the plasma membrane (Fig. 3.3C), suggesting that SAP102 is inside of cone pedicles and not in their plasma membrane. One punctum was typically found in the center of each rod spherule (Fig. 3.3B). Similar to the situation in cones, the SAP102 label was found in a gap in syntaxin 3 labeling, suggesting that SAP102 was present in a process invaginating the rod spherule.

Double labeling using an antibody to the synaptic ribbon protein ribeye revealed that SAP102 was closely associated with photoreceptor synaptic ribbons, but ribeye and SAP102 were not colocalized (Fig. 3.3D). SAP102 immunoreactivity was always localized below the cone and rod synaptic ribbons, suggesting that it is post-synaptic to the photoreceptors, but localized well within the invaginating synapses of the photoreceptors. Two cell types have processes post-synaptic to photoreceptors within the invaginating synapses: ON (depolarizing) bipolar cells and horizontal cells. To determine whether SAP102 was associated with ON bipolar cell

dendrites, we performed double labeling studies using an antibody to the ON bipolar cell glutamate receptor mGluR6 (Fig. 3.3E). ON bipolar cell dendrites were also closely associated with SAP102-IR puncta, but the two were not colocalized. The SAP102-IR puncta were always located above ON bipolar cell dendrites (Fig. 3.3F).

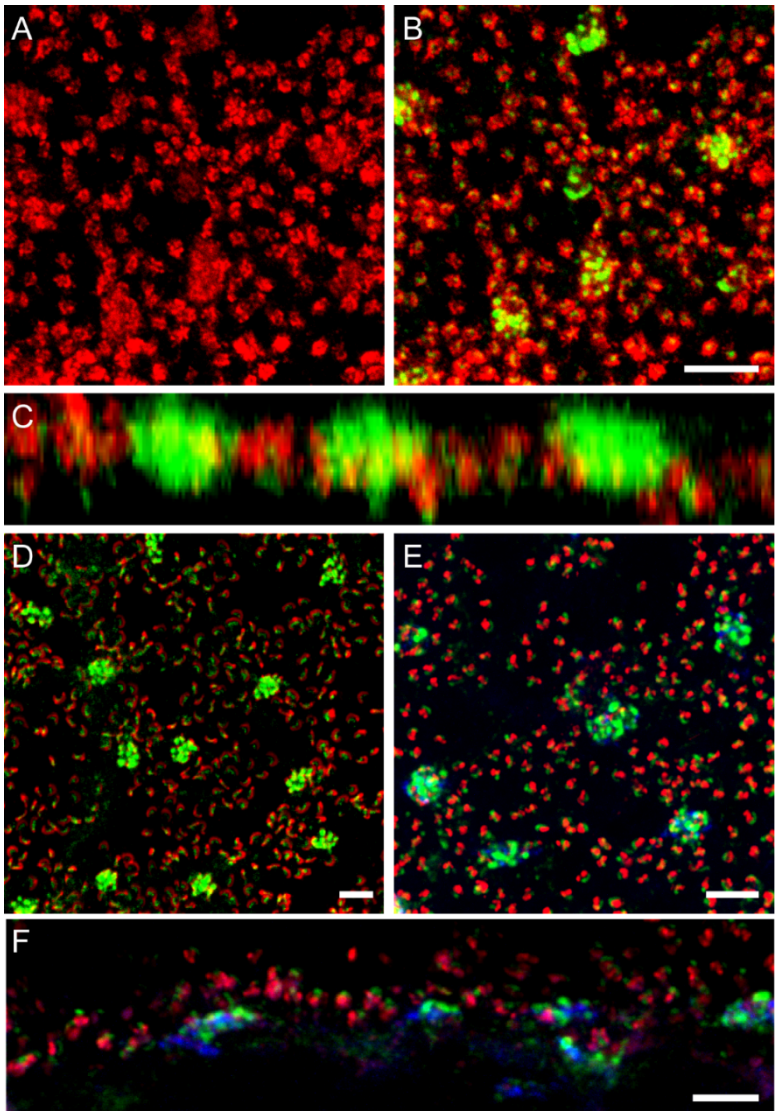

Figure 3.3. Association of SAP102 with synaptic elements in the OPL. A. Wholemount immunofluorescence labeling in the OPL of syntaxin 3 (red), revealing small clusters labeling synaptic terminals of rods, and diffuse cellular staining in cone terminals. **B.** Single optical section through the OPL double labeled for

SAP102 (green) and syntaxin 3 (red). SAP102 labeling appears in gaps in syntaxin 3 labeling. **C.** Z-axis projection of a series of optical sections taken at 0.35 μm intervals through the OPL. SAP102 puncta in clusters were localized slightly above the cone plasma membrane labeled with syntaxin 3, suggesting that SAP102 is inside of cone pedicles and not in their plasma membrane. One punctum was typically found per rod spherule. **D.** Wholemount immunofluorescence labeling in the OPL of SAP102 (green) and the synaptic ribbon protein ribeye (red). **E.** Wholemount immunofluorescence labeling in the OPL of SAP102 (green) and mGluR6 (red), labeling the tips of ON bipolar cell dendrites. **F**, Vertical section through the OPL with labeling of SAP102 (green), mGluR6 (red) and GluR5 (blue). The SAP102-IR puncta were always located above ON bipolar cell dendrites (mGluR6) in rods and slightly above OFF bipolar cell basal contacts (GluR5) in cones. Scale bars: 5 μm.

3.2.2. SAP102 is located in B-type horizontal cells.

The lack of co-localization of SAP102 immunoreactivity with either ON or OFF bipolar cell markers and its apparent post-synaptic localization suggests that it may be located in horizontal cells. In the rabbit, A-type horizontal cells (HCs) send dendritic processes only into the invaginating synapses in cone pedicles, while B-type HCs send dendritic processes to cone pedicles and axon terminal processes to rod spherules. To examine whether SAP102 was expressed by horizontal cell dendrites, the lateral elements of the triads, cell bodies of HCs were visualized with DAPI and injected with Neurobiotin using intracellular electrodes. Injection of A-type

HCs and double labeling with anti-SAP102 revealed that the tips of A-type HC processes were closely associated with SAP102 clusters, but the two markers failed to colocalize (Fig. 3.4 A-D).

In contrast to the results with A-type HCs, double-labeling experiments with Neurobiotin-filled B-type HCs and SAP102 antibodies showed dendritic processes colocalized with SAP102 (Fig. 3.4E-H). Dendrites of B-type horizontal cells sent one or more processes to clusters of SAP102 puncta located at cone terminals (Fig. 3.4F) while the axon terminal complex sent fine processes ending with a single contact on a rod (Fig. 3.4H). Co-localization was complete at the tips of the HC processes, confirming that B-type horizontal cells contain the SAP102 clusters. Pan and Massey (2007) have previously shown that rods in rabbit retina are contacted by a single B-type horizontal cell axon terminal process and that each B-type HC axon terminal process contacts only about 10% of immediately adjacent rods due to the extensive overlap with other HCs. Thus the extension of processes contacting a limited number of rods within the axon terminal field (Fig. 3.4H) is expected. Likewise, the extension of B-type HC dendritic processes to make a single contact with a cone (Fig. 3.4F) is also expected. The presence of SAP102 in both cone and rod invaginating synapses suggests that whatever mechanism is supported by this protein complex is present in both types of photoreceptors. These proteins may be involved in either feedforward or feedback signaling between the photoreceptors and the horizontal cell.

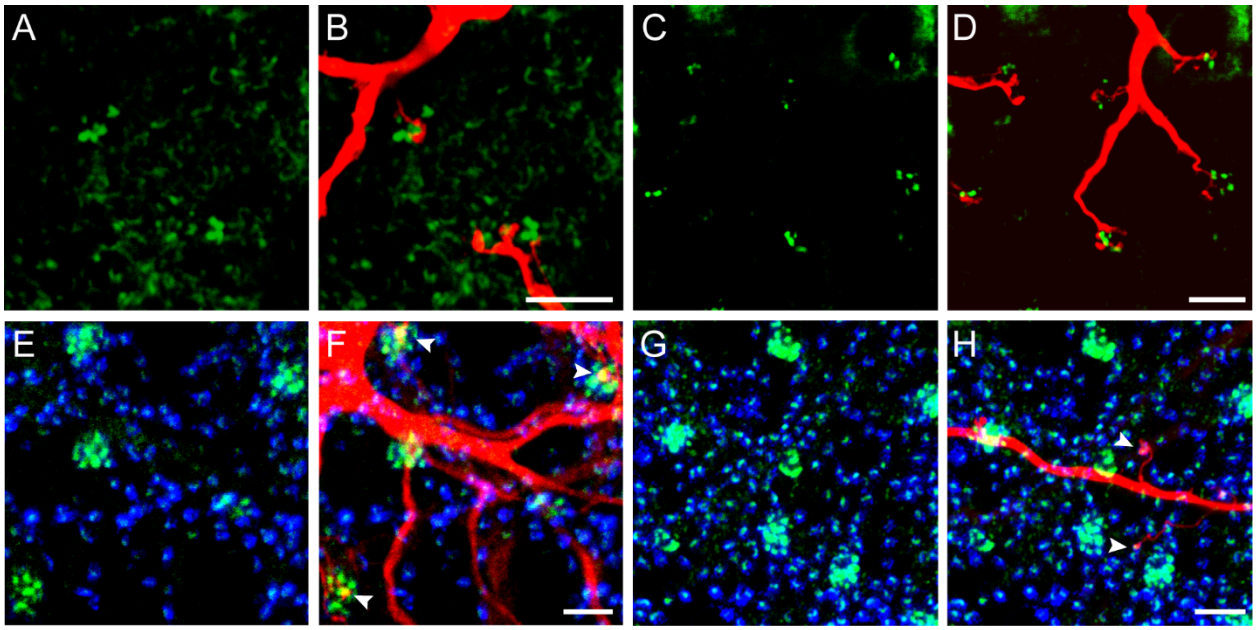

Figure 3.4. SAP102 is located in B-type horizontal cells. (A-D) Distribution of SAP102 (green) immunoreactivity relative to a Neurobiotin-injected A-type HC (red) in the OPL. **A and C**: Distribution of SAP102 immunoreactivity in the OPL. **B and D**: Stacks from 15 single optical sections at 0.25 µm increments are shown. A-type HC dendrites labeled with Neurobiotin were closely associated with clusters of SAP102 immunoreactive puncta in cones, but not co-localized. **(E-H):** Distribution of SAP102 immunoreactivity relative to a Neurobiotin-injected B-type HC in the OPL. **E and G**: Distribution of SAP102 immunoreactivity in the OPL. The location of photoreceptor terminals is shown with syntaxin 3 labeling (blue). Stacks from 17 single optical sections at 0.25 µm increments are shown. **F and H**, Relationships of B-type HC dendrites (**F**) and axon terminals (**H**) with SAP102. Both B-type HC dendrites (F) and axon terminals (H) colocalized with SAP102 (arrowheads) at contacts with cone terminals and rod spherules respectively. Christopher Whitaker Ph.D performed the HC injections for this figure and I did the immunostaining and imaging. Scale bars: 5 µm.

3.3. SAP102 complex in rabbit retina

3.3.1 Proteins known to bind to SAP102 are present in HC synapses

To determine whether SAP102 in horizontal cells was associated with some of its known interacting partners, we double- and triple stained specimens with specific antibodies against glutamate receptors and potassium channels. The kainate receptor GluR6 has been found to bind to SAP102 in vitro (Cai et al., 2002) and an antibody against GluR6/7 has previously been found to label processes of horizontal and bipolar cells in mammalian retina (Peng et al., 1995). We found strong GluR6/7 staining distributed in the OPL, where the protein had a punctate appearance with the formation of aggregates adjacent to cone pedicles (Fig. 3.5A, B). These aggregates colocalized completely with SAP102 at cone pedicles. Higher magnification images showed less pronounced GluR6/7 immunoreactivity in the form of single puncta above the level of cone pedicles, colocalizing with SAP102 (Fig. 3.5C). In vertical sections (Fig. 3.5D) GluR6/7 labeling was clearly colocalized with the clusters of SAP102 associated with the invaginations of rod spherules. The localization of the kainate receptor GluR6/7 was quite different than that of AMPA receptors, which are predominantly localized just outside of the synaptic cleft at desmosome-like junctions below cone pedicles and at comparable locations along the shaft of processes leading to rods (Haverkamp et al., 2001b; Pan and Massey, 2007).

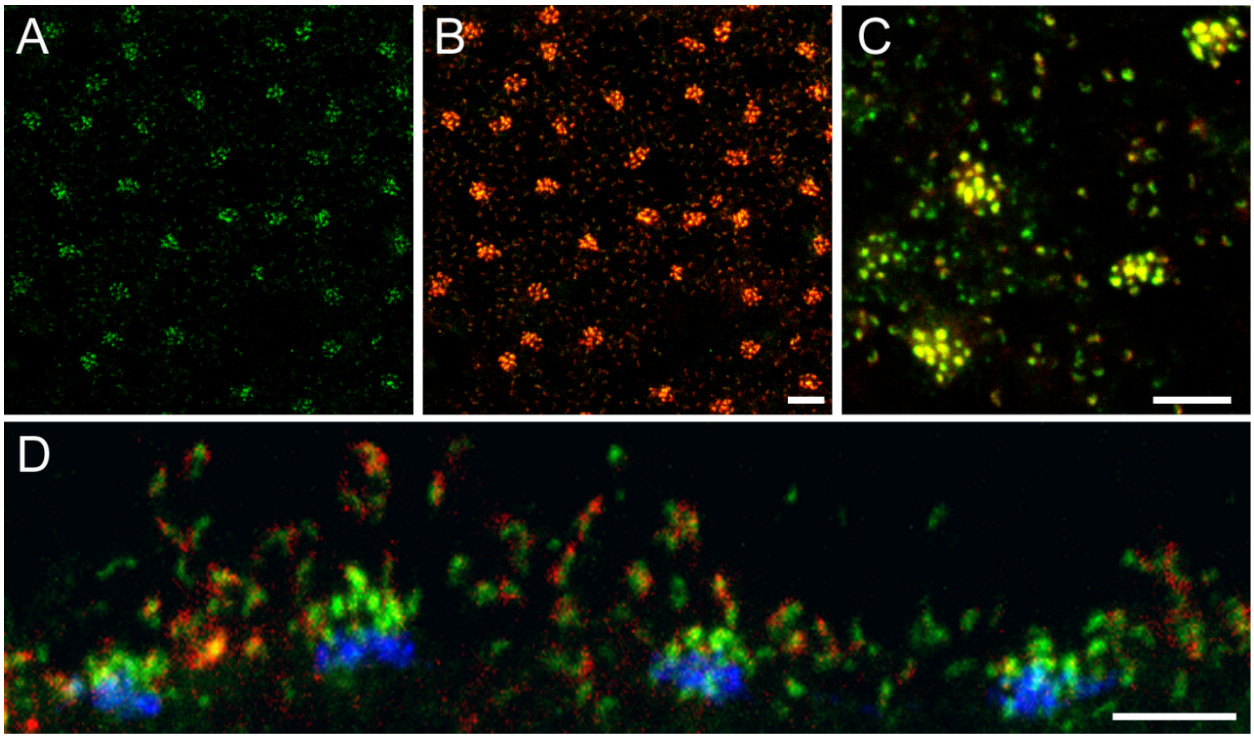

Figure 3.5. Association of SAP102 with kainate receptor GluR6/7. (A-C), Wholemount immunofluorescence labeling in the OPL of SAP102 (green; alone in A) and GluR6/7. **B**, A stack from 6 single optical sections at 0.35 µm increments is shown. GluR6/7-IR appeared as discrete puncta colocalized with SAP102. **C**, Single optical section confirming that GluR6/7 colocalization with SAP102 was not due to projection of labels at different depths. **D**, Vertical section through the OPL labeled for SAP102 (green), GluR6/7 (red) and GluR5 (blue). GluR6/7 labeling was clearly colocalized with the clusters of SAP102 associated with the invaginations of rod spherules. Scale bars: 5 µm

Another protein that has been demonstrated to associate with SAP102 is the inward rectifier potassium channel Kir2.1 (Leonoudakis et al., 2004). Kir2.1 immunolabeling exhibited a mixture of diffuse and punctate patterns in the OPL and

surrounded the somas of HCs (Fig. 3.6A). Labeling for Kir2.1 extended to the outermost part of the OPL and sometimes localized to specific areas close to photoreceptors. To evaluate whether Kir2.1 was present in HCs, we triple-labeled sections with antibodies to Kir2.1, SAP102, and GluR6/7 (Fig. 3.6B-E). Figure 3.6B (SAP102 alone) and C (triple label) show one SAP102 cluster at a cone terminal with surrounding rod spherule contacts. The numbers 1, 2 and 3 designate single SAP102 puncta contacting a cone (1) or rods (2 and 3). Figure 3.6C shows the triple-labeled specimen and the insets 1-3 show enlarged single optical sections of the three single puncta at the level of the cone contacts. Figure D and E show the same sample 0.35 μm higher in the OPL, at the level of the rod contacts, and insets 4-6 show the same SAP102 puncta as 1-3. Kir.2.1 immunoreactivity was found directly colocalized with SAP102 puncta at the invaginated tips of both HC dendritic processes contacting cones and axon terminal processes contacting rods in the OPL. Only Kir2.1 puncta were colocalized in the outermost portion of the OPL, suggesting that Kir2.1 was clustered by SAP102 in the tips of HC processes.

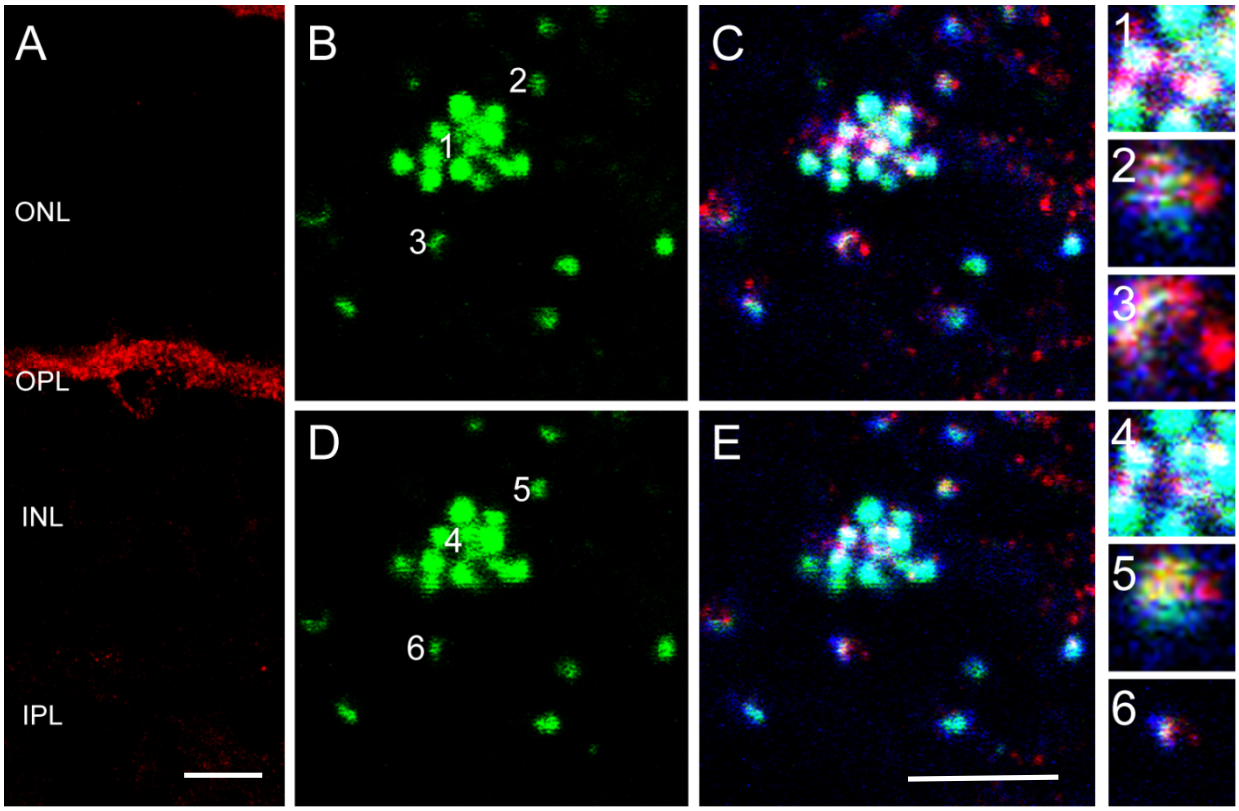

Figure 3.6. Association of SAP102 with inward-rectifier potassium channel Kir2.1. A, Vertical section through the retina labeled for Kir2.1. Kir2.1 exhibited a mixture of diffuse and punctate patterns in the OPL and surrounded the somas of HCs. **(B-E),** Wholemount immunofluorescence labeling in the OPL of SAP102 (green), Kir2.1 (red) and GluR6/7 in two consecutive optical sections. B and C represent a single optical section in the lower portion of the OPL separated by 0.35 µm from a higher section in the OPL represented in D and E. **B and D**, SAP102 alone. **C and E**, Kir2.1-IR (red) was diffusely present below SAP102 clusters, but puncta were colocalized with SAP102 at the tips of HC processes. Numbers in B and D indicate individual SAP102 puncta at contacts with cone (1, 4) and rod (2-3, 5-6) terminals that are shown in the insets. Kir2.1 colocalizes with SAP102 at the level

of the cones (inset 1) and at the level of the rods (insets 5 and 6). Scale bar: 10 and 5 μm respectively.

3.3.2 Proteins thought to mediate ephaptic feedback signaling were not present in the scaffolded complex.

Connexin hemichannels at the tips of HC dendrites have been proposed to function as a current source for ephaptic feedback from HCs to cones (Kamermans et al., 2001). To evaluate whether SAP102 was associated with connexin hemichannels we performed double labeling studies using antibodies against Cx57 and Cx59. We found Cx57 immunoreactive clusters in the OPL and scattered through the nuclear layers (Fig. 3.7A). Labeling in the nuclear layers with this antibody has previously been found to be non-specific, while labeling in the OPL detected Cx57 gap junctions (Pan et al., 2012). Cx57 gap junctions in the OPL were located mostly below the SAP102-IR puncta (Fig. 3.7A), suggesting that Cx57 plaques lie at the bottom of the HC processes. No apparent relationship between the Cx57 plaques and either cone pedicles or rod spherules was observed. Labeling for Cx59 in the OPL similarly showed small puncta that did not have any relationship to the SAP102 clusters associated with cones or rods (figure 3.7B). Thus, neither connexin was associated with SAP102 nor was either detectable at the tips of horizontal cell processes.

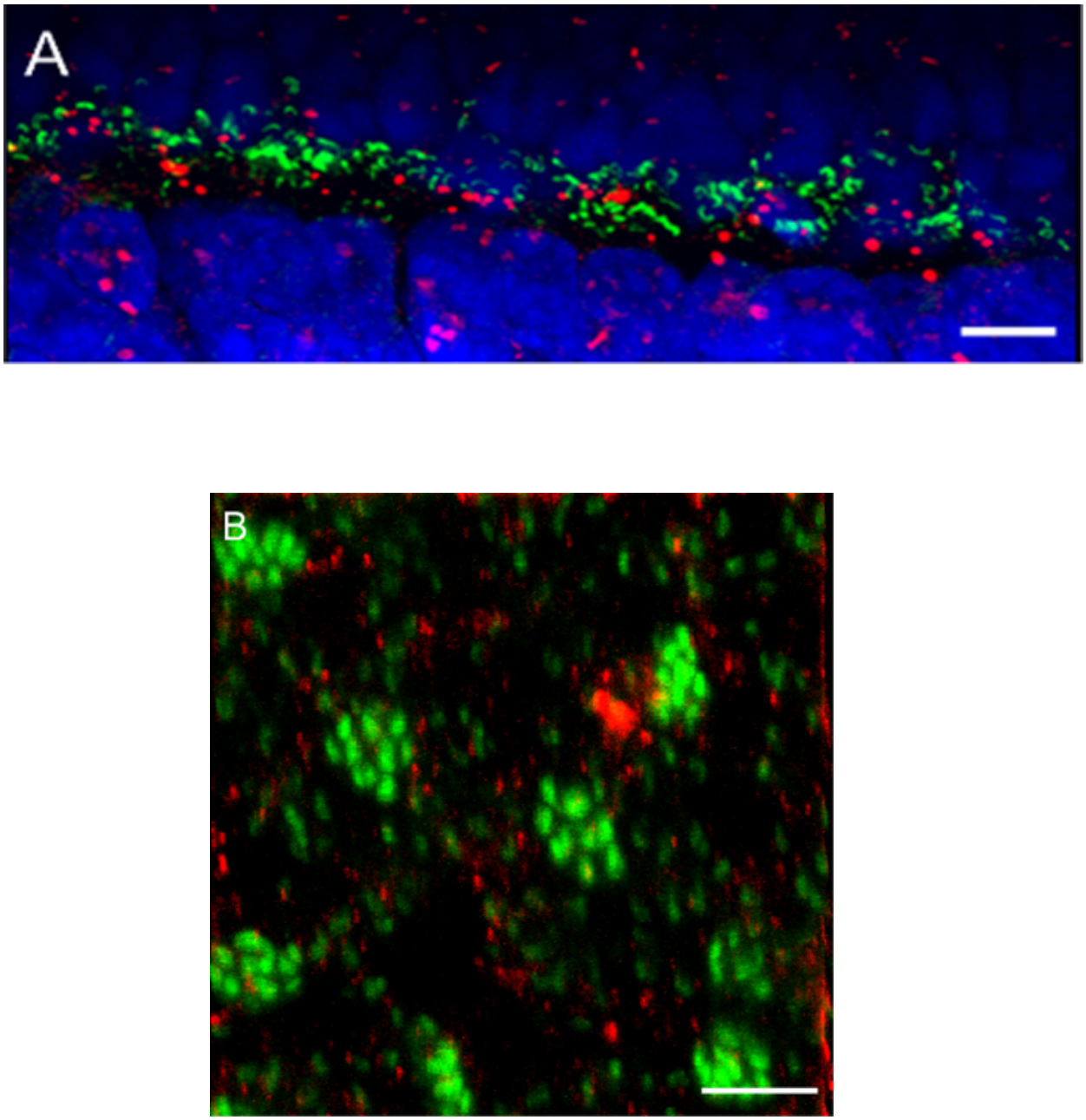

Figure 3.7. **Connexins 57 and 59 make gap junctions in OPL but do not colocalize with SAP102. A,** Vertical section through the OPL showing labeling of SAP102 (green) and Cx57 (red). Cell nuclei are labeled with DAPI (blue). No apparent relationship between the Cx57 plaques and SAP102 at either cone pedicles or rod spherules was observed. **B**, Wholemount immunofluorescence

labeling in the OPL of SAP102 (green) and Cx59 (red). Cx59 labeling was located mostly below the SAP102-IR puncta, but was not colocalized. Scale bars: 5 μm.

3.3.3 Close associations of SAP102 with ion channels in the OPL

The placement of ion channels at the tips of horizontal cell processes deep within the invaginating synapses in cones and rods gives them preferential access to the physical environment of the synapse, which may be particularly important for post-synaptic signaling and feedback signaling from HCs to photoreceptors. We hypothesize that the role of the synaptic scaffold SAP102 is to hold these channels in this location to facilitate synaptic signaling. To assess whether SAP102 is bound to GluR6/7 and Kir2.1 in the OPL, we used in situ proximity ligation assays (PLA). The indirect method we used detects protein proximity up to about 40 nm apart, suggesting that positive signals represent either direct protein-protein interactions or very close association of proteins that could be via indirect interactions. Figure 3.8 shows SAP102 labeling in a section of rabbit retina (A) and PLA reaction product for interaction between SAP102 and GluR6/7 (B) in a sequential section. While SAP102 immunoreactivity occurred in both the OPL and IPL, the PLA reaction product was restricted to the OPL and appeared punctate. In a similar fashion, the PLA reaction product for interaction between SAP102 and Kir2.1 was restricted to a narrow band of puncta in the OPL (Fig. 3.8E). This distribution was much more restricted than that of SAP102 immunoreactivity in an adjacent section (Fig. 3.8D) or the observed distribution of Kir2.1 in the OPL (see Fig. 3.8A). Figure 3.8G-I shows a negative control experiment in which an interaction between SAP102 and syntaxin 3

was tested by PLA. Although these proteins occur very close to each other on opposite sides of the photoreceptor synapses, no reaction product was detected in the OPL (Fig. 3.8H). The results indicate that GluR6/7 and Kir2.1 are very closely associated with SAP102 in the OPL, and thus supports the hypothesis that SAP102 likely interacts with these proteins to form a complex within the tips of HC processes. To our knowledge, this is the first time that interactions between SAP102 and either kainite receptors or potassium channels have been reported by in situ proximity ligation assay (PLA).

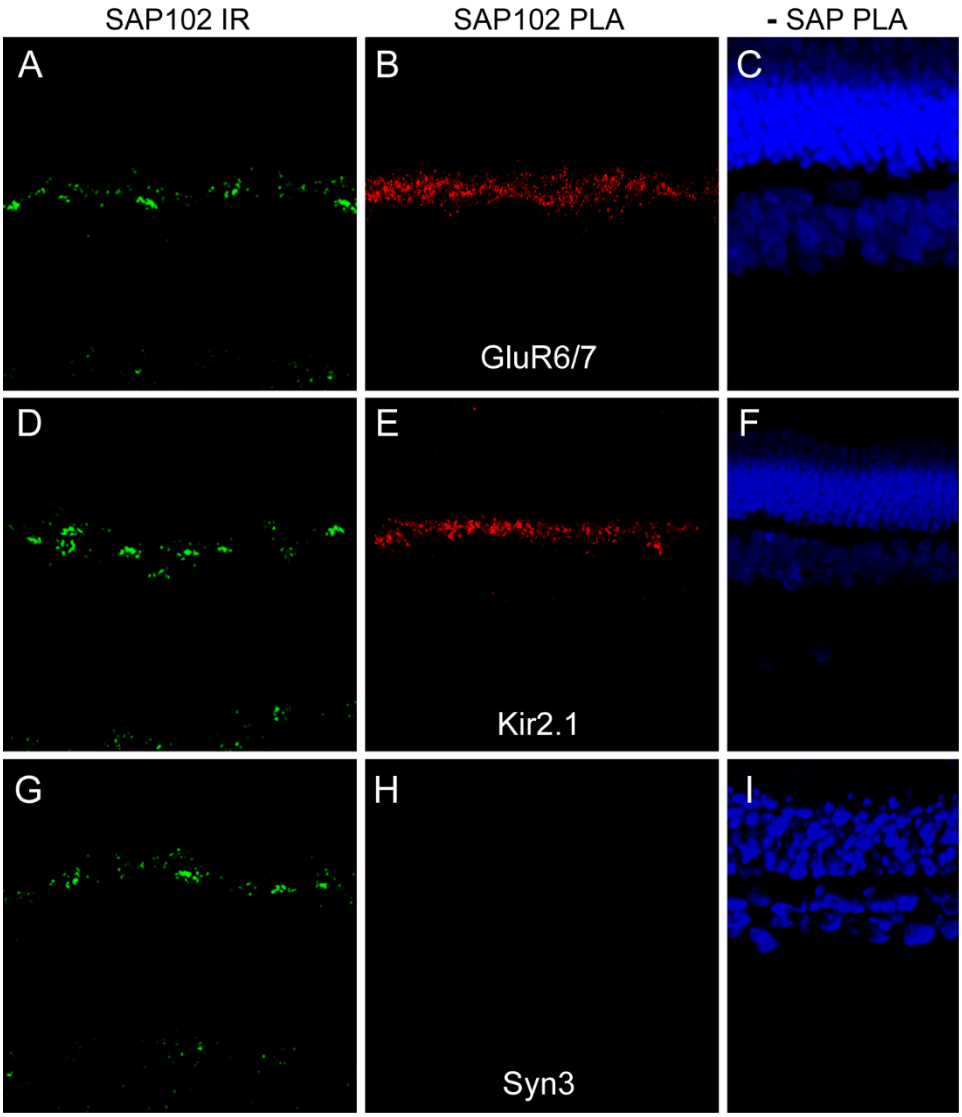

Fig 3.8. In situ proximity ligation assays (PLA) to show SAP102 association with ion channels. SAP102 labeling (green) in a section of rabbit retina **(A)** and PLA reaction product (red) for interaction between SAP102 and GluR6/7 **(B)** in a sequential section. While SAP102 immunoreactivity occurred in both the OPL and IPL, the PLA reaction product was restricted to the OPL and appeared punctate. **C,** Negative control PLA reaction in which the SAP102 antibody was omitted; nuclei are labeled with DAPI (blue). **D-F,** PLA experiment for interaction between SAP102 and Kir2.1 using the same order and color scheme as in A-C. PLA reaction product was

restricted to a narrow band of puncta in the OPL **(E)**. This distribution was much more restricted than that of Kir2.1 in the OPL (see Fig. 3.6A). **G-I,** Negative control PLA experiment in which an interaction between SAP102 and syntaxin 3 was tested, using the same order and color scheme as in A-C. Although these proteins occur very close to each other on opposite sides of the photoreceptor synapses, no reaction product was detected in the OPL **(H).**

3.4 DISCUSSION

In this chapter, we show SAP102 and its interacting partners associated with processes postsynaptic to photoreceptors, extending previous studies demonstrating the localization of some MAGUKs to photoreceptor synapses (Koulen et al., 1998a; Koulen et al., 1998b). We found that SAP102 organized a complex containing GluR6/7 and Kir2.1 in the tips of dendritic and axon terminal processes of B-type horizontal cells where they invaginate cone and rod photoreceptors. Chapsyn110 was also likely a component of this complex. Most previous studies show AMPA-type glutamate receptors to be the predominant form of glutamate receptor in mammalian horizontal cells, with dense clusters localized below cone and rod terminals and only a small fraction localized to the invaginating tips of dendritic or axon terminal processes (Haverkamp et al., 2001b; Pan and Massey, 2007). Targeted knockout of AMPA receptor GluA4 in mouse horizontal cells reveals a very small persistent glutamate receptor current, amounting to just a few percent of the glutamate-induced current in isolated cells, attributable to kainate receptors (Ströh et al., 2013). Thus the kainate receptor GluR6/7 likely serves a very limited but

potentially specialized role in horizontal cell signaling. We hypothesize that this role is in feedback of horizontal cells onto cone and rod photoreceptors.

Inhibitory receptive fields can be imposed by feedback of HC onto photoreceptors. The HC feedback provides dynamic gain control for the photoreceptor synapse and enhances contrast between the center of the receptive field and the surround; this contrast makes for better vision. HC feedback is caused by a shift in the activation curve of the Ca^{2+} current of the photoreceptor (Verweij et al., 1996; Kamermans and Fahrenfort, 2004). The mechanisms that cause this change have been controversial for decades, but appear to include a mechanism that regulates the concentration of protons in the synaptic cleft, modulating the level of inhibition of the photoreceptor voltage-gated Ca^{2+} channel, an ephaptic mechanism that modulates the apparent voltage across the photoreceptor synaptic membrane, and potentially a GABA-based mechanism (Thoreson and Mangel, 2012).

A great deal of evidence has accumulated recently in support of proton-mediated feedback mechanisms. Proton concentration increases in the synaptic cleft of cones when HCs are depolarized in response to glutamate, and is reduced when HCs hyperpolarize (Wang et al., 2014), as would be expected for a dynamic feedback mechanism. Strong pH buffering and alkalinization of the extracellular medium enhance photoreceptor Ca^{2+} current and prevent further enhancement caused by surround illumination that hyperpolarizes HCs, indicating that feedback has been blocked (Hirasawa and Kaneko, 2003; Vessey et al., 2005; Cadetti and Thoreson, 2006). Recent studies propose that protons responsible for acidifying the

synaptic cleft come from HCs via a Na^+:H^+ exchanger (Warren et al., 2016), but that regulation of extracellular buffering by bicarbonate is responsible for the modulation of pH (Liu et al., 2013; Warren et al., 2016). An alternative hypothesis proposes that changes in phosphate buffering that is developed via ATP release through Pannexin 1 channels and extracellular hydrolysis of ATP is responsible for the change in cleft pH (Vroman et al., 2014).

A series of studies has indicated that proton-mediated feedback of HCs to photoreceptors is dependent on Ca^{2+}-driven vesicular GABA release from HCs (Liu et al., 2013; Hirano et al., 2016). This is proposed to operate through an unconventional signaling pathway in which GABA activates $GABA_A$ autoreceptors on the horizontal cells, opening a channel permeable to both Cl^- and HCO_3^- (Liu et al., 2013). At depolarized potentials, this would result in an inward flux of HCO_3^- and acidification of the extracellular space, while the reverse would occur at more hyperpolarized potentials negative to the HCO_3^- equilibrium potential. The Ca^{2+} driving GABA release was found to derive largely from voltage-gated Ca^{2+} channels, although some feedback could not be blocked with inhibitors of N- or P/Q-type Ca^{2+} channels (Liu et al., 2013). It is possible that direct Ca^{2+} influx through glutamate receptors could contribute to GABA release. Glutamate receptors of horizontal cells in general have been found to be Ca^{2+}-permeable (Molina et al., 2004). Indeed the GluR6 receptor coded by the unedited mRNA has a Ca^{2+}:monovalent cation permeability ratio of 1.2 (Egebjerg and Heinemann, 1993), suggesting that the kainate receptors we have described at the tips of horizontal cell processes could provide a localized Ca^{2+} signal to support GABA release.

Several studies with isolated horizontal cells have examined modulation of extracellular proton fluxes near the HC plasma membrane. These studies have consistently shown a resting flux of protons out of HCs with a reduction or reversal of flux driven by glutamate stimulation (Molina et al., 2004; Kreitzer et al., 2007; Jacoby et al., 2012). In these studies, proton uptake could be attributed at least partially to Ca^{2+}-dependent activation of the plasma membrane Ca^{2+} ATPase, which functions as a Ca^{2+}/H^{+} antiporter. While these results seem to be at odds with findings that HC depolarization enhances proton-mediated feedback to photoreceptors, they reveal mechanisms at work in HCs that may not be detected in the synaptically connected network. We suggest that GluR6/7 kainate receptors at the tips of HC processes could contribute a localized Ca^{2+} signal that activates the Ca^{2+} ATPase.

It is important to consider that receptor desensitization may significantly influence the behavior of kainate receptors on horizontal cells. In isolated horizontal cells from *gluA4* knockout mice, kainate receptor currents were almost completely desensitized until potentiated by the addition of the lectin concanavalin A (Stroh et al., 2013). In general kainate receptors desensitize rapidly upon exposure to glutamate, and kainate receptors deep in the invaginated synaptic cleft of photoreceptors might be expected to be substantially desensitized in the continued presence of glutamate at the dark, resting state in the retina. On the other hand, binding of concanavalin A reduces GluR6 desensitization and binding to the scaffold PSD95 speeds recovery from desensitization (Bowie et al., 2003). While neither of these proteins specifically interacts with kainate receptors on HCs, extracellular matrix proteins may have effects similar to lectins and SAP102 or Chapsyn110

binding may have effects similar to PSD95; neither topic has been specifically investigated. Even in the absence of modulators, kainate receptors on the tips of HC processes would be expected to resensitize somewhat during light exposure on the receptive field center, priming the receptors to signal reductions in brightness.

Horizontal cells have also been proposed to feed back to photoreceptors through an ephaptic mechanism (Kamermans et al., 2001). In this scenario, there is no messenger that is mediating communication between HC and photoreceptor terminal. Rather, it is an electrical effect due to the voltage drop produced by the flow of synaptic current through the extracellular space. Because the synapse is invaginated and the space between the HC dendrites and the photoreceptor is restricted, the extracellular space has a finite non-zero resistance. Current flow through this space produces a voltage drop that influences the potential across the photoreceptor plasma membrane. Thus, the ephaptic signal causes a change in Ca^{2+} channel activity and the rate of neurotransmitter release.

Negative ephaptic feedback to photoreceptors requires that ion channels in the horizontal cell processes remain open when horizontal cells hyperpolarize, leading to higher synaptic current and higher current through the extracellular space. In the simplest sense, glutamate receptor channels should not provide this service in the receptive field center, as illumination would reduce glutamate release and close the channels. Indeed, glutamate receptors in the synaptic invagination would provide a form of positive ephaptic feedback in the receptive field center (Byzov and Shura-Bura, 1986). Glutamate receptors would still contribute to surround-imposed feedback, and would likely contribute during modest light excursions that do not fully

prevent glutamate release. Indeed resensitization of kainate receptors discussed above could contribute in the latter situation with enhancement of current through the synaptic cleft.

In proposing the ephaptic feedback hypothesis, Fahrenfort and Kamermans implicated connexin hemichannels at the tips of HC dendrites to provide the current source (Kamermans et al., 2001). This proposal immediately met with resistance (Deans and Paul, 2001; Dmitriev and Mangel, 2006), but a variety of evidence has supported the presence of connexin hemichannels and their role in feedback in various species (Fahrenfort et al., 2009; Klaassen et al., 2012; Sun et al., 2012; Kemmler et al., 2014), and the presence of Pannexin 1 channels is also thought to provide a route for current flow (Prochnow et al., 2009). It is perhaps surprising that we did not find Cx57 or Cx59 associated with SAP102 in the OPL, which would be expected if either of these connexins formed hemichannels that participated in feedback. One caveat of this result is that the Cx59 antibody has not been well characterized, so it is not certain that this negative result is completely reliable. We did not find antibodies to Pannexin 1 that worked in the rabbit retina, so we were not able to assess whether this channel might be involved in feedback.

One significant finding of our study was identification of Kir2.1 as a component of the postsynaptic complex in photoreceptor invaginating synapses. Under physiological conditions, this inward rectifier channel opens upon hyperpolarization, generating a large inward K^+ conductance at potentials negative to E_K (Hibino et al., 2010). Unlike connexin hemichannels or pannexin channels that should be open at the dark resting potential and provide instantaneous ephaptic

feedback upon hyperpolarization, Kir2.1 channels would open upon hyperpolarization, developing ephaptic feedback with a time constant dependent on the time constant of channel opening. Horizontal cell feedback develops with a relatively slow time course (Kamermans et al., 2001), which has been attributed to alleviation of proton-mediated Ca^{2+} channel inhibition by dissipation of an ATP-ADP-H^{+} buffer in the synaptic cleft (Vroman et al., 2014). The delayed activation time course of Kir2.1 channels would be more consistent with observed feedback signals, making it a plausible channel for the generation of ephaptic feedback.

Two types of positive feedback have recently been observed at the horizontal cell to photoreceptor synapse. One form is imposed by the surround and enhances the gain of the photoreceptor synapse (VanLeeuwen et al., 2009). This form is a corollary to the negative feedback, resulting from the shift of the voltage dependence of the Ca^{2+} channel activation curve. The other form of positive feedback is local (Jackman et al., 2011). The mechanism of this feedback is not fully elucidated, but it depends on Ca^{2+} rise in the horizontal cell and activation of AMPA-type glutamate receptors. It is unclear if kainate-type glutamate receptors could contribute to this mechanism, but the relatively high Ca^{2+} permeability of GluR6 receptors suggests that these receptors could provide Ca^{2+} to support this mechanism. This remains a possible role for the GluR6/7 receptors we find localized in the tips of horizontal cell processes contacting photoreceptors.

Chapter 4. Synaptic scaffolds in Mouse retina

4.1. Introduction

Previously, we identified a complex formed by SAP102 and its interacting partners in the tips of HC in rabbit. In order to move our discovery to a genetically modifiable background we sought to examine the presence of this complex and its associated neuronal scaffold proteins that reside in the synapse between photoreceptors and HCs in mouse retina. We hypothesized that synaptic scaffolding proteins could assemble components of the signaling mechanism into a similar complex in mouse retina. We found evidence that different synaptic scaffolds are restricted to the tips of horizontal cells contacting photoreceptors, and assemble a complex of similar proteins that are likely involved in synaptic signaling between photoreceptors and horizontal cells in mouse retina.

4.2. Distribution of MAGUK-containing synaptic scaffold proteins in the retina

Because MAGUKs are the substrate for the anchoring of proteins at specialized synapses we hypothesize that the complex we found in rabbit retina is important to control synaptic signaling in HCs, and should be present in mouse. We found SAP102 and possibly Chapsyn 110, was predominantly localized in the invaginating processes of HCs contacting both rod and cone photoreceptors in the rabbit. To determine whether synaptic scaffolds are found at the synapse between HC and cone photoreceptors we examined the distribution of the MAGUK-containing synaptic scaffold proteins in the mouse outer plexiform layer (OPL).

In contrast to the distribution in rabbit retina, SAP102 immunoreactivity was found in photoreceptor terminals in the mouse OPL (Fig. 4.1). The distribution of SAP102 was scarce and small punctate in the IPL (data not shown). SAP97 labeling was not punctate and appeared to label axons in the IPL (data not shown). Labeling for PSD95 had a similar pattern as a pre-synaptic marker encircling the plasma membranes of both rod and cone terminals as previously found in rabbit retina (Fig. 4.2).

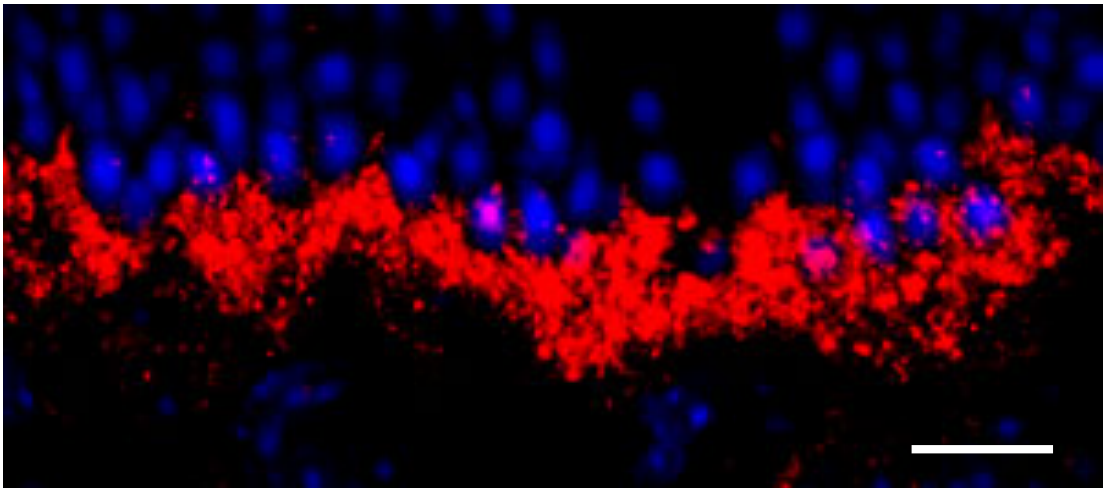

Figure 4.1: SAP102 distribution in the mouse retina. SAP102-IR was found in the OPL, where rod and cone photoreceptor terminals were labeled intensively. Strong labeling was concentrated in the cytoplasm of rod spherules and cone pedicles. In the IPL immunofluorescence was found in the form of sparse puncta (data not shown). Scale bar: 10 μm.

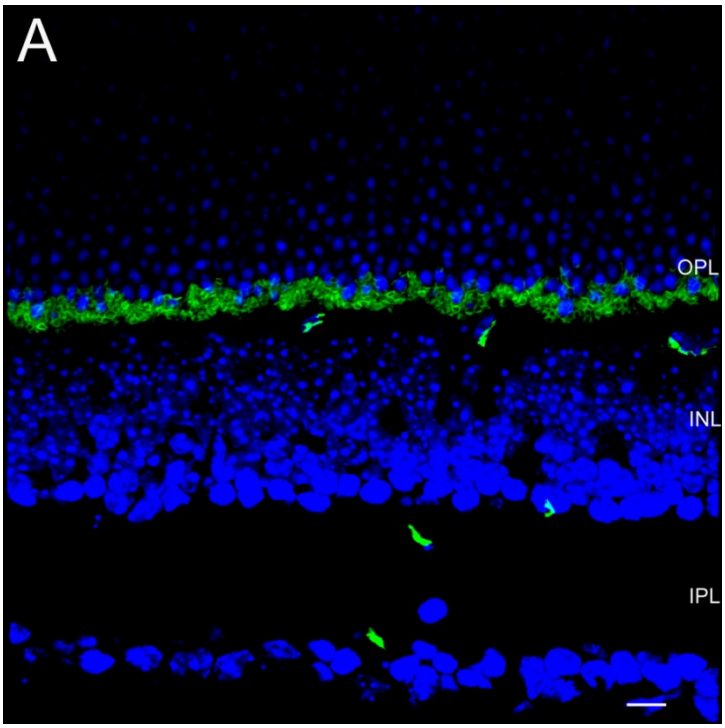

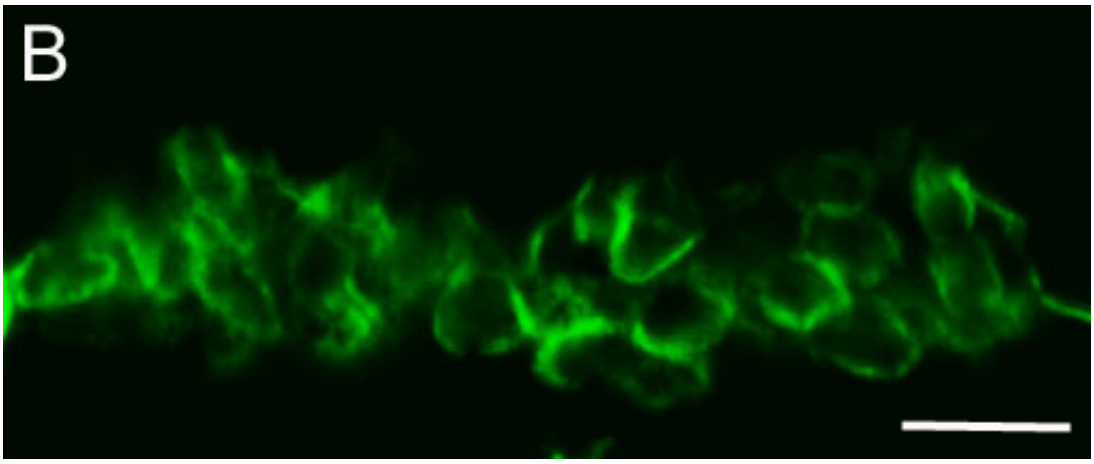

Figure 4.2: PSD95 immunolabeling in the mouse retina. A. Vertical section of mouse retina labeled for PSD-95. Prominent immunoreactivity in the OPL encircled photoreceptor terminals, as previously shown in rabbit. In the IPL immunofluorescence was faint. Large blood vessels were strongly labeled

throughout the retina. **B**. High magnification immunolabeling for PSD95 showing the termninal labeling. Scale bars: 5 µm.

In rabbit, we also found Chapsyn110/PSD93 in the HC tip complex. When we used antibodies against SAP102 our immunolabeling was negative, suggesting that SAP102 is not a scaffold in horizontal cells in the mouse retina. A major finding was Chapsyn110 immunoreactivity had a strong punctate distribution in the OPL and quite abundant and punctate in the IPL (Fig. 4.3). These results suggest that Chapsyn110 may be the main scaffold in horizontal cells in the mouse retina.

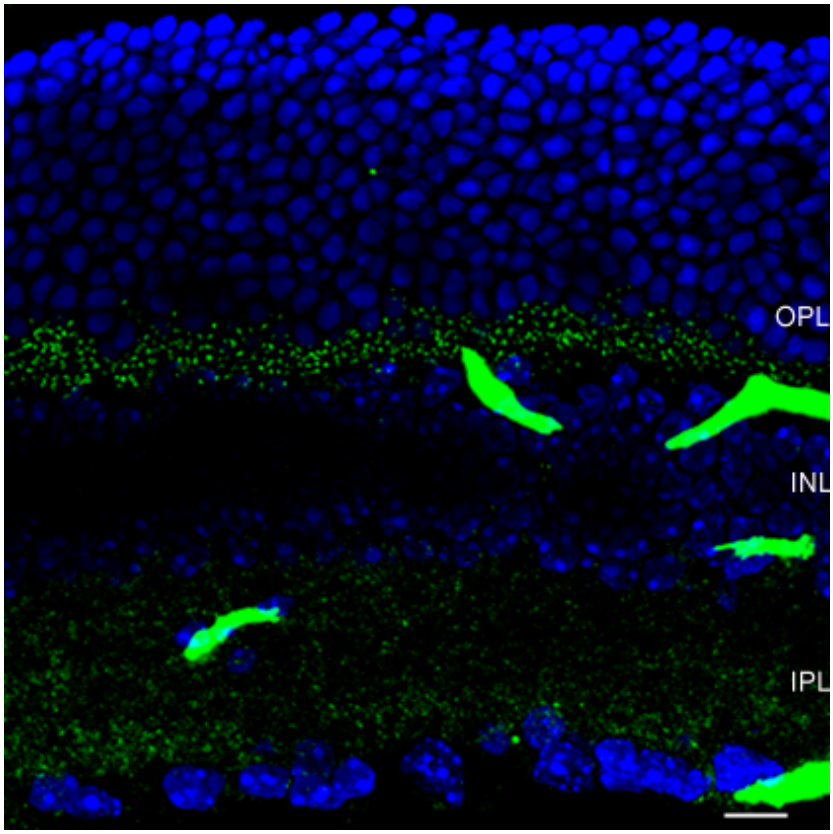

Figure 4.3: Chapsyn110/PSD93 distribution in the mouse retina. Chapsyn110/PSD93-IR appeared as clusters of puncta in the OPL surrounded by sparser puncta. Immunolabeling in the IPL was weak and

punctate. Large blood vessels were strongly labeled throughout the retina. Scale bar: 10 µm.

4.2.1. Chapsyn110/PSD93 is a postsynaptic element of photoreceptor synapses

Chapsyn110 labeling had similar distribution as observed with SAP102 in rabbit suggesting that this scaffold might be post-synaptic in the OPL in mouse retina. HCs dendrites are post-synaptic to photoreceptors and their lateral processes flank a total of two ON bipolar cell dendrites in rods and one or perhaps more dendrites into the cone invaginating synapse. To determine whether Chapsyn110 was associated with ON bipolar cell dendrites, we performed double labeling studies using an antibody to the ON bipolar cell glutamate receptor mGluR6 (Fig. 4.4). ON bipolar cell dendrites were also closely associated with Chapsyn110-IR puncta, but the two were not colocalized. The Chapsyn110-IR puncta were always located above ON bipolar cell dendrites. mGluR6 immunolabeling is located within the dendritic tips of rod and ON-cone bipolar cells and forms a pattern of doublets and clusters, respectively. Our results confirm Chapsyn110 was associated with mGluR6 at both rod spherules and at cone pedicles.

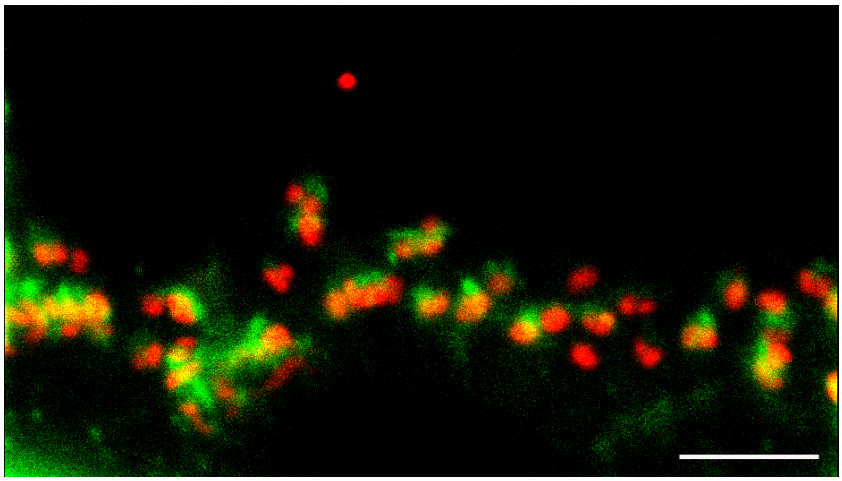

Figure 4.4: **Association of Chapsyn110/PSD93 with synaptic elements in the OPL:** Vertical section through the OPL with labeling of Chapsyn110/PSD93 (green) and mGluR6 (red). The Chapsyn110/PSD93-IR puncta were always located above ON bipolar cell dendrites (mGluR6) in rods and cones. Chapsyn110 was associated with mGluR6 at both rod spherules (isolated doublets of mGluR6) and at cone pedicles (clusters). Scale bar: 10 µm

4.2.2. Chapsyn110/PSD93 is located in horizontal cells.

The lack of co-localization of Chapsyn110/PSD93 immunoreactivity with ON bipolar cell markers and its apparent post-synaptic localization suggests that it may be located in horizontal cells. In the mouse retina, a unique type of axon-bearing HC, which is morphologically similar to B-type HC in the rabbit, sends dendritic processes contacting both cone pedicles and rod spherules (Peichl and Gonzalez-Soriano, 1994). To examine whether Chapsyn110/PSD93 was expressed by horizontal cell dendrites, the lateral elements of the triads, HCs were labeled with antibodies against Calbindin. Double labeling of Chapsyn110/PSD93 with Calbindin revealed that the tips of HC processes were colocalized with Chapsyn110

immunoreactive puncta (Fig. 4.5A-C). Figure 4.6 is a high magnification image showing double labeling of Chapsyn110/PSD93 (green) with Calbindin (blue). Co-localization was complete at the tips of the HC processes, confirming that HCs contain the Chapsyn110/PSD93 clusters.

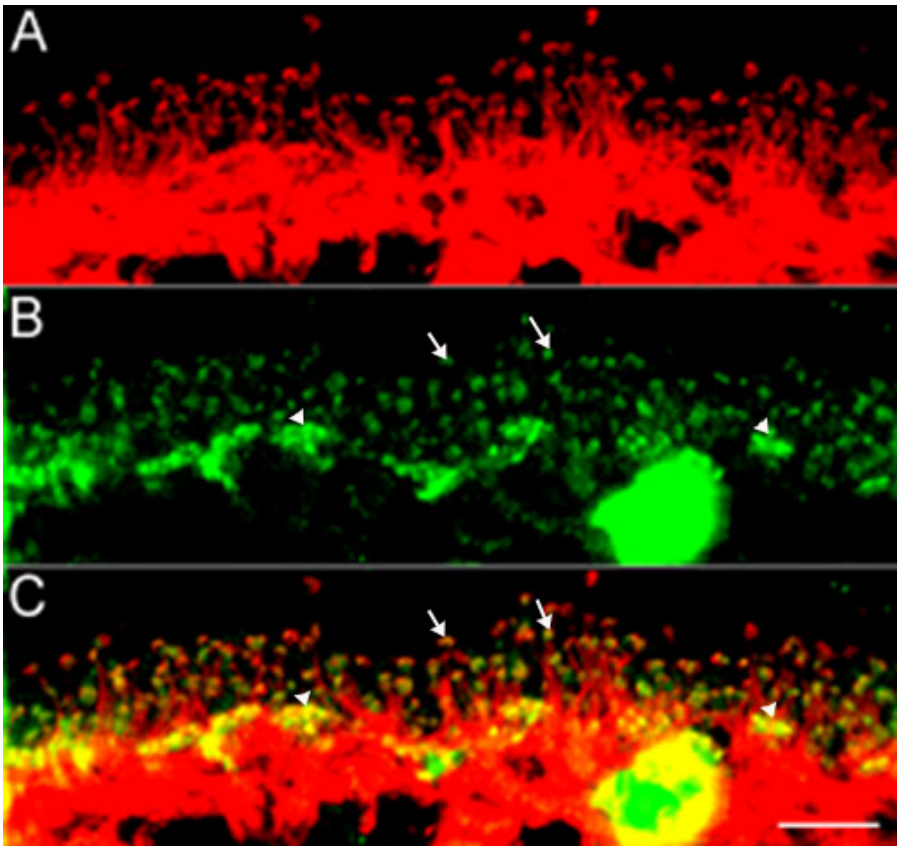

Figure 4.5. Chapsyn110/PSD93 is located in mouse horizontal cells. (A-C) Distribution of Chapsyn110 (green) immunoreactivity relative to Calbindin (red) in the OPL. **B:** Distribution of Chapsyn110 immunoreactivity with strong labeling in the OPL. **(A-C)** Stacks from 17 single optical sections at 0.25 µm increments are shown. Both HC dendrites and axon terminals colocalized with Chapsyn110 at contacts with cone terminals (arrowheads) and rod spherules (arrows) respectively. Scale bars: 10 µm.

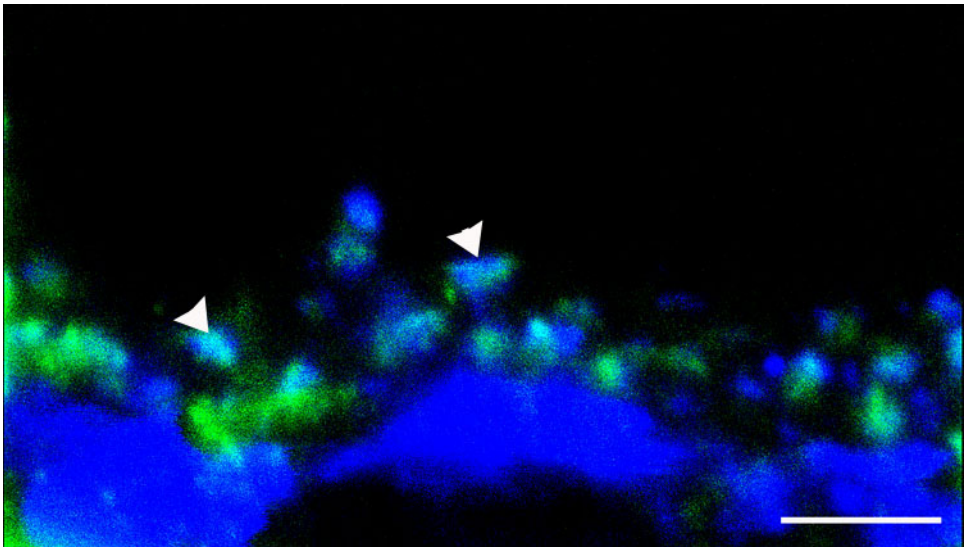

Figure 4.6. High magnification image of Chapsyn110/PSD93 in the tips of HC dendrites. Distribution of Chapsyn110 (green) immunoreactivity relative to Calbindin (blue) in the OPL. Stacks from 10 single optical sections at 0.25 µm increments are shown. The tips of HC dendrites colocalized with Chapsyn110 at contacts with rod spherules (arrows). Scale bars: 10 µm.

4.3. Chapsyn110/PSD93 complex in mouse retina

4.3.1 Chapsyn110 collects inward rectifying channels in HC synapses

We found Chapsyn110 as synaptic scaffold localized at invaginating dendritic tips (cones) and at axon terminals (rod) in the mouse retina. Our first objective was to identify whether Kir2.1 is preserved in HC tips of the mouse. Kir2.1 immunolabeling was diffuse around the somas of HCs surrounded by clusters of puncta in the OPL (Fig. 4.7A). Labeling for Kir2.1 extended to the outermost part of the OPL and sometimes localized to specific areas close to photoreceptors. To

evaluate whether Kir2.1 was present in HCs, we double-labeled sections with antibodies to Kir2.1 and Calbindin, (Fig. 4.7B). Figure 4.7B show Kir2.1 clusters at a cone terminal with surrounding rod spherule contacts. The arrowheads designate Kir2.1 labeling contacting cones and rods are labeled with circles. Kir.2.1 immunoreactivity was found directly colocalized with Calbindin labeling at the invaginated tips of both HC dendritic processes contacting cones and axon terminal processes contacting rods in the OPL. Only Kir2.1 puncta were colocalized in the outermost portion of the OPL, suggesting that Kir2.1 was clustered in the tips of HC processes. High magnification images confirmed colocalization of Calbindin labeled HC dendritic processes with Kir2.1 immunoreactive punctate patterns in the OPL (Fig. 4.8).

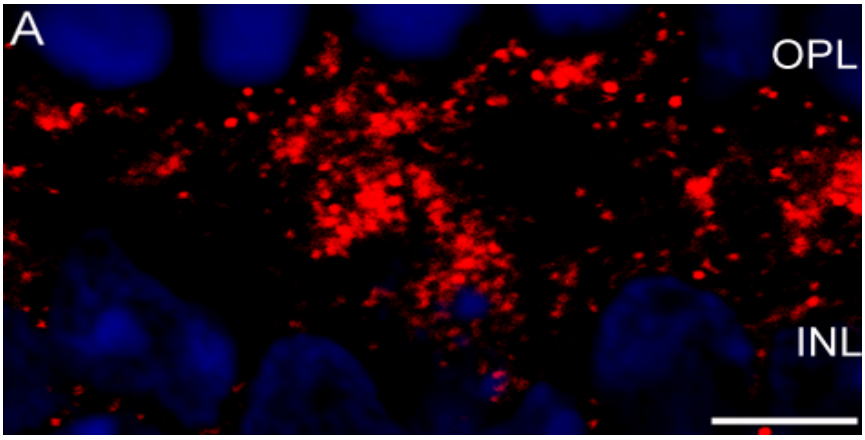

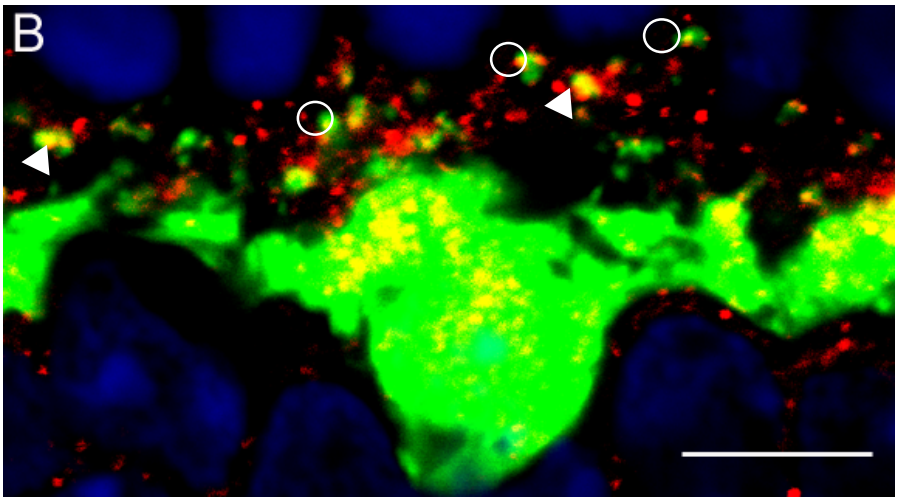

Figure 4.7. Kir2.1 is located in tips of horizontal cells contacting cone and rod photoreceptors. Distribution of Kir2.1 (red) immunoreactivity relative to Calbindin (green) in the OPL. **A:** Distribution of Kir2.1 immunoreactivity exhibited a mixture of diffuse and punctate patterns in the OPL. **(B)** Stacks from 13 single optical sections at 0.25 µm increments are shown. Both HC dendrites and axon terminals colocalized with Kir2.1 at contacts with cone terminals (arrowheads) and rod spherules (circles) respectively. Scale bar: 5 µm.

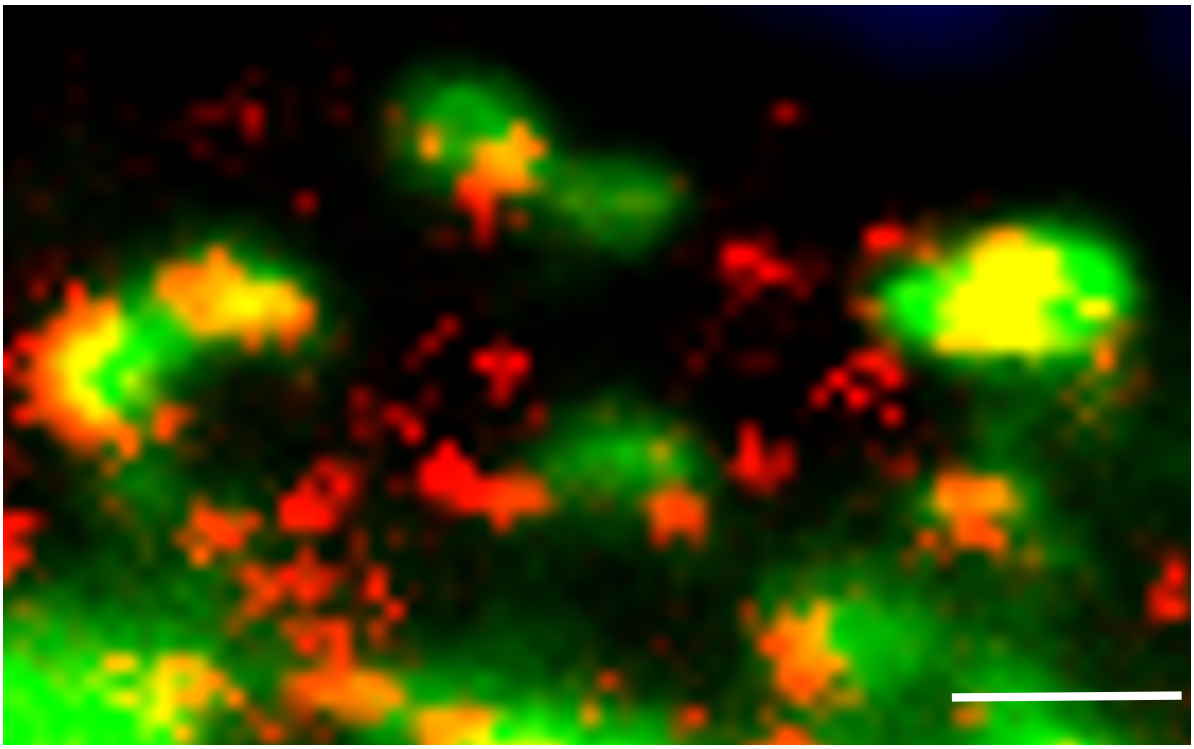

Figure 4.8. High magnification of Kir2.1 in tips of horizontal cells. Distribution of Kir2.1 (red) immunoreactivity relative to Calbindin (green) in the OPL. Distribution of Kir2.1 immunoreactivity exhibited a mixture of diffuse and punctate patterns in the OPL. A single optical section through the OPL shows colocalization of Kir2.1 with HC dendrites. Scale bar: 5 µm.

Double labeling studies with mGluR6 and GluR6/7 appeared to cross-react with each other and other proteins. Further tests should be performed using different fixation conditions to reduce background fluorescence and preserve the epitopes that can be detected with these antibodies. Recent studies suggest that using subclass-specific secondary antibodies matching the IgG subclass of the monoclonal antibody increases specificity of immunolabeling in comparison to standard anti-mouse IgG secondary antibodies (Manning et al., 2012).

4.4. Evidence for pannexin channels in the mouse retina

One of the proposed mechanisms for ephaptic feedback is the presence of hemichannels in the invaginating HCs processes. Although little is known about their regulation hemichannels are presumably voltage independent and provide constant current flow into HCs. There is some immunohistochemical evidence of connexins at the tips of HCs, suggesting they contribute to ephaptic signals (Kamermans et al., 2001). We found strong Pannexin 1 immunolabeling in the OPL, which is consistent with recent findings of Pannexin 1 expression at the lateral elements of the triad synapse (Kranz et al., 2013). Immunoreactive puncta were also present in the inner layers and some Müller cell inner processes were labeled in the GCL (Fig 4.9A). Furthermore, some labeling in the form of small puncta can be seen above the OPL, suggesting pannexin 1 could be present in HC dendrites (Fig 4.9B). Of course, we would need to confirm colocalization of Pannexin 1 channels with calbindin, a known marker that labels HCs in mouse retina.

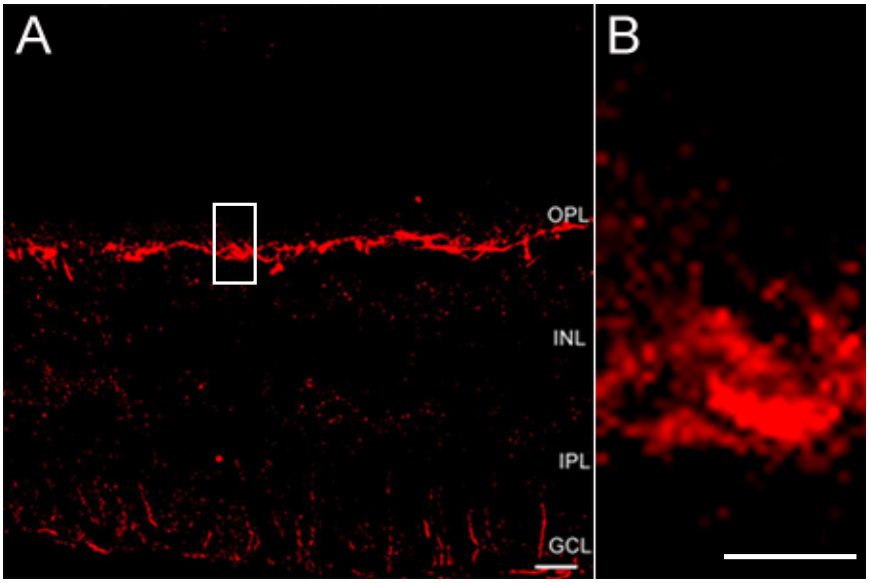

Figure 4.9 Pannexin 1 immunolabeling in the mouse retina. A: Immunolabeling of pannexin 1 was particularly strong in thick processes of the OPL. Some fraction of muller cell processes were labeled near the GCL but no end feet labeling was observed. Labeling was predominantly strong in the form of puncta in the inner layers and above immunoreactive processes the OPL. **B:** High magnification of inset shows Pannexin 1 immunoreactive puntacte labeling above the OPL, suggesting Pannexin 1 is present in HC invaginating processes. Scale bars: 10 and 5 μm respectively

4.5 Changes of polyamine content in the OPL

We know that feedback disappears at night but this effect could be due to the fact that HCs are especially widely coupled causing a reduction of their voltage signals (Pandarinath et al., 2010). Alternatively, it is possible that there is a built in mechanism that regulates the activity of feedback such as polyamines. Many channels are regulated by polyamine binding. One of the key ways that Kir2.1 channel acquires its inward rectification is to polyamines which block the channel when the cell is depolarized and become unblocked and allowed current when the cell hyperpolarizes. We hypothesize that release of polyamines through some unknown mechanism is a natural mechanism that regulates the activity of Kir2.1 as a feedback channel. Polyamine antibodies will allow us to study whether feedback is regulated by the time of the day. For this purpose, we measured different levels of polyamines in day time vs. night time. Polyamines are largely taken up by glia

(Skatchov et al., 2000) but they are made in neurons, suggesting polyamines are released. Through a collaboration with our colleague Dr. Cristophe Ribelayga we used mice from daytime and nightitime conditions. We sampled mice under different light conditions: 1 hour before noon and 1 hour past midnight, corresponding to day and night phase conditions respectively. Muller cells in the retina are involved in potassium homeostasis and express inward rectifying potassium channels (Biedermann et al., 1998). Because polyamines are modulators of these channels we expect to find polyamine immunolabeling concentrated in Müller cells. In Figure 4.10 we stained mouse sections with antibodies against glutamine synthetase to label Müller cells. Double labeling studies show that some of the polyamine labeling in the form of puncta in the inner retinal layers is in Müller cells.

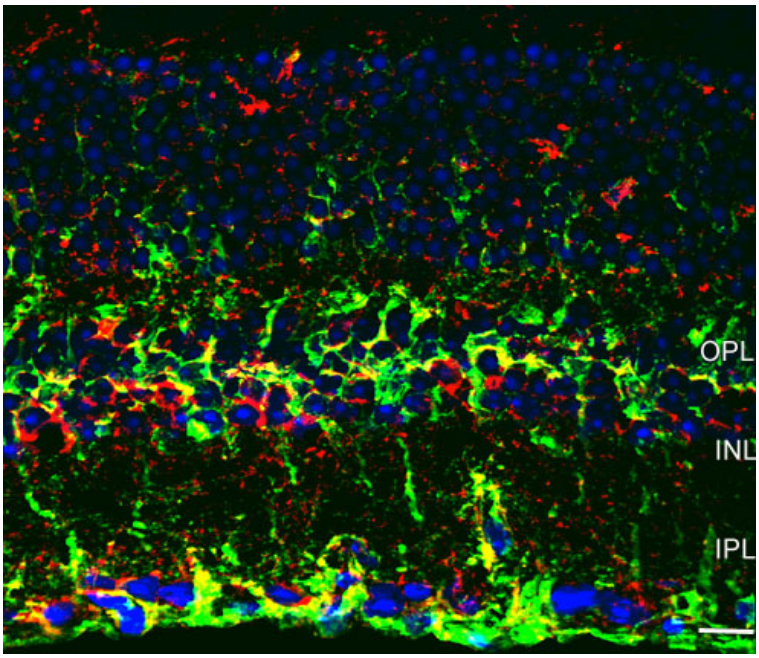

Fig 4.10 Association of Spermine with glial cells in the retina. Distribution of spermine (red) immunoreactivity relative to glutamine synthetase (green) in the

mouse retina. Distribution of polyamine immunoreactivity was sparse throughout the retina. Some of the polyamine labeling was colocalized with the inner layers of the IPL in Müller cells. Stacks from 10 single optical sections at 0.45 µm increments are shown. DAPI is shown in blue. Scale bar: 10 µm.

Figure 4.10 and 4.11 show labeling of mouse retinal sections stained with spermine antibodies from the light phase condition. To our surprise, spermine immunolabeling in these animals appeared to be concentrated in the outer most layer of the OPL corresponding to photoreceptor terminals. Based on these results we sought to investigate whether changes in polyamine content are driven by day light cycles. We stained some sections from animals corresponding to night phase and immunolabeling was specially reduced in the photoreceptor layer (Fig 4.12C) when compared to light phase (Fig 4.12B).

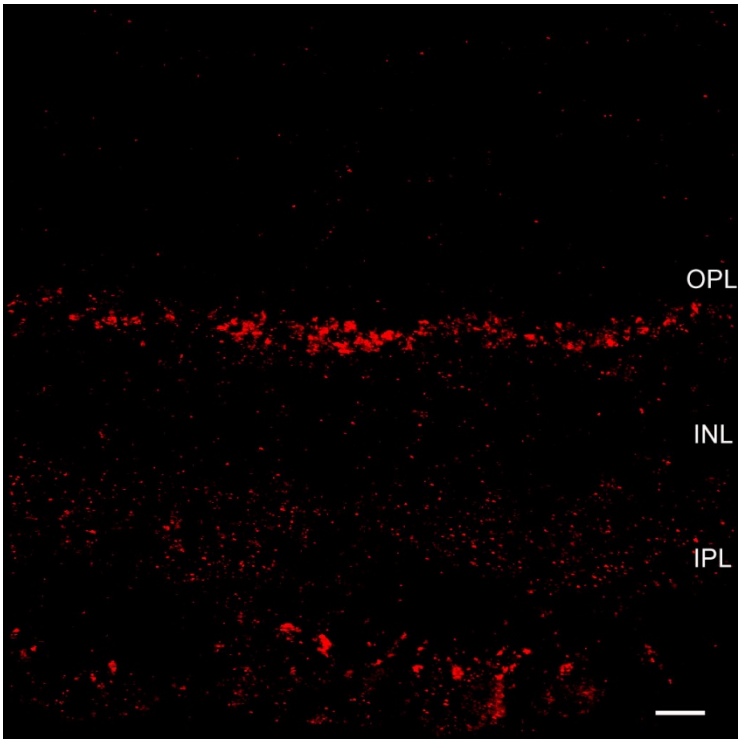

Fig 4.11. Spermine immunolabeling throughout the entire mouse retina. Strong Immunolabeling was confined in photoreceptor terminals in daytime retinal sections. Weak immunoreactive labeling was found in the form of small puncta in the IPL. Some labeling was confined to the most inner portion of the IPL, suggesting spermine labeling is present in bipolar cell terminals. Scale bar: 10 μm.

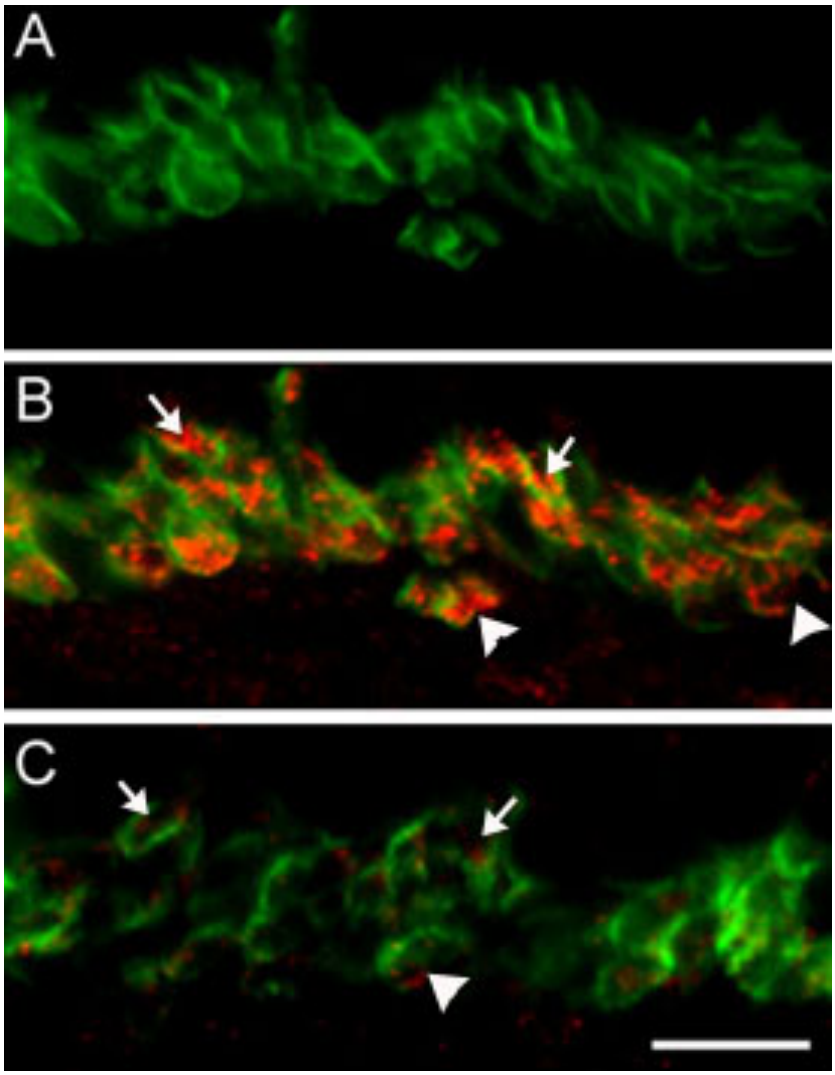

Fig 4.12 Polyamine immunolabeling varied across photoreceptors and with time of the day. All images were taken from OPL in mouse retina. (A) PSD95

monoclonal antibody labeling was used as marker for photoreceptor terminals. Cones were identified as trapezoidal structures weakly stained with PSD95 in the outer ring (arrowheads) whereas rod spherules were analyzed by the typical round shape strongly labeled (arrows). (B) Merged image of A and B. Many photoreceptors were strongly labeled by the spermine antibody in daytime retina, including the cones. We found spermine labeling was not uniformly distributed in the OPL. C: Merge image for spermine and monoclonal anti-PSD95 immunolabeling in nightime retina. Spermine antibody labeling was markedly reduced on photoreceptors in nightime retina, and some photoreceptors showed no labeling at all. Scale bar: 10 μm.

Our results showed an increase in the amount of polyamines present in the photoreceptor terminals during the day vs. night condition, suggesting that polyamine levels are regulated by the time of the day (Fig. 4.12B and C). We measured the amount of polyamines from high magnification optical sections taken in the OPL. These sections were double labeled with PSD95 to visualize the terminals of rod and cone photoreceptors. The amount of spermine labeling in rods and cones was compared between animals from day and night phase (Fig 4.13). Five measurements were taken from each animal corresponding to rods and cones at day and night conditions respectively. A mixed effect model was used to compare intensity measurements from both conditions. There was a significant difference between day conditions ($p<0.001$): on average, at night the intensity was 44.13% less than in day condition. The difference between rods and cones was negligible ($p=0.083$). These findings suggest that polyamines could regulate HC feedback by changing the efficacy by which Kir2.1 channels open up. With more rectification HCs would require more hyperpolarization in the day time and less hyperpolarization at

night bringing out more ephaptic signal at night. The underlying mechanism that controls ephaptic signals is yet to be resolved.

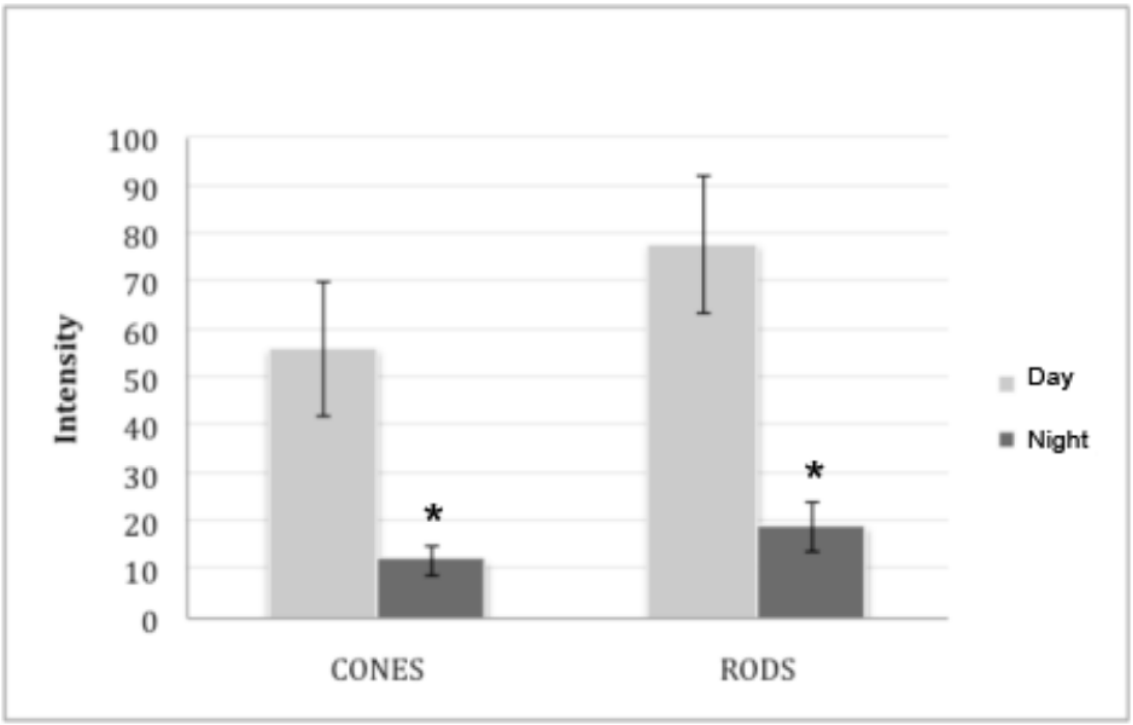

Figure 4.13: Polyamine intensity measurements in the OPL day vs night animals. A total of 5 animals per condition was used. The same level of adjustment for brightness and contrast was maintained across samples. There was no interaction term between time of the day and cell type (p=0.35). This indicated that amount of changes between day and night were similar between rods and cones. Asterisks represent difference between day and night condition is statistically significant

4.5.1 Immunohistochemical evidence for polyamine transporter

We found the amount of polyamines is increased in photoreceptor terminals during the daytime. The differences in polyamine content of photoreceptor terminals could impose different regulatory states on the inward rectifier potassium channels in HCs. Furthermore, polyamines could also potentiate kainate receptors we found in

HCs. We hypothesize this could only work if polyamines are released. Recent evidence suggests that a gene that encodes for vesicular monoamine transporter (SLC18B1) could be involved in the packaging of polyamines (Hiasa et al., 2014). We sought to investigate whether this transporter could be present in photoreceptors, which would suggest that polyamines are packaged into vesicles and are released. To determine whether a vesicular mechanism is present we stained mouse retinas with antibodies against the monoamine transporter SLC18B1. SLC18B1 immunoreactivity was not clearly associated with photoreceptors and may have been present in glial cells (Fig 4.14A). Double labeling studies using PSD95, an antibody which is known to label rod and cone photoreceptor terminals, failed to confirm colocalization with SLC18B1 immunoreactivity (Fig 4.14B). To our knowledge this is the first report examining vesicular polyamine transporter localization in the retina.

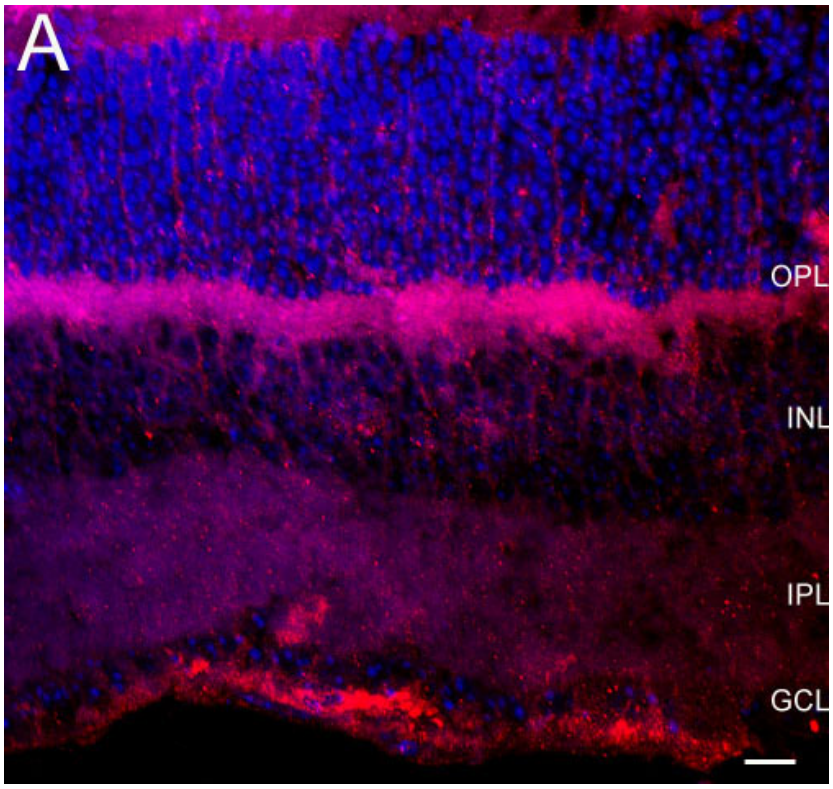

Fig 4.14A. Distribution of vesicular polyamine transporter SLC18B1 in the mouse retina. Immunoreactivity for an antibody against the gene that encodes a vesicular polyamine transporter (red) was abundant in the photoreceptor layer and labeled processes spanning across the entire retina consistent with glial cells. Some labeling was observed in the end feet of Muller cells. Scale bar: 10 μm.

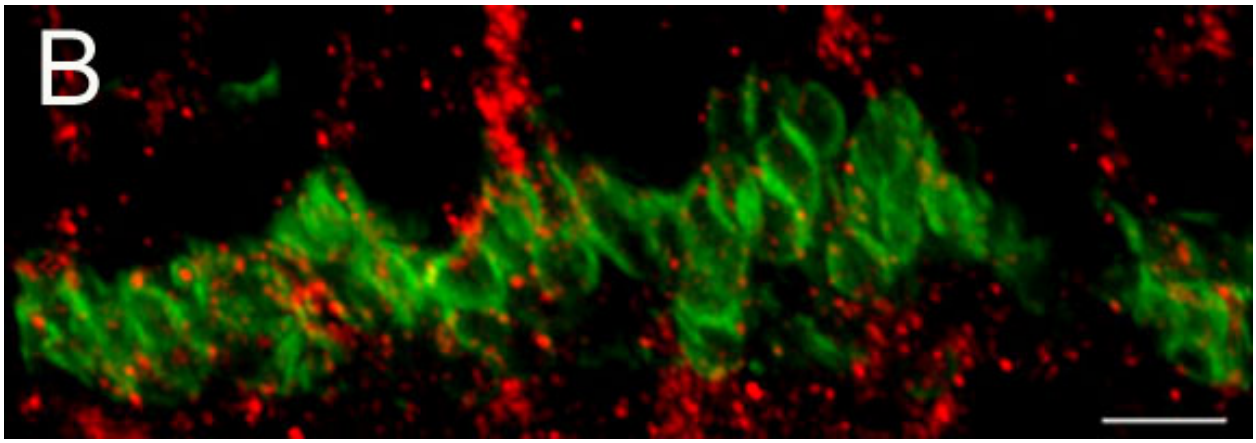

Fig 4.14B. Distribution of vesicular polyamine transporter SLC18B1 in the OPL. Immunoreactivity for an antibody against the gene that encodes a vesicular polyamine transporter (red) was sparse and labeled processes surrounding the photoreceptors. Immunostaining was absent in photoreceptor terminals as demonstrated with lack of colocalization with PSD95 (green) antibodies Scale bar: 5 µm.

4.6 DISCUSSION:

In contrast to SAP102 and Chapsyn110/PSD93 being present as post-synaptic scaffolds in rabbit, we found only the latter in HC tips of the mouse retina. Furthermore, Kir2.1 immunoreactive puncta were present in the tips of HCs reinforcing the idea that this channel could play a role in regulating synaptic communication between HCs and cone photoreceptors. Kir2.1 channel immunoreactivity was similar to what we found in rabbit.

We hypothesize Kir2.1 is a feedback channel. The polyamines spermidine, spermine and putrescine are essential for cell growth in both eukaryotic and

prokaryotic systems. Polyamines are composed of single carbon chains with amino groups attached to them that become protonated at physiological pH. Under these conditions their chemical structure interacts with negatively charged molecules including nucleic acids and a variety of ion channels (Williams, K 1997). In the retina, spermine is found to modulate inward rectifying currents through K^+ channels (Solessio et al., 2001). Activation of Kir channels is associated with hyperpolarization and binding of polyamines to internal residues within the channel pore which appears to be essential for blocking of the channel. (Igarashi and Kashiwagi, 2010; Pegg, 2016. Refer to Figure 1.7 and 1.8 taken from Traynelis et al., 2010.

During depolarization, the channel becomes blocked by Mg^{2+} and polyamines (Fakler et al., 1995) and outward current decreases, suggesting the pore conducts K^+ ions only at negative membrane potentials. On hyperpolarization, the inward current increases by unblocking Mg^{2+} and polyamines from the channel pore just like NMDA receptors when they depolarize. We hypothesized that polyamines regulate the opening and closing of Kir2.1 channel. The higher the internal concentration of polyamines is the more blocked the channel is and more hyperpolarization is required to activate Kir2.1. This provides an opportunity for the cell to regulate its activity metabolically. Thus, polyamines could reduce the contribution of Kir2.1 to ephaptic feedback. Our measurements of polyamine content suggests there is a natural mechanism to regulate the activity of Kir2.1 channel. See Figures 4.12 B and C.

We used commercially available antibodies against polyamines to measure whether the amount of polyamines change at different times of the day. This would

suggest that the inward rectification properties of Kir2.1 could be regulated by changes in polyamine content. To our surprise, polyamine immunolabeling was confined to photoreceptor terminals. Though other areas of the retina were immunoreactive for polyamine content, labeling was specially prominent in the OPL. Furthermore, we found significant increase in the amount of polyamines present in photoreceptors during the day. Given the proximity of photoreceptor terminals to HC processes it is possible polyamines can be released by some unknown mechanism and modulate the activity of Kir2.1 channels at the tips of these cells. Some evidence points to polyamine release by uptake mechanisms in brain synaptosomes (Masuko et al., 2003). This would suggest that polyamines can be released and transported back into the cell via vesicular mechanism. In support to our hypothesis, a vesicular monoamine transporter (VMAT) family was associated with the vesicular storage of polyamines in neurons (Hiasa et al., 2014). Immunolabeling for this transporter did not reveal its presence in photoreceptors. However, we cannot rule out the possibility that a different transporter may package polyamines into vesicles in photoreceptors.

Our results suggest polyamines are regulated by the time of the day. If polyamines are released then they could potentially reduce the contribution of Kir2.1 for ephaptic feedback causing more rectification and require more hyperpolarization to open the channels in a day time. The underlying mechanism of polyamine release is unknown but we think some type of vesicular transporter is involved. Whether polyamines are released via vesicular mechanism or transporters remains to be elucidated.

Chapter 5. FUTURE DIRECTIONS:

Our study shows how the unique assembly of suites of proteins are anchored by synaptic scaffolds at invaginating processes of photoreceptors terminals. We found SAP102 and Chapsyn110 are associated with photoreceptor synapses that formed a complex containing GluR6/7 and Kir2.1 in the tips of HCs. However, Chapsyn110 is more likely to be the key synaptic scaffold since it is present in both rabbit and mouse. Together these findings suggest this complex plays a role in synaptic signaling. Our synaptic model includes the presence of Chapsyn110 scaffold together with GluR6/7 and Kir2.1 channels forming a complex near the release sites. See model below.

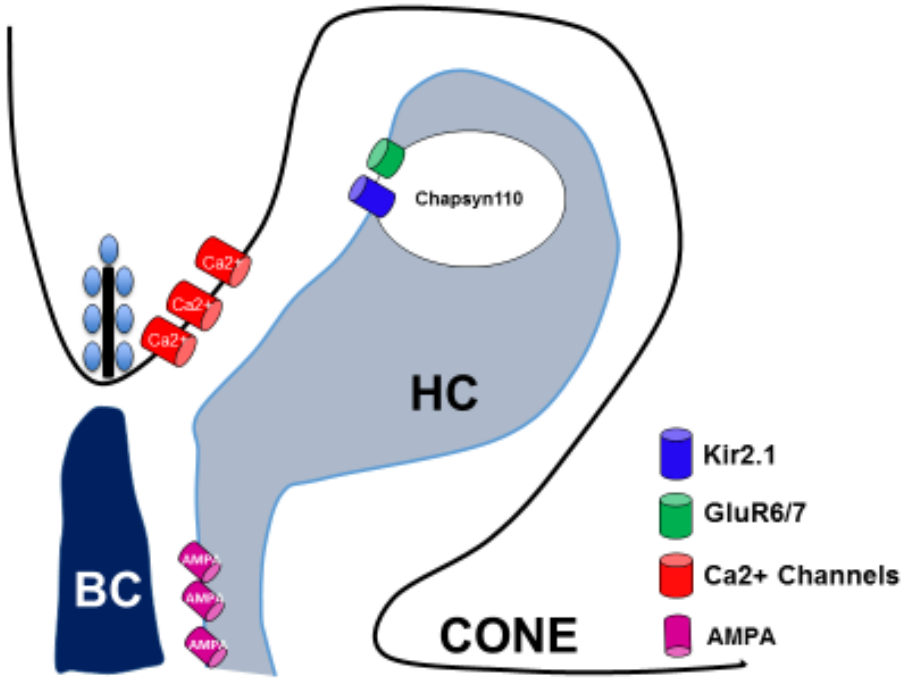

Scaffolds anchors a complex: implications for synaptic signaling

We hypothesize that Chapsyn110/PSD93 is required to hold the complex in place to direct the signals to the invaginated synaptic cleft. To test this hypothesis we would use knockout models to determine whether immunoreactivity for GluR6/7 and Kir2.1 is reduced in the outer retina where HCs receive photoreceptors inputs. By comparing labeling with wild type animals we would confirm whether Chapsyn110 is the key synaptic scaffold that assembles its binding partners in the photoreceptor synapse.

Kainate receptor subunit GluR6/7:

We hypothesize GluR6/7 receptors contribute to feedback of HCs to rod and cone photoreceptors. The AMPA receptors dominate the polarization of HCs but in rabbit these receptors have GluR2 which is not Ca^{2+} permeable (Pan et al., 2007). Recently, AMPA receptor GluR4 subunit knockout reveals a small residual kainate receptor current in mouse HCs (Ströh et al., 2013). We found kainate receptors (GluR6/7) at the tips of HCs being anchored up in the cleft near the release sites. One possibility is that a portion of that Ca^{2+} current flowing through GluR6/7 subunits of kainate receptors could be used to drive GABA release and reduce HC feedback (Liu et al., 2013). To test whether kainate receptors contribute to acidification of the synaptic cleft we would need to measure local changes in pH and compared them at depolarized and hyperpolarized conditions.

Kir2.1 could participate in ephaptic signaling:

The underlying mechanism that generates ephaptic feedback is controversial. The original hypothesis proposed positive feedback effects via open channels at the tips of HC dendrites; however HC cells generate negative feedback signals in the dark by relieving lateral inhibition, suggesting the presence of different type of channels in these cells. We found Kir2.1 channels are anchored by Chapsyn110 in the invaginating synapses contacting photoreceptors. We do not know whether Kir2.1 plays a physiological role but localization of the channel deep in the cleft is consistent with having functional significance in HC signaling. Unlike other channels, inward rectifying channels contribute to K^+ conductances when cells are hyperpolarized and they turn off upon depolarization. This particular characteristic makes Kir2.1 channels attractive for the generation of ephaptic signals.

It is well established that the inward rectification of Kir2.1 can be blocked by external barium or cesium. This offers the possibility to test pharmacologically whether this channel contributes to the generation of ephaptic signals from HCs to cone phototoreceptors. Our colleague Wallace Thoreson tested the effects of blocking inward rectifying channels using cone-horizontal cell pair recordings to different voltage clamp steps and measuring calcium currents with 10 mM CsCl in amphibian slices (personal communication). However, blocking the channel did not have any effect on the development of the shift of the Ca^{2+} activation curve of the cones. It is unknown whether Kir2.1 plays a role on the amplitude or kinetics of the response. It could be that Kir2.1 channels are simply not present in the invaginating processes of amphibian species.

Alternatively, we could measure whether Kir2.1 plays a role on ephaptic feedback using a conditional knockout mouse line where the channel is not expressed in horizontal cells. This could be accomplished by crossing an already available knockin mouse line expressing a Cre recombinase under the promoter of Cx57 (Ströh et al., 2013) with mouse line in which coding sequence for Kir2.1 is flanked by two loxP sites. To test whether Kir2.1 channel plays a role in ephaptic feedback we would expect to see a change in the polarization of the cones. We could record from cones in whole mount preparations using a large size annulus to maximize feedback signals and record light responses of the cones.

Polyamines could regulate signaling through the day or could be regulating Gi signaling:

Polyamines are associated with increase rectification of Kir2.1 channels. We used antibodies to measure whether changes in polyamine content are regulated by the time of the day. One hypothesis is that polyamines are released by photoreceptor terminals and regulate feedback by blocking the inward rectifier channel found directly apposed to release sites in the synaptic invagination. It is unknown whether polyamines are released by photoreceptors. However, a vesicular amino transporter was recently identified in purified brain preparations suggesting a possible release mechanism for polyamines (Hiasa et al., 2014). We performed immunolabeling with antibodies raised against a gene that encodes for this vesicular polyamine transporter but immunoreactivity was only found in glia. Together these results are not consistent with vesicular release of polyamines from photoreceptors

due to lack of colocalization with PSD95 and the transporter. However, we cannot rule out the possibility that other transporters are present in photoreceptor terminals.

Our measurements show high level of polyamines in photoreceptor terminals during the day and low levels at night suggesting a natural mechanism to regulate the activity of feedback. However, it is unclear whether light adaptation mediates changes in the amount of polyamine being released. This is a group of animals we did not include in our experimental paradigm. Thus, from our experiments we cannot determine whether the difference between day and night times is circadian driven or light adaptation driven.

One potential alternative to the release mechanism is whether polyamines regulate photoreceptor behavior. Giα is the type of G protein that is regulating Adenylate cyclase (AC) in photoreceptors. Dopamine receptor (D4) and Adenosine receptors (A1) are coupled to Giα in photoreceptors. Spermine has been found to regulate Giα proteins by inhibiting GTPase activity (Daeffler et al., 1999). This would prolong the activated state of Giα. Thus, we would expect in the day time activation by dopamine and very low activation of adenosine receptors to be enhanced (meaning the action of AC would be enhanced) by the polyamine content we found. At night time, on the other hand, we would expect less polyamine and less DA prolonging the activation of Giα, suggesting polyamine metabolism may regulate AC through its effects on G proteins. D4 receptor signaling and AC activity both control photoreceptor coupling as well as photoreceptor calcium channel activity (Li et al., 2013).

Components for ephaptic mechanism in HCs:

The presence of gap junctions and pannexin channels has been associated with ephaptic feedback signaling (Kamermans et al., 2001; Klaassen et al., 2011). Our immunolabeling of connexin channels is consistent with gap junctional expression in the OPL but our antibodies did not colocalize with synaptic scaffolding proteins. We found strong Pannexin 1 immunoreactivity in processes above the OPL, consistent with the ability of this channel to provide a current source for ephaptic feedback. Because HCs release ATP via Pannexin channels their unique localization in the invaginating processes of the photoreceptor synapse is consistent with proton-mediated feedback (Vroman et al., 2014). Presumably, Pannexin 1 channels localized in the tips of HCs release ATP in the cleft and is hydrolyzed to protons and phosphate buffers producing an acidification of the cleft and inhibiting the calcium current of the cone photoreceptor. We would need to confirm whether Pannexin 1 labeling is localized to tips of HCs by performing double labeling studies with Calbindin, a marker that labels horizontal cells in mammalian retina.

.

LITERATURE CITED

Anastassiou C, Koch C. 2015.Ephaptic coupling to endogenous electric field activity: why bother?. Current Opin Neurobiol (31):95-103

Bader C, Bertrand D, Schwartz E. 1982. Voltage-activated and calcium-activated current studied in solitary rod inner segments from the salamander retina. J. Physiol 80:517-536

Barnes S, Bui Q. 1991. Modulation of calcium-activated chloride current via pH-induced changes of calcium channel properties in cone photoreceptors. J Neurosci 11(12):4015-4023

Barnes S, Merchant V, Mahmud F. 1993. Modulation of transmission gain by protons at the photoreceptor output synapse. PNAS 90(21): 10081-10085

Baylor D, Fuortes, M, O'Bryan P. 1971. Receptive fields of cones in the retina of the turtle. J Physiology 214, 265-294

Bichet D, Haass F, Jan L. 2003. Merging functional studies with structures of inward-rectifer K channels. Nature Reviews Neuroscience 4:957-967

Biedermann B[1], Skatchkov SN, Brunk I, Bringmann A, Pannicke T, Bernstein HG, Faude F, Germer A, Veh R, Reichenbach A. 1998. Spermine/spermidine is expressed by retinal glial (Müller) cells and controls distinct K+ channels of their membrane. Glia_;23(3):209-20.

Brecha N, Lee H. 2010. Immunocytochemical evidence for SNARE protein-dependent transmitter release from guinea pig horizontal cells. EJN 31(8): 1388-1401

Bowie D, Garcia EP, Marshall J, Traynelis SF, Lange GD. 2003. Allosteric regulation and spatial distribution of kainate receptors bound to ancillary proteins. J Physiol 547(Pt 2):373-385.

Bruzzone R, Hormuzdi SG, T. Barbe M, Herb A, Monyer H. 2003. Pannexins, a family of gap junction proteins expressed in brain. PNAS:2233464100.

Burkhardt DA. 1993. Synaptic feedback, depolarization, and color opponency in cone photoreceptors. Vis Neurosci 10(6):981-989.

Byzov AL, Shura-Bura TM. 1986. Electrical feedback mechanism in the processing of signals in the outer plexiform layer of the retina. Vision Res 26(1):33-44.

Cadetti L, Thoreson WB. 2006. Feedback effects of horizontal cell membrane potential on cone calcium currents studied with simultaneous recordings. J Neurophysiol 95(3):1992-1995.

Cai C, Coleman SK, Niemi K, Keinanen K. 2002. Selective binding of synapse-associated protein 97 to GluR-A alpha-amino-5-hydroxy-3-methyl-4-isoxazole propionate receptor subunit is determined by a novel sequence motif. J Biol Chem 277(35):31484-31490.

Catterall W, Few A. 2008. Channel regulation and presynaptic plasticity. Neuron 59(6): 882-901

Chen XH, Tsien RW.1997. Aspartate substitutions establish the concerted action of P-region glutamates in repeats I and III in forming the protonation site of L-type Ca2+ channels. *The Journal of Biological Chemistry*. 28;272(48):30002-8
.

Chen X, Levy JM, Hou A, Winters C, Azzam R, Sousa AA, Leapman RD, Nicoll RA, Reese TS. 2015. PSD-95 family MAGUKs are essential for anchoring AMPA and NMDA receptor complexes at the postsynaptic density. Proc Natl Acad Sci U S A 112(50):E6983-6992.

Ciolofan C, Lynn BD, Wellershaus K, Willecke K, Nagy JI. 2007. Spatial relationships of connexin36, connexin57 and zonula occludens-1 in the outer plexiform layer of mouse retina. Neuroscience 148(2):473-488.

Cuthbert PC, Stanford LE, Coba MP, Ainge JA, Fink AE, Opazo P, Delgado JY, Komiyama NH, O'Dell TJ, Grant SG. 2007. Synapse-associated protein 102/dlgh3 couples the NMDA receptor to specific plasticity pathways and learning strategies. J Neurosci 27(10):2673-2682.

Darstein M, Petralia RS, Swanson GT, Wenthold RJ, Heinemann SF. 2003. Distribution of kainate receptor subunits at hippocampal mossy fiber synapses. J Neurosci 23(22):8013-8019.

Deans MR, Paul DL. 2001. Mouse horizontal cells do not express connexin26 or connexin36. Cell Adhes Commun 8(4-6):361-366.

Dedek K, Pandarinath C, Alam NM, Wellershaus K, Schubert T, Willecke K Prusky G,Weiler R, Nirenberg S. 2008. Ganglion Cell Adaptability: Does the Coupling of Horizontal Cells Play a Role? PLoS ONE 3(3): e1714.

Deng Q, Wang L, Dong W, He S. 2006. Lateral components in the cone terminals of the rabbit retina: Horizontal cell origin and glutamate receptor expression. The Journal of Comparative Neurology 496(5):698-705

DeVries SH (2001) Exocytosed protons feedback to suppress the Calcium current in mammalian cone photoreceptors. Neuron 32:1107–1117.

Dmitriev AV, Mangel SC. 2006. Electrical feedback in the cone pedicle: a computational analysis. J Neurophysiol 95(3):1419-1427.

Doering CJ, McRory JE. 2007. Effects of extracellular pH on neuronal calcium channel activation. Neuroscience. 25;146(3):1032-43.

Dong C, Werblin F. 1995. Inwardly rectifying potassium conductance can accelerate the hyperpolarizing response in retinal horizontal cells. J Neurophysiolo 74(6):2258-65

Egebjerg J, Heinemann SF. 1993. Ca2+ permeability of unedited and edited versions of the kainate selective glutamate receptor GluR6. Proc Natl Acad Sci U S A 90(2):755-759.

Endeman D, Fahrenfort I, Sjoerdsma T, Steijaert M, Eikelder H. 2012. Chloride currents in cones modify feedback from horizontal cells to cones in goldfish retina. The Journal of Physiology 590 (22): 5581-5595

Fahrenfort I, Klooster J, Sjoerdsma T, Kamermans M. 2005. The involvement of glutamate-gated channels in negative feedback from horizontal cells to cones.

Progress in Brain Research 147:219-229

Fahrenfort I, Steijaert M, Sjoerdsma T, Vickers E, Ripps H, van Asselt J, Endeman D, Klooster J, Numan R, ten Eikelder H, von Gersdorff H, Kamermans M. 2009. Hemichannel-mediated and pH-based feedback from horizontal cells to cones in the vertebrate retina. PLoS One 4(6):e6090.

Ficker, E., Taglialatela, M., Wible, B. A., Henley, C. M., and Brown, A. M. (1994). Spermine and spermidine as gating molecules for inward rectifier K^+ channels. *Science* 266 1068–1072. doi: 10.1126/science.7973666

Forgac M , Cantley L, Wiedenmann B, Altstiel L, Branton D. 1983. Clathrin-coated vesicles contain an ATP-dependent proton pump. Proc Natl Acad Sci U S A. 1983 Mar; 80(5): 1300–1303.

Gastinger MJ, Barber AJ, Vardi N, Marshak DW. 2006. Histamine receptors in mammalian retinas. J Comp Neurol 495(6):658-667.

Giovannardi S, Forlani G, Balestrini M, Bossi E, Tonini R, Sturani E, Peres A, Zippel R. 2002. Modulation of the inward rectifier potassium channel IRK1 by the Ras signaling pathway. J Biol Chem 277(14):12158-12163.

Glanzman D. 2010. Common Mechanisms of Synaptic Plasticity in Vertebrates and Invertebrates. Current Biology. Minireview 20(1):R31-R36

Guo C, Hirano A, Stella S, Bitzer M, Brecha N (2010) Guinea pig horizontal cells express GABA, the GABA-synthesizing enzyme GAD_{65}, and the GABA vesicular transporter. JCN 518 (10): 1647-1669

Hartline H, Ratliff F. 1957. Inhibitory interaction of receptor units in the eye of limulus.

Haverkamp S, Grunert U, Wassle H. 2000. The cone pedicle, a complex synapse in the retina. Neuron 27(1):85-95.The Journal of General Physiology 40 (3): 357-376

Haverkamp S, Grunert U, Wassle H. 2001a. Localization of kainate receptors at the cone pedicles of the primate retina. J Comp Neurol 436(4):471-486.

Haverkamp S, Grunert U, Wassle H. 2001b. The synaptic architecture of AMPA receptors at the cone pedicle of the primate retina. J Neurosci 21(7):2488-2500.

Hiasa M, Miyaji T, Haruna Y, Takeuchi T, Harada Y, Moriyama S, Yamamoto A, Omote H, Moriyama Y. 2014. Identification of a mammalian vesicular polyamine transporter. Scientific Reports 4 Article number: 6836

Hibino H, Inanobe A, Furutani K, Murakami S, Findlay I, Kurachi Y. 2010. Inwardly rectifying potassium channels: their structure, function, and physiological roles. Physiol Rev 90(1):291-366.

Hille B (2001) Ion channels of excitable membranes, Ed 3, p 294. Sunderland, MA: Sinauer.

Hirano AA, Liu X, Boulter J, Grove J, Perez de Sevilla Muller L, Barnes S, Brecha NC. 2016. Targeted Deletion of Vesicular GABA Transporter from Retinal Horizontal Cells Eliminates Feedback Modulation of Photoreceptor Calcium Channels. eNeuro 3(2).

Hirasawa H, Kaneko A. 2003. pH changes in the invaginating synaptic cleft mediate feedback from horizontal cells to cone photoreceptors by modulating Ca2+ channels. J Gen Physiol 122(6):657-671.

Igarashi K, Kashiwaqi K. 2010. Characteristics of cellular polyamine transport in prokaryotes and eukaryotes. Plant Physiolo Biochem 48(7):506-12

Iijima T, Ciani S, Hagiwara S. 1986. Effects of the external pH on Ca channels: Experimental studies and theoretical consideration using a two-site, two-ion model. Proc Nat Acad Sci USA 83:654-658

Jackman SL, Babai N, Chambers JJ, Thoreson WB, Kramer RH. 2011. A positive feedback synapse from retinal horizontal cells to cone photoreceptors. PLoS Biol 9(5):e1001057.

Jacoby J, Kreitzer MA, Alford S, Qian H, Tchernookova BK, Naylor ER, Malchow RP. 2012. Extracellular pH dynamics of retinal horizontal cells examined using electrochemical and fluorometric methods. J Neurophysiol 107(3):868-879.

Johnson J, Chen T, Rickman D, Evans C, Brecha N (1996) Multiple γ-aminobutyric acid plasma membrane transporters (GAT-1, GAT-2, GAT-3) in the rat retina. JCN 375 (2):212-224

Kamermans M, Spekreijse H. 1999. The feedback pathway from horizontal cells to cones. A mini review with a look ahead. Vision Res 39(15):2449-2468.

Kamermans M, Fahrenfort I, Schultz K, Janssen-Bienhold U, Sjoerdsma T, Weiler R. 2001. Hemichannel-mediated inhibition in the outer retina. Science 292(5519):1178-1180.

Kamermans M, Fahrenfort I, Sjoerdsma. 2002. GABAergic modulation of ephaptic feedback in the outer retina. IOVS Vol 43, 2920

Kamermans M, Fahrenfort I. 2004. Ephaptic interactions within a chemical synapse: hemichannel-mediated ephaptic inhibition in the retina. Curr Opin Neurobiol 14(5):531-541.

Kamboj,S. K. , Swanson,G. T. & Cull-Candy,S. G. 1995. Intracellular spermine confers rectification on rat calcium-permeable AMPA and kainate receptors. J. Physiol. (Lond.) 486, 297–303.

Kaneko A. 1971. Electrical connexions between horizontal cells in the dogfish retina. The Journal of Physiology 213 (1): 95-105

Katsumata O, Ohara N, Tamaki H, Niimura T, Naganuma H, Watanabe M, Sakagami H. 2009. IQ-ArfGEF/BRAG1 is associated with synaptic ribbons in the mouse retina. Eur J Neurosci 30(8):1509-1516.

Kemmler R, Schultz K, Dedek K, Euler T, Schubert T. 2014. Differential regulation of cone calcium signals by different horizontal cell feedback mechanisms in the mouse retina. J Neurosci 34(35):11826-11843.

Klaassen LJ, Fahrenfort I, Kamermans M. 2012. Connexin hemichannel mediated ephaptic inhibition in the retina. Brain Res 1487:25-38.

Kolb and Nelson 1983. Kolb H, Nelson R. Rod pathways in the retina of the cat. Vision Res 23: 301–312, 1983

Koulen P. 1999. Localization of synapse-associated proteins during postnatal development of the rat retina. Eur J Neurosci 11(6):2007-2018.

Koulen P, Fletcher EL, Craven SE, Bredt DS, Wassle H. 1998a. Immunocytochemical localization of the postsynaptic density protein PSD-95 in the mammalian retina. J Neurosci 18(23):10136-10149.

Koulen P, Garner CC, Wassle H. 1998b. Immunocytochemical localization of the synapse-associated protein SAP102 in the rat retina. J Comp Neurol 397(3):326-336.

Krafte DS, Kass RS (1988) Hydrogen ion modulation of Ca channel current in cardiac ventricular cells. J Gen Physiol 91:641-657.

Kranz K, Dorgau B, Pottek M, Herrling R, Schultz K. 2013. Expression of Pannexin1 in the outer plexiform layer of the mouse retina and physiological impact of its knock-out. J Comp Neurol 521(5): 1119–1135.

Kreitzer MA, Collis LP, Molina AJ, Smith PJ, Malchow RP. 2007. Modulation of extracellular proton fluxes from retinal horizontal cells of the catfish by depolarization and glutamate. J Gen Physiol 130(2):169-182.

Kurata H, Zhu E, Nichols C. 2010. Locale and chemistry of spermine binding in the archetypal inward rectifier Kir2.1. J Gen Physiol 135: 495-508

Lee H, Brecha N. 2010. Immunocytochemical evidence for SNARE protein-dependent transmitter release from guinea pig horizontal cells. Eur J Neurosci. 2010 Apr;31(8):1388-401

Leonoudakis D, Conti LR, Anderson S, Radeke CM, McGuire LM, Adams ME, Froehner SC, Yates JR, 3rd, Vandenberg CA. 2004. Protein trafficking and anchoring complexes revealed by proteomic analysis of inward rectifier potassium channel (Kir2.x)-associated proteins. J Biol Chem 279(21):22331-22346.

Leuchowius KJ, Weibrecht I, Soderberg O. 2011. In situ proximity ligation assay for microscopy and flow cytometry. Current protocols in cytometry / editorial board, J Paul Robinson, managing editor [et al] Chapter 9:Unit 9 36.

Li H, Chuang AZ, O'Brien J. 2009. Photoreceptor coupling is controlled by connexin 35 phosphorylation in zebrafish retina. J Neurosci 29(48):15178-15186.

Li H, Zhang Z, Blackburn MR, Wang SW, Ribelayga CP, O'Brien J. 2013. Adenosine and Dopamine Receptors Coregulate Photoreceptor Coupling via Gap Junction Phosphorylation in Mouse Retina. J Neurosci 33(7):3135-3150.

Lin B, Masland RH, Strettoi E. 2009. Remodeling of cone photoreceptor cells after rod degeneration in rd mice. Exp Eye Res 88(3):589-599.

Liu X, Hirano AA, Sun X, Brecha NC, Barnes S. 2013. Calcium channels in rat horizontal cells regulate feedback inhibition of photoreceptors through an unconventional GABA- and pH-sensitive mechanism. J Physiol 591(13):3309-3324.

Lüscher C, Malenka R. 2012. NMDA Receptor-Dependent Long-Term Potentiation and Long-Term Depression (LTP/LTD). Cold Spring Harb Perspect Biol. 4(6): a005710

Manning C, Bundros A, Trimmer J. 2012. Benefits and Pitfalls of Secondary Antibodies:
Why Choosing the Right Secondary Is of Primary Importance. PLOS ONE 7:e38313

Masuko T, Kusama-Eguchi K, Sakata K, Kusama T, Chaki S, Okuyama S, Williams K,Kashiwagi K, Igarashi K. 2003. Polyamine transport, accumulation, and release in brain. J Neurochem.84(3):610-7.

McMahon D, Knapp A, Dowling J. 1989. Horizontal cell gap junctions: single-channel conductance and modulation by dopamine. Proceedings of the National Academy of Science (USA) 86, 7639-7643

Miller R. 2004. D-Serine as a glial modulator of nerve cells. Glia 47(3):275-83

Mills SL, Massey SC. 1994. Distribution and coverage of A- and B-type horizontal cells stained with Neurobiotin in the rabbit retina. Visual Neuroscience 11(3):549-560.

Mills SL, O'Brien J, Li W, O'Brien J, Massey S. 2001. Rod pathways in the mammalian retina use connexin 36. JCN 436(3):336-350

Molina AJ, Verzi MP, Birnbaum AD, Yamoah EN, Hammar K, Smith PJ, Malchow RP. 2004. Neurotransmitter modulation of extracellular H+ fluxes from isolated retinal horizontal cells. J Physiol 560(Pt 3):639-657.

Morgans CW, Brandstatter JH, Kellerman J, Betz H, Wassle H. 1996. A SNARE complex containing syntaxin 3 is present in ribbon synapses of the retina. J Neurosci 16(21):6713-6721.

Murakami M, Shimoda Y, Nakatani K, Miyachi E, Watanabe S. 1982. GABA-mediated negative feedback from horizontal cells to cones in carp retina. Jpn J Physiol 32(6):911-926.

Nagura H, Ishikawa Y, Kobayashi K, Takao K, Tanaka T, Nishikawa K, Tamura H, Shiosaka S, Suzuki H, Miyakawa T, Fujiyoshi Y, Doi T. 2012. Impaired synaptic clustering of postsynaptic density proteins and altered signal transmission in hippocampal neurons, and disrupted learning behavior in PDZ1 and PDZ2 ligand binding-deficient PSD-95 knockin mice. Mol Brain 5:43.

O’Brien J, Chen X, MacLeish P, O’Brien J, Massey S. 2001. Photoreceptor Coupling mediated by Connexin 36 in the Primate Retina. J Neurosci 32(13):4675-4687

O'Brien J. 2014. The ever-changing electrical synapse. Curr Opin Neurobiol. 0:64-72

Oliva C, Escobedo P, Astorga C, Molina C, Sierralta J. 2012. Role of the MAGUK protein family in synapse formation and function. Dev Neurobiol 72(1):57-72.

Pan F, Keung J, Kim IB, Snuggs MB, Mills SL, O'Brien J, Massey SC. 2012. Connexin 57 is expressed by the axon terminal network of B-type horizontal cells in the rabbit retina. J Comp Neurol 520(10):2256-2274.

Pan F, Massey SC. 2007. Rod and cone input to horizontal cells in the rabbit retina. J Comp Neurol 500(5):815-831.

Paik SS, Park N, Lee S, Han H, Jung C, Bai S. 2003. GABA receptors on horizontal cells in the goldfish retina. Vision Research 43 (20): 2101-2106

Pearson RA, Dale N, Llaudet E, Mobbs P. 2005. ATP released via gap junction hemichannels from the pigment epithelium regulates neural retinal progenitor proliferation. Neuron. 2;46(5):731-44.

Pegg A. 2016. Functions of Polyamines in Mammals. The Journal of Biological Chemistry 291 (29):14904-14912

Peng YW, Blackstone CD, Huganir RL, Yau KW. 1995. Distribution of glutamate receptor subtypes in the vertebrate retina. Neuroscience 66(2):483-497.

Prochnow N, Hoffmann S, Vroman R, Klooster J, Bunse S, Kamermans M, Dermietzel R, Zoidl G. 2009. Pannexin1 in the outer retina of the zebrafish, Danio rerio. Neuroscience 162(4):1039-1054.

Pruss H, Derst C, Lommel R, Veh RW. 2005. Differential distribution of individual subunits of strongly inwardly rectifying potassium channels (Kir2 family) in rat brain. Brain Res Mol Brain Res 139(1):63-79.

Puthussery T, Percival KA, Venkataramani S, Gayet-Primo J, Grunert U, Taylor WR. 2014. Kainate receptors mediate synaptic input to transient and sustained OFF visual pathways in primate retina. J Neurosci 34(22):7611-7621.

Schmitz F, Konigstorfer A, Sudhof TC. 2000. RIBEYE, a component of synaptic ribbons: a protein's journey through evolution provides insight into synaptic ribbon function. Neuron 28(3):857-872.

Schwartz E. 2002. Transport-mediated synapses in the retina. Physiological Reviews 82 (4): 875-891

Shen W, Finnegan S, Slaughter M. 2004. Glutamate receptor subtypes in human retinal horizontal cells. Vis Neurosci 21(1):89-95

Sherry DM, Mitchell R, Standifer KM, du Plessis B. 2006. Distribution of plasma membrane-associated syntaxins 1 through 4 indicates distinct trafficking functions in the synaptic layers of the mouse retina. BMC Neurosci 7:54.

Sohl G, Joussen A, Kociok N, Willecke K. 2010. Expression of connexin genes in the human retina. BMC Ophthalmol 10:27.

Sohl G, Willecke K. 2003. An update on connexin genes and their nomenclature in mouse and man. Cell Commun Adhes 10(4-6):173-180.

Solessio E, Rapp K, Perlman I, Lasater EM. 2001. Spermine mediates inward rectification in potassium channels of turtle retinal Müller cells. J Neurophysiology 85(4): 1357-67

Stella S, Hu D, Vila A, Brecha N. 2007. Adenosine inhibits voltage-dependent Ca2+ influx in cone photoreceptor terminals of the tiger salamander retina. J Neurosci Res 85(5):1126-37

Stroh S, Sonntag S, Janssen-Bienhold U, Schultz K, Cimiotti K, Weiler R, Willecke K, Dedek K. 2013. Cell-specific cre recombinase expression allows selective ablation of glutamate receptors from mouse horizontal cells. PLoS One 8(12):e83076.

Sun Z, Risner ML, van Asselt JB, Zhang DQ, Kamermans M, McMahon DG. 2012. Physiological and molecular characterization of connexin hemichannels in zebrafish retinal horizontal cells. J Neurophysiol 107(10):2624-2632.

Tang L, Gamal El-Din TM, Payandeh J, Martinez GQ, Heard TM, Scheuer T, Zheng N, Catterall WA. 2014. Structural basis for Ca2+ selectivity of a voltage-gated calcium channel. Nature. 2;505(7481):56-61

Tatsukawa T, Hirasawa H, Kaneko A, Kaneda M. 2005. GABA-mediated component in the feedback response of turtle retinal cones. Visual Neuroscience 22(3): 317-324

Thoreson W, Burkhardt D. 1990. Effects of synaptic blocking agents on the depolarizing responses of turtle cones evoked by surround illumination. Visual Neuroscience 5(6): 571-583

Thoreson W, Babai N, Bartoletti T. 2008. Feedback from horizontal cells to rod photoreceptors in vertebrate retina. J Neurosci 28(22): 5691-5695

Thoreson WB, Mangel SC. 2012. Lateral interactions in the outer retina. Prog Retin Eye Res 31(5):407-441.

Tomita S, Nicoll RA, Bredt DS. 2001. PDZ protein interactions regulating glutamate receptor function and plasticity. J Cell Biol 153(5):F19-24.

Traynelis SF, Wollmuth LP, McBain CJ, Menniti FS, Vance KM, Ogden KK, Hansen KB, Yuan H, Myers SJ, Dingledine R. 2010. Glutamate receptor ion channels:structure, regulation, and function.62(3): 405-96

Trenholm S, Baldridge WH. 2010. The effect of aminosulfonate buffers on the light responses and intracellular pH of goldfish retinal horizontal cells. Journal of Neurochemistry. 115:102–11.

VanLeeuwen M, Fahrenfort I, Sjoerdsma T, Numan R, Kamermans M. 2009. Lateral gain control in the outer retina leads to potentiation of center responses of retinal neurons. J Neurosci 29(19):6358-6366.

Vardi N, Duvoisin R, Wu G, Sterling P. 2000. Localization of mGluR6 to dendrites of ON bipolar cells in primate retina. J Comp Neurol 423(3):402-412.

Verweij J, Kamermans M, Spekreijse H. 1996. Horizontal cells feed back to cones by shifting the cone calcium-current activation range. Vision Res 36(24):3943-3953.

Vessey JP, Stratis AK, Daniels BA, Da Silva N, Jonz MG, Lalonde MR, Baldridge WH, Barnes S. 2005. Proton-mediated feedback inhibition of presynaptic calcium channels at the cone photoreceptor synapse. J Neurosci 25(16):4108-4117.

Vila A, Satoh H, Rangel C, Mills SL, Hoshi H, O'Brien J, Marshak DR, Macleish PR, Marshak DW. 2012. Histamine receptors of cones and horizontal cells in Old World monkey retinas. J Comp Neurol 520(3):528-543.

Vilin Y, Nunez JJ, Kim RY, Dake GR, Kurata HT. 2013. Paradoxical activation of an inwardly rectifying potassium channel mutant by spermine: "(b)locking" open the bundle crossing gate. Mol Pharmacol 84(4): 572-81

Vroman R, Klaassen LJ, Howlett MH, Cenedese V, Klooster J, Sjoerdsma T, Kamermans M. 2014. Extracellular ATP hydrolysis inhibits synaptic transmission by increasing ph buffering in the synaptic cleft. PLoS Biol 12(5):e1001864.

Wang TM, Holzhausen LC, Kramer RH. 2014. Imaging an optogenetic pH sensor reveals that protons mediate lateral inhibition in the retina. Nat Neurosci 17(2):262-268.

Warren TJ, Van Hook MJ, Supuran CT, Thoreson WB. 2016. Sources of protons and a role for bicarbonate in inhibitory feedback from horizontal cells to cones in Ambystoma tigrinum retina. J Physiol.

Williams. 1997. Modulation and Block of Ion Channels: A New Biology of Polyamines. C Cell Signal 9 (1):1-13

Wu S. 1992. Feedback connections and operation of the outer plexiform layer of the retina. Current Opinion in Neurobiology 2 (4): 462-468

Xie L, John S, Weiss J. 2003. Inward rectification by polyamines in mouse Kir2.1 channels: synergy between blocking components. J Physiol 550(Pt 1): 67-82

Yazulla S, Studholme K, Pinto L. 1997. Differences in the retinal GABA system among control spastic mutant and retinal degeneration mutant mice. Vision Research 37 (24): 3471-3482

Yang X and Wu S. Effects Effects of prolonged light exposure, GABA, and glycine on horizontal cell responses in tiger salamander retina. J Physiology 61:1025-1035

Zheng CY, Seabold GK, Horak M, Petralia RS. 2011. MAGUKs, synaptic development, and synaptic plasticity. Neuroscientist 17(5):493-512.

Vita

Alejandro Vila Ymbert was born in Barcelona, Spain on July 17, 1973, the son of Ramon Vila Rodriguez and Monica Ymbert Rosselli. After completing high school at Colegi Claret in Barcelona in 1991, he studied for three years to become a dental technician. In 1994, he moved to US to pursue a career in science. He received the degree of Bachelor of Science with a major in Molecular, Cell and Developmental Biology from UCLA in August, 2000. In August of 2006, he entered The University of Texas Graduate School of Biomedical Sciences at Houston. In 2009, he received the degree of Master of Science in Neuroscience and continued working on his Ph.D in Ophthalmology and Vision Science Department at McGovern Medical School in Houston.

Permanent address:

2220 Bering Dr. Suite # 25
Houston, Texas 77057